ADDIS ABABA UNIVERSITY

ADDIS ABABA INSTITUTE OF TECHNOLOGY (AAiT)

School of Electrical and Computer Engineering

ANALYSIS OF DYNAMIC VOLTAGE STABILITY ON THE PENETRATION OF ADAMA II WIND FARM IN ETHIOPIAN GRID

BY

ANCHINESH MENGISTU

September, 2017

ADDIS ABABA, ETHIOPIA

ADDIS ABABA UNIVERSITY

ADDIS ABABA INSTITUTE OF TECHNOLOGY (AAiT)

School of Electrical and Computer Engineering

ANALYSIS OF DYNAMIC VOLTAGE STABILITY ON THE PENETRATION OF ADAMA II WIND FARM IN ETHIOPIAN GRID

A thesis submitted to Addis Ababa Institute of Technology, School of Graduate Studies, Addis Ababa University in Partial Fulfillment of the Requirements for the Degree of Master of Science in Electrical Engineering
(Electrical Power Engineering)

By

Anchinesh Mengistu

Advisor: Dr.- Ing. Fekadu Shewarega

September, 2017

ADDIS ABABA UNIVERSITY

ADDIS ABABA INSTITUTE OF TECHNOLOGY (AAiT)

School of Electrical and Computer Engineering

ANALYSIS OF DYNAMIC VOLTAGE STABILITY ON THE PENETRATION OF ADAMA II WIND FARM IN ETHIOPIAN GRID

By: **Anchinesh Mengistu**

APPROVED BY BOARD OF EXAMINERS

Mr. Amare Assefa (MSc) _____
Chairman, Department of Graduate Committee Signature

Dr.-Ing Fekadu Shewarega _____
Advisor Fekadu Shewarega Signature

Prof. N.P Singh _____
Internal Examiner Signature

Dr.-Ing Getachew Biru _____
External Examiner Signature

Dedication

This thesis is dedicated to the **Lord Jesus Christ** - the donor of wisdom, knowledge, and understanding.

Declaration

I, the undersigned, declare that this MSc thesis work is my original work, has not been presented for fulfillment of a degree in this or any other universities, and all sources of materials used for the thesis work have been duly acknowledged.

Name : Anchinesh Mengistu

Signature : _____

Place: Addis Ababa Institute of Technology, Addis Ababa University, Addis Ababa

Date of Submission: September, 2017

This thesis has been submitted for examination with my approval as a university advisor.

Dr.- Ing. Fekadu Shewarega
Advisor‘s Name

_____
Signature

Acknowledgement

Primarily, I would like to give all honor and glory to my Lord and Savior Jesus Christ without which the completion of this thesis would have been unthinkable.

I would like to express my deepest and sincere gratitude to my advisor Dr.-Ing. Fekadu Shewarega, for all his expert guidance, suggestions, encouragement and kind patience during the course of this thesis work. He has made a great effort in keeping me focused in my thesis in all ups and downs of the thesis journey. In addition, I appreciate and acknowledge the valuable support and critical comments regarding the work. He has been a constant source of inspiration throughout my thesis period. Once more I would like to say thank you.

I am indeed very grateful to Prof. Nagandra Prasad Singh for his invaluable guidance, patience and assistance in the writing of the thesis. I am highly privileged to have worked under him.

I also like to acknowledge the support from Mr. Melaku Yigzaw, for using the PSS/E software that has been used for my thesis work. Thanks go to Adama II wind project office in providing with the necessary data and also I would like to give credit to Mr. Yalewayker Mandefro for his kind helps and assistance to collect the necessary data from the site for conducting this study.

I want to appreciate my husband Dr. Alemayehu Mekonnen for his motivation, and encouragement in this Master studies and my children- Samuel and Lidet Alemayehu for their immense love. Many thanks go to my parents: my brother Dr. Shimelis Mengistu for his valuable assistance, contributions and guidance and my mother Yeshi Kebede for her words of encouragement, and constant prayers.

Finally, I would like to be grateful Mr. Hiwot Eshetu, Mr. Mesfin Megra, Mr. Mohammed Shikur and Mr. Mikyas Wondimu who has contributed to this work directly or indirectly. Last but not least, I would like to thank my friends who stood always with my side.

Anchinesh Mengistu

Abstract

Wind energy is one of the most available and exploitable forms of renewable energy. The importance of wind farm penetration is that it can reduce or replace the existing conventional generators. The integration of wind farm to the existing grid introduces new challenges regarding power system which need to be addressed. Among power system stability concerns, voltage stability due to the integration of wind farms is the one that considerably affect the grid.

By now, Ethiopia has wind energy sources with installed capacity of 324 MW that consist of three wind farms. Among them the largest operational wind farm is Adama II, which has been considered in this thesis, uses Doubly Fed Induction Generator Wind Turbine (DFIG WT).

In this study, Adama II wind farm is aggregated from 102 wind turbines to single turbine representation. Thus, the dynamic model of DFIG WT has been developed and verified using load flow analysis. And the simplified grid model has been developed also. This model is used to analyze the dynamic voltage stability as regards the penetration of Adama II wind farm in Ethiopian existing national grid. The modeling, simulation studies and analysis has been done using Power System Simulator for Engineering (PSS /E) software.

The compliance of the grid code behavior of the wind farm has been investigated based on the detailed analysis of the contingency scenario of that a bolted symmetrical three-phase fault applied at the point of common coupling (PCC) for 150 ms. After fault clearance, the voltage recovers to 1.032 p.u at the PCC and within 0.6 second following the fault clearance other buses restored to the super grid voltage. The active power output and the reactive power restored to 0.9 of the level available immediately before the fault. The results show that Adama II wind farm integrated to the Ethiopian power grid fulfills the wind grid code requirements in response to the short circuit event. The thesis also analyzes the voltage control capability of Adama II wind farm voltage controller on the power system dynamic voltage stability. To study its influence, wind generator equipped with /without voltage controller is considered. The voltage at the PCC gradually recovers to 1.038 p.u and 1.059 p.u with and without voltage controller respectively after the clearance of short circuit fault .It is observed that the voltage with out voltage control strategy exceeds the normal limit of 1.05 p.u. Finally, the analysis of wind farm performance in weak grid has been done . It can be observed that the voltage on the far end substation bus bar is 0.934 p.u and 1.0639 p.u with low and maximum load respectively. In this case, the results show that voltages are violated the standard voltage range.

The simulation results depict that, the contribution of voltage controller is visible since it enhances the wind farm capability during the fault as compared with no voltage control is enabled. Therefore, the wind farm is able to fulfill the control characteristic of the controller that can improve power system dynamic behavior such as voltage stability as spelt out in international grid codes. And also it is recommended that EEP has to implement and equipped with voltage controller for all wind farms.

Key words: wind farm, DFIG, dynamic voltage stability, aggregated wind farm, PSS/E, wind farm penetration, contingency scenario, national grid, PCC, grid code, voltage control

Table of Contents

List of Figures

List of Tables

Nomenclature

AC	Alternating Current
AVR	Automatic Voltage Regulator
DC	Direct Current
DFIG	Doubly-fed induction generator
EAPP IC	East African Community Interconnection Code
EAPP	Eastern Africa Power Pool
EEP	Ethiopian Electric Power
ENTGC	Ethiopia National Transmission Grid Code
ETS	Ethiopian Transmission System
FACT	Flexible AC Transmission
FRT	Fault Ride Through
FSR	Full System Representation
GE	Generic models in simulation platform that are typically used in Siemens-PTI PSSE
GP	Generating Plant
GSC	Grid Side Converter
HEEP	Hydro Electric Power Plant
HV	High voltage
IGBT	Insulated Gate Bipolar Transistor
LDC	Load Dispatch Center
M base	Base apparent power
MV	Medium voltage
p.u	Per Unit
PCC	Point of Common Coupling
PI	Proportional Integrator
Pmax	Maximum power
Pmin	Minimum power
POI	Point of Interconnection
PSS/E	Power System Simulator /Engineering
PWM	Pulse-width modulation
Qmax	Maximum reactive power
Qmin	Minimum reactive power

RPP	Renewable Power plants
RSC	Rotor Side Converter
SCADA	Supervision Control and Data Acquisition
SG	Synchronous generator
Sn	Apparent power
STATCOM	Static Synchronous Compensator
STR	Single Turbine Representation
SVC	Static Var Compensator
TSO	Transmission System Operator
Type-1	Fixed speed wind turbines
Type-2	Limited variable speed
Type-3	Variable speed with partial scale frequency converter
Type-4	Variable speed with full-scale frequency converter
Unp/Uns	Wind turbine transformer voltage ratio(primary voltage/secondary voltage)
VSWT	Variable Speed Wind Turbines
WEF	Wind Energy Facility
WF	Wind farm
WPP	Wind Power Plant
WTG	Wind Turbine Generator
Ytr	Transformer impedance
Ztr	Transformer admitance
Z source	Source impedance

CHAPTER 1

Introduction

1.1 Background

Energy demand has increased year by year that led energy sector to seek the use of new ways to produce energy in environmental friendly way. This was found in the development of renewable energy resources.

Renewable energy resources are the best energy options due to the environmental concerns and to reduce dependency on conventional energy resources with finite nature of supplies.

Ethiopia has a lot of renewable energy source like wind power, solar power, hydropower, etc. Among those renewable energy sources, wind energy is one of those renewable energies and assumed to have the most favorable technical and economic prospects. Presently the electric supply system of Ethiopia is mainly from hydro power plants and wind farms.

Wind power is undergoing the fastest rate of growth of any form of electricity generation in the world. The resource potential is large; with many countries having wind regimes that could serve as a significant energy source. Since Ethiopia has high wind resource potential EEP has a plan to increase the power generated from wind significantly. Consequently when level of wind power penetration in to the grid increases, it has its own impact on the stability of the power system that requires detailed analysis for its impact on the steady state and dynamic behavior of the power system.

Experiences to date indicate that wind generation has both positive and negative impacts on power system dynamics. Modern wind turbines come with power electronic converters with fast acting controllers, which provide control options and speed of response that are normally not available in conventional synchronous machine based generation plants. On the other hand, the dynamic behavior of the power system due to the increasing share of wind in power generation will change considerably by the reason of these technologies used for wind. Therefore, both steady-state load flow and dynamic system-stability analysis are needed when determining adequacy of the grid. And also for system stability reasons, operation and control properties will be required from wind power plants at some stage, depending on wind power penetration and power system robustness [1].

Countries like Ethiopia, where power development mostly focused on hydro, can severely be affected by a drastic weather change in case of dry hydrologic conditions. The paramount and time honored solution for such kind of problems using diversified sources of energy is imperative. In Ethiopia, wind and geothermal sources are good options and opportunities for generating mix in the energy development.

The past three years has seen the emergence of wind as growing energy source in Ethiopia. Currently three wind farms are in operation. These are Ashegoda, Adama I and Adama II wind farms that found in different part of the country. The installed wind generation (WG) capacity already surpassed 300 MW by the end of the year 2015 in Ethiopia which is more than 7% of the total installed capacity.

The Adama II wind farm is the largest wind farm in Ethiopia. It has 102 turbines and can produce 153MW electric power. Thus, it helps and has significant role to start diversifying electricity generation, which would otherwise remain entirely from hydropower and thus susceptible to extreme weather events.

The Ethiopian government has projected transformation and development plan to achieve 720 MW of power from wind energy with the near future. Therefore, a significant amount of a system's energy is come from wind and will start to replace the output of conventional synchronous generators. As a result, it may also begin to influence overall power system behavior and poses challenges for the system operators which will need to be addressed. Among power system stability concerns, voltage stability due to the integration of WFs will affect the national grid, and this is one of the major concerns and has to be carried out.

Hence, this thesis is needed to investigate the dynamic voltage stability analyses and phenomenon due to the integration of large-scale wind farm. Adama II wind farm has been selected as a case study due to the fact that it is the largest WPP which is operational in Ethiopia.

1.2 Statement of the Problem

Grid integration concerns have come to the fore in recent years as wind power penetration levels have increased in a number of countries like Ethiopia as an issue that may impede the widespread deployment of wind power systems. The challenges to wind power penetration into Ethiopian grid are:

- Voltage stability is the main problem that will affect the operation and security of wind farms and power grids, since voltage stability deterioration is mainly due to the large amount of

reactive power absorbed by the WTs during their continuous operation and system contingencies.

- Wind farms could cause serious voltage stability problems due to their output variability and intermittency.
- Additionally Wind turbines possess limited capability to inject reactive power into the PCC to support the voltage during short-circuit.

Currently federal government of Ethiopia has developed policy and strategy aimed at production of electric energy from wind and solar. Therefore, in the near future these increase of wind power will take place and those wind farms with hundreds megawatts connected to the high voltage grid are expected to be built. Thus, the dynamic behavior of the power system will change considerably by the reason of different technologies used for wind generators due to the increasing share of wind in power generation. Therefore, integration of wind parks has to be considered in power system dynamic stability (voltage stability) studies.

Various papers [2, 3, 4, 5 and 6] have been published dwelling on impacts of wind farms on power system stability. However most of the papers include the impacts of integration of wind farms on rotor angle stability in general. But this thesis particularly studies the dynamic voltage stability when Adama II wind farm has been penetrated in the existing Ethiopian grid.

The problem considered in this thesis is to study and investigate the effects of penetration of Adama II wind farm on dynamic voltage stability on Ethiopian grid.

1.3 Objectives of the Thesis

General Objective

The general objective of this thesis is to investigate and analyze dynamic voltage stability of the existing Ethiopian grid integrated with Adama II wind farm.

Specific Objectives

The specific objectives of this thesis are as follows:

- To collect and analyze various data sourced from EEP and Siemens PTI standards.
- To develop aggregated Adama II wind farm and validate the model.
- To develop the simplified aggregated grid model.

- To investigate and analyze the dynamic voltage stability behavior of the power system integrated with Adama II wind farm.
- To carry out dynamic simulation of three phase short circuit fault at the PCC.
- To investigate the contribution of wind power plant controllers on power system dynamic voltage stability.
- To draw conclusions based on results analysis and observations with regard to the dynamic voltage stability of Ethiopian grid integrated with Adama II wind farm.

1.4 Literature Review

In this section, different studies around this thesis idea have been done, that the power system impact of wind power integration has been reviewed, proposed and analyzed.

F. Shewarega, I. Erlich and José L. Rueda 2009 [2] tried to deal with the impact of large scale wind power integration on transient stability performance of power systems. The aim is to investigate the effect of wind turbines on the transient stability of conventional synchronous generator units operating on the system and explore some of the possible control measures that can help stabilize the system in the post fault scenario. The paper has been analyzed the effect of increased wind power generation on the transient stability performance of the interconnected system using a complete modeling of DFIG wind turbine and a number of simulation and analysis using DIgSILENT software. It concluded that the electro-mechanical power oscillations, which typically occur following a grid fault in conventional synchronous generators, are not prevalent in wind generation plants. The overall impact of wind on the transient stability performance of the network, as it increases the fault clearing time and can be characterized as adverse. But in this study steady state and dynamic analysis has been performed using PSS/E simulation software to map the impacts of the injected power of the wind farm on the existing system with different scenarios were proposed and analyzed to fulfill the grid requirements in response to the contingency events .

Getachew Bekele, Abdulfetah Abdela 2012 [3] investigated on Adama I wind farm interaction with Ethiopian electric power corporation's grid. It concerned with only specific scenario Fault Ride-Through (FRT) capability, which includes voltage recovery at the wind turbines terminal; active and reactive power behavior of the wind farm after the applied three phase short circuit fault is cleared. In the study only PMSG wind turbine was considered and using DIgSILENT simulation software it tried

to model Adama I wind farm by representing the 34 wind turbines with a single turbine. After modeling a three phase fault of 150 ms duration was introduced on the high voltage terminal of the wind farm and concluded that PMSG wind turbines provided to be promising in which it comply with the grid requirements for the EEPCO power system, after the three phase short circuit fault showing its immunity. But the paper study only PMSG wind turbines were analyzed and their impact on the transient stability of the power system was not studied and also only a single location of fault which is near to the wind farm was considered. But in this study the impact of DFIG wind turbine technologies on power system stability will be investigated and also the impact of wind power plant with different fault locations will be analyzed using PSS/E simulation software.

Belachew Bantyirga Gessesse 2013 [4] tries to conduct integration of large wind farms into weak power grids considered on the Ethiopian Interconnected System. The main focus of the study is the impact of increased wind power on the steady state and dynamic behavior of the Ethiopian power system. The study has investigated the impact of wind power penetration level and concluded that the impact of wind turbines penetration level on the operational indices was more pronounced in the vicinity of the wind farm but the power angle oscillation is seen to propagate throughout the system independent of the location of the wind farm and also deals with the investigation of the effect of large scale wind power integration on small signal stability of the Ethiopian power system. Dynamic stability investigation is carried out using eigen value and eigenvector techniques while transient stability study is carried out using time domain simulation. The investigations conducted on the impact of system load levels with no wind power and with maximum wind generation on the damping performance of the system suggests that the damping performance of the system is not significantly affected either by the level of system load or the amount of wind generation. It is concluded on the basis of the studies that the integration of large scale wind generation does not appear to affect the small signal stability on the Ethiopian power system.

MOHAMMAD SEYEDI 2009[5] assesses DFIG wind turbine built-in model in PSS/E. It tries to investigate the responses of the model subjected to grid disturbances. The built-in dynamic model for DFIG wind turbine in PSS/E is illustrated and it is used to study the dynamic behavior of DFIG subjected to a symmetrical short circuit at the point of common coupling of a large wind farm. The load flow study for a network where a wind farm consisting 67 numbers of DFIG wind turbines and each one with 1.5MW rated power connected to the grid are presented and the output results from load

flow study is used to perform dynamic simulation. The voltage, current, output power, speed and pitch angle profiles are presented in the dynamic study. The dynamic simulation results shows that the DFIG dynamic model presented in PSS/E is not able to fully represent the limitations of the wind turbine due to the parameters used in the model.

Gabriele Michalke 2008 [6] deals with the modeling, control, and the impact of variable speed wind turbines on the power system. It focuses on the dynamic behavior of wind turbines and their interaction with the power system. DFIG and PMSG wind turbine technologies are selected for the investigation. Comprehensive dynamic simulation models of both of these wind turbine concepts are implemented in the power system simulation software DIgSILENT Power Factory. Furthermore advanced control strategies for the wind turbine concepts in normal and fault operation are developed. Finally, an aggregated model of a large offshore wind farm consisting of eighty 2 MW wind turbines is implemented for each wind turbine concept, a 160 MW DFIG wind farm and a 160 MW PMSG wind farm, respectively. These models serve to illustrate how such large wind farms can contribute with reactive power and help to reestablish the voltage in case of a grid fault. The wind farms´ fault ride-through capability and their contribution to voltage control is assessed and evaluated by means of simulations with the use of a generic but realistic transmission power system model delivered by the Danish Transmission System Operator Energinet.dk. Several case studies are performed in order to analyze the power system impact of both considered wind turbines concepts. The simulation results illustrate how the DFIG wind farm as well as the PMSG wind farm equipped with voltage control participate to re-establish properly the voltage during a grid fault.

Anca D. Hansen,Gabriele Michalke,Poul Sørensen and Torsten Lun 2006 [9] presents a simulation model for DFIG wind turbines equipped with co-ordinated voltage control to enable uninterrupted operation during a grid fault using DIgSILENT simulation software. The objective of this article is to enhance the capability of DFIG WTs to provide grid support during grid faults. Issues on modeling and control of a DFIG wind turbine, with focus on the converter protection under grid fault operation, are discussed and illustrated. The controllability of the DFIG during grid faults is enhanced by the design of a proper co-ordination of three additional controllers, namely a damping controller, a rotor-side converter voltage controller and a grid side converter reactive power boosting. The influence of such a control set-up on the performance of an active stall wind farm located nearby is also investigated. The conclusion is that the DFIG wind farm equipped with voltage control can help a nearby active stall

wind farm to ride through a grid fault, without implementation of any additional ride-through control set-up in the nearby active stall wind farm.

Akhmatov V 2002 [18] described the considerations and the results of the investigation on short-term voltage stability carried out on a large wind power network model. In the investigation, a distinction was made between large wind farms connected to the transmission network which must ride through three-phased as well as unbalanced short-circuit faults and local wind turbines connected to the distribution networks which could disconnect in case of a grid fault. The large power grid model was implemented in the PSS/E and as a result; access to the strong power grid stated very favorable for the connection of the large offshore wind farms to reduce the demands on the control applied to the grid as well as to the wind turbines.

L. Munteanu, A. L. Bratcu, N.-A. Cutulilis, and E. Ceanga n.d. [19] focuses on the development of an equivalent representation of a WPP collector system for power system planning studies. Although it uses a specific large WPP as a case study, the concept is applicable for any type of WPP.This reports ummarized the dynamic model development of four types of wind turbine generators,data collectionnee ded for model validation, power flow wind power plant equivalencing, model validation, and modeling guidelines developed for the Western Electricity Coordinating Council.

Considerable numbers of studies has been conducted on the impact of wind power integration on power system stability. However most of the papers include the analysis of power system stability in general. Stability study is becoming particularly important given the fact that utilities have to ensure the same stability margin even in cases where wind power constitutes a significant component of the total power generation.

This thesis attempts to analyze the voltage stability when Adama II Wind farm wind has been penetrated in the Ethiopian grid along with conventional generators.

1.5 Methodology

The main focus of this thesis is to study and analyze the dynamic voltage stability of Adama II Wind farm penetration into an existing Ethiopian grid. The general methodologies employed in this thesis work to achieve the specific objectives are presented as follows.

Primarily literatures on the experience on the area of voltage stability when wind generation is penetrating into power system are studied. A review on literatures are conducted concerning investigation on voltage stability as large wind generation is integrating into the power system from available books; journals, case studies, and previous research papers . Theoretical descriptions on wind turbine types, modeling of wind turbine and control system with Doubly Fed Induction Generator (DFIG) are reviewed. It also includes empirical literature survey on power system stability and wind power generation with the area of voltage stability and voltage control. These aids in getting the relevant information and adopting different concepts and methodologies as required.

Secondly, mathematical model for the wind farm aggregation has been developed for aggregation of Adama II wind farm. Then, the aggregated model has gone through steady state analysis to map the impacts of injected power on the existing system and the model has been validated using load flow analysis. This also helps to model the grid model that is used for this study. In general, the grid model representing the Ethiopian national grid with the aggregated Adama II wind farm that has been used for static and dynamic studies.

The data collection, modeling, simulation and analysis are the general methods adopted for this thesis. Accordingly the various input data required for the model has been collected, organized, refined, analyzed and verified to make the model complete.

The requested data has mainly been sourced from EEP generally from Adama II wind farm project office, site of where the wind farm is located, LDC and corporate planning office and the generic wind turbine models are obtained from built in model in PSS/E.

With the aim of investigating the dynamic voltage stability of the grid and the compliance and capability of Adama II wind farm connecting to the existing grid, the steady state and dynamic simulations have been performed with realistic contingency scenarios on the grid model under analysis to carry out the objectives of the thesis. Finally based on detailed analysis and simulation results, it can be observed that how the wind farm penetration is affecting the dynamic voltage stability of the existing Ethiopian grid and lastly conclusion is drawn from the simulation results of PSS/E software.

1.6 Scope of the Thesis

All studies for each of the above stated objectives has been modeled and simulated in PSS®E 33 simulation software. The wind turbine models will be created to be generic in nature but are practical.

All the data and equipment specifications are obtained from Ethiopian Electric Power (EEP) and Siemens Power Technologies International (PTI) standards. The main scope of this study is to investigate the impact of the penetrated Adama II wind farm on dynamic voltage stability at the point of common coupling of the developed grid model when transporting electric power between different parts of Ethiopian grid.

1.7 Organization of the Thesis

This thesis consists of five chapters. The present chapter gives the introduction, statement of the problem, objectives of the thesis, literature review, methodology, and scope of the thesis.

Chapter two is dedicated to theoretical back ground; primary the main mathematical equations and modeling control system of DFIG are discussed in detail. subsequently, types of WT, Power system stability and also wind power plant voltage control are explained. Finally, a brief description on the performance requirements in operation of wind farms connected to the Ethiopian grid has been described in detail.

In chapter three mathematical modeling and analysis of Adama II wind farm has been described. Wind farm aggregation methods has been given consequently, Adama II wind farm aggregation is developed and the model has been verified using power flow results after that, the model used for study has been described in detail. The simulation software used for this thesis work is also described in this chapter.

Chapter four is simulation result analysis and discussion. The simulation on the model under study has been carried out in order to analyze power system stability impact or the dynamic behavior of the system with wind integration when subjected to various fault scenarios, particularly, dynamic voltage performance on the system under study are discussed and analyzed using the results obtained from the simulations with PSS/E.

Finally, Chapter Five presents conclusions, recommendation and future work.

CHAPTER 2

2 Performance Characteristics of Wind Farms

2.1 Introduction

In this chapter the theories have been laid out. First the main mathematical equations, that describe the relationship between voltage and fluxes in DFIG and which are the basic equations to establish dynamic model, are presented with a short description, then, types of WT and model of DFIG wind turbine are discussed in detail. Modeling control system of DFIG, power system stability and wind power generation with the area of voltage stability and also wind power plant voltage control are explained. Finally, integration and performance requirements of wind farm are also presented in detail.

2.2 Mathematical Modeling of DFIG

The conventional T-equivalent circuit is used to represent the dynamic model of induction generator (IG). This model consists of stator winding and rotor winding with slip rings. The three phase stator windings directly connected to the grid through a step-up transformer. The rotor also has a three phase winding but it is connected to the rotor power supply through slip rings and brushes. The power supply of the rotor comes from the rotor-side converter.

The rotor current is controlled by the rotor-side converter and consequently the active and reactive power can be controlled. The equivalent diagram of the stator and rotor and the grid-side and rotor-side converters is shown in Figure 2.1.

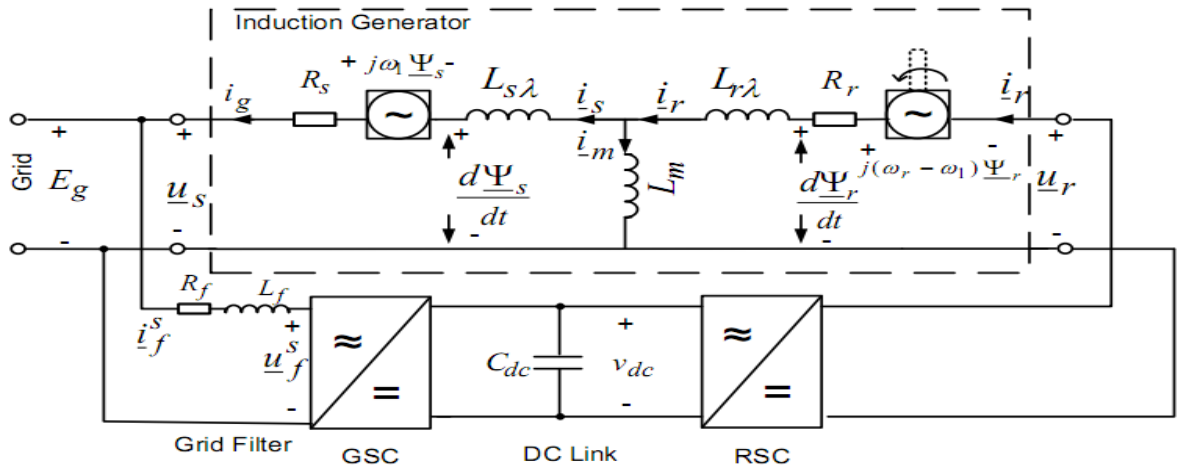

Figure 2. 1: Dynamic equivalent circuit of the DFIG and converters

Based on the equivalent circuit presented in Figure 2.1, the electrical dynamics equations using the space vector approach can be derived. By applying Kirchhoff's voltage law in the stator and rotor and in per unit system it can be written as

$$\underline{u}_s = R_s \underline{i}_s + \frac{d\underline{\Psi}_s}{dt} + j\omega_1 \underline{\Psi}_s \quad (2.1)$$

$$\underline{u}_r = R_r \underline{i}_r + \frac{d\underline{\Psi}_r}{dt} - j(\omega_1 - \omega_r)\underline{\Psi}_r \quad (2.2)$$

where

R_s= stator resistance

R_r= rotor resistance

L_m=mutual inductance

u_s= stator voltage

$\underline{\Psi}_s$= stator Flux

ω_1= synchronous frequency

$\omega_1 - \omega_r = \omega_2$= slip frequency

$\underline{i}_s$=Stator current

$L_{s\lambda}$=stator leakage inductance

$L_{r\lambda}$=rotor leakage inductance

$(\omega_1 - \omega_r)\underline{\Psi}_r$= rotor back emf

u_r= rotor voltage

$\underline{\Psi}_s$= rotor Flux

ω_r= rotor frequency

$\underline{i}_r$= rotor current

The subscripts s and r refer to quantities of the stator and rotor, respectively. The dynamic model of an induction machine is usually presented by means of a so called fifth-order model that represents IG by a system of five general differential equations of an idealized induction machine.

$$\underline{\Psi}_s = L_s \underline{i}_s + L_m \underline{i}_r \quad (2.3)$$

$$\underline{\Psi}_r = L_r \underline{i}_r + L_m \underline{i}_s \quad (2.4)$$

Where

$$L_s = L_{s\lambda} + L_m \quad (2.5)$$

$$L_r = L_{r\lambda} + L_m \quad (2.6)$$

The electromechanical torque is

$$T_e = \mathrm{Im}\left[\underline{\Psi}_s^s \underline{\mathrm{i}}_{\mathrm{s}}^*\right] = -(\Psi_{sd} i_{sq} - \Psi_{sq} i_{sq}) \quad (2.7)$$

The electrical power will be

$$P_e = \mathrm{Im}\left\{\underline{\Psi}_r \underline{\mathrm{i}}_{\mathrm{r}}^*\right\} \quad (2.8)$$

In power system studies, it is desirable to reduce the complexity of the system by using

reduced-order models that can be obtained by assuming some of the derivatives as being equal to zero. For example, a third-order model of IG is obtained when we neglect the stator flux transients.

Under balanced network conditions, the amplitude and rotating speed of the stator and rotor fluxes are assumed to be constant. The flux dynamics are canceled to get a fast response to the commands from electric controls of converter. Consequently, in the dq reference frame, the stator and rotor fluxes remain constant, i.e.

$$\frac{d\underline{\Psi}_s}{dt} = 0 \text{ and } \frac{d\underline{\Psi}_r}{dt} = 0 \quad (2.9)$$

Thus the voltage equations can be written as

$$u_{sd} = R_s i_{sd} - \omega_1 \Psi_{sd} \quad (2.10)$$

$$u_{sq} = R_s i_{sq} - \omega_1 \Psi_{sd} \quad (2.11)$$

$$u_{rd} = R_s i_{rd} - s\omega_1 \Psi_{rd} \quad (2.12)$$

$$u_{rq} = R_s i_{rq} - s\omega_1 \Psi_{rd} \quad (2.13)$$

If d-axis of the synchronous frame is fixed to the stator voltage, then

$$u_{sd} = 0 \quad (2.14)$$

The flux linkage equations are as follows:

$$\Psi_{sd} = L_s i_{sd} - L_m i_{rd} \quad (2.15)$$

$$\Psi_{sq} = L_s i_{sq} - L_m i_{rq} \quad (2.16)$$

$$\Psi_{rd} = L_r i_{rd} - L_m i_{sd} \quad (2.17)$$

$$\Psi_{rq} = L_r i_{rq} - L_m i_{sq} \quad (2.18)$$

We can also neglect the stator resistance because it is considerably small compared to the stator reactance, hence

$$u_{sd} = 0 \quad (2.19)$$

Subsequently

$$i_{sd} = \frac{L_m}{L_s} i_{rd} \quad (2.20)$$

$$u_{sd} = \omega_1 \Psi_{sd} \quad (2.21)$$

The electromechanical torque is calculated as:

$$T_e = (\Psi_{rq} i_{rd} - \Psi_{rd} i_{rq}) \quad (2.22)$$

$$T_e = L_m (i_{sd} i_{rq} - i_{sq} i_{rd}) \quad (2.23)$$

The active power of stator, rotor, grid-side converter and the injected active power to the grid can be determined as:

$$P_s = Re\left[\underline{u}_s \underline{i}^*_s\right] = -u_{sd} i_{sd} + u_{sq} i_{sq}) \quad (2.24)$$

$$P_r = Re\left[\underline{u}_r \underline{i}^*_r\right] = -u_{rd} i_{rd} + u_{rq} i_{rq}) \quad (2.25)$$

$$P_c = Re\left[\underline{u}_c \underline{i}^*_c\right] = -u_{cd} i_{cd} + u_{cq} i_{cq}) \quad (2.26)$$

$$P_g = P_s + P_c \quad (2.27)$$

Where P_s, P_r, P_c, andP_g are the stator, rotor, dc link grid-side converter active power and the total generator active power, respectively .

If the losses in the converter ignored the converter power will be equal to the power injected to the rotor (Pc=Pr), thus it can be written as

$$P_g = u_{sd} i_{sd} + u_{rd} i_{rd} + u_{rq} i_{rq} \quad (2.28)$$

The reactive power can be calculated as:

$$Q_s = -u_{sq} i_{sq} \quad (2.29)$$

$$P_c = u_{rq} i_{rd} - u_{rd} i_{rq} \quad (2.30)$$

By assuming the grid-side converter reactive power is zero, the generated reactive power will be

$$Q_g = Q_s + Q_r \quad (2.31)$$

$$Q_g = -u_{sd} i_{sq} + u_{rd} i_{rd} - u_{rq} i_{rq} \quad (2.32)$$

2.3 Types of Wind Turbine

The wind turbines are classified into four basic types according to differences in generation technology: fixed speed wind turbine with induction generator, limited variable-speed wind turbine with variable rotor resistance, variable speed wind turbine with doubly fed induction generator (DFIG) and variable speed wind turbine with full converter .

Fixed-Speed Wind Turbine

Fixed speed wind turbine, are equipped with an induction generator (squirrel cage or wound rotor) that is directly connected to the grid as in Figure 2.2. The rotor of a fixed-speed wind turbine rotates at a fixed speed determined by the frequency of the grid, the gear ratio and the pole pairs of generator. It is connected to the grid through a soft-starter, and a capacitor bank for reducing reactive power compensation. The induction generator absorbs reactive power from the grid, so capacitor bank is

necessary to provide reactive power compensation. A gear box is used to transform power from the turbine with lower-rotational speed to the generator rotor with high-rotational speed. The generator terminal voltage is increased with a step-up unit transformer to a medium voltage level.

This type of wind turbines has the advantage of being simple, robust and the cost of its electrical parts is low compared to the other wind turbine types. Its disadvantages are an uncontrollable reactive power consumption, mechanical stress and limited power quality control. Owing to its fixed-speed operation, all fluctuations in the wind speed are further transmitted as fluctuations in the mechanical torque and then as fluctuations in the electrical power on the grid. In the case of weak grids, the power fluctuations can also lead to large voltage fluctuations, which, in turn, will result in significant line losses. [7]

Loss of synchronism due to over-speed in case of voltage dips and increasing of reactive power consumption, especially after fault clearance, is other disadvantages of this type of wind turbine. Generally, the dynamics stability of this type of generator cannot be improved. But , the preventive or corrective measures can be done to limit acceleration during voltage dip through improvement of pitch control and to provide reactive power support during and after clearing of fault, via FACTS devices such as SVCs and STATCOMs is a potential but it can be costly. Compatibility with grid code requirements not satisfied also other disadvantages of this type of wind turbine.

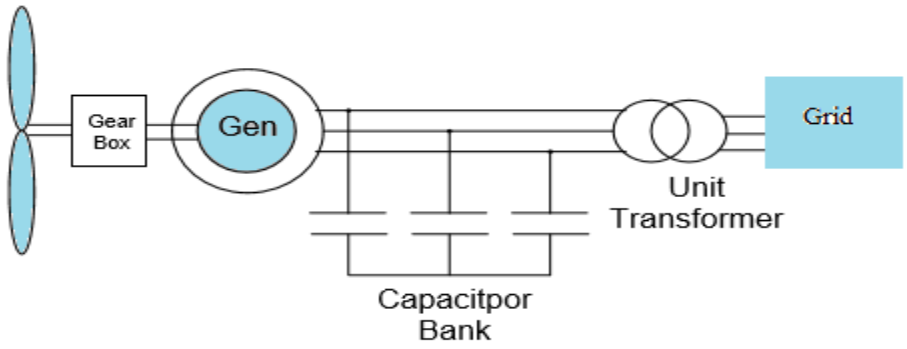

Figure 2.2:Fixed speed wind turbine

Limited Variable Speed Turbine with Variable Rotor Resistance

Wind turbine with variable rotor resistance uses a wound rotor induction generator that is directly connected to the grid. Like a fixed-speed wind turbine, a capacitor provides reactive power compensation. The unique feature of this configuration is that it has a variable additional rotor resistance which can be changed by an optically controlled converter mounted on the rotor shaft. This gives a small variable speed range than fixed-speed turbine type. Typically the speed range is 0-10%

above synchronous speed. Speed and power controls allow these turbines to extract more energy from a given wind regime than fixed-speed turbines can. This type of wind turbine is shown in Figure 2.3.

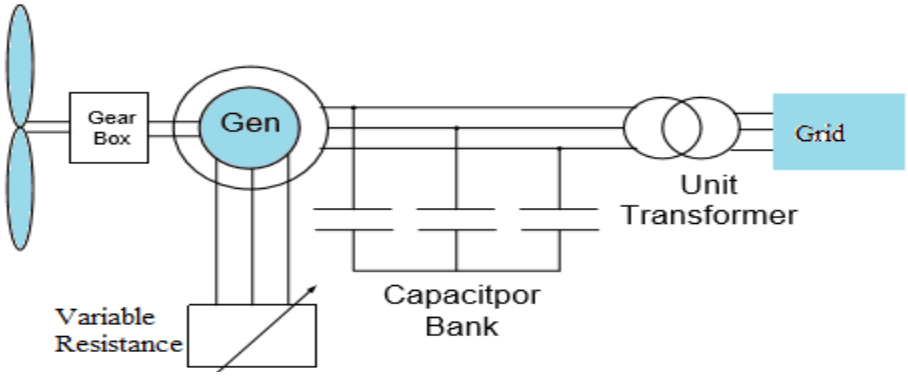

Figure 2.3: Limited variable speed wind turbine with variable rotor resistance

Variable-Speed Wind Turbine with Doubly-Fed Induction Generator

A power electronic converter is used in the variable-speed wind turbine with doubly fed induction generator as shown in Figure 2.4. In this type of wind turbine, the stator directly connected to the grid, while the rotor circuit is connected to a power converter by means of slip rings and brushes. The frequency converter is rated at approximately 30% of the generator power so it is more suitable than the one with full converter for high power wind turbines. The converter also allows for control of the reactive power. This type of wind turbine gives possibility to design the converter with smaller size, and as a result, lower cost and lower power electronic losses [8].

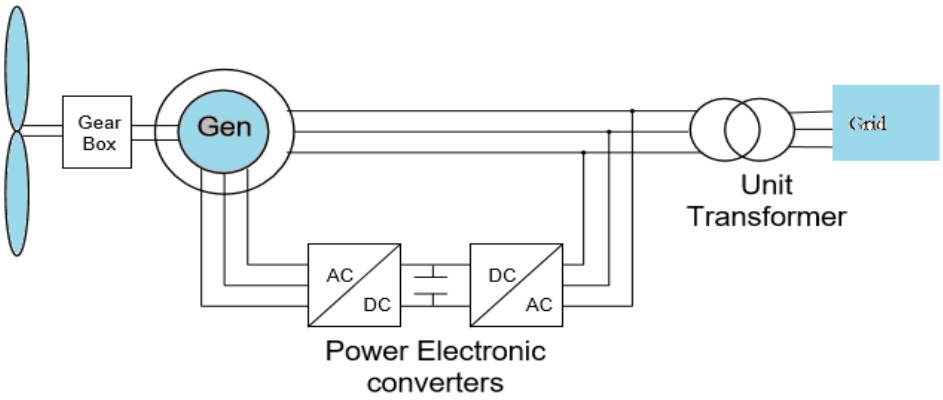

Figure2.4: Variable-speed wind turbine with doubly fed induction generator

Variable-Speed Wind Turbine with Full Converter

This type of wind turbine concept has a full variable speed range, with a squirrel-cage induction generator or a synchronous generator which is connected to the grid via a power electronic converter as shown in Figure 2.5.

The whole power output from generator goes through the converter and therefore the converter is rated at full power. The electronic converter performs the reactive power compensation and the smoother grid connection.

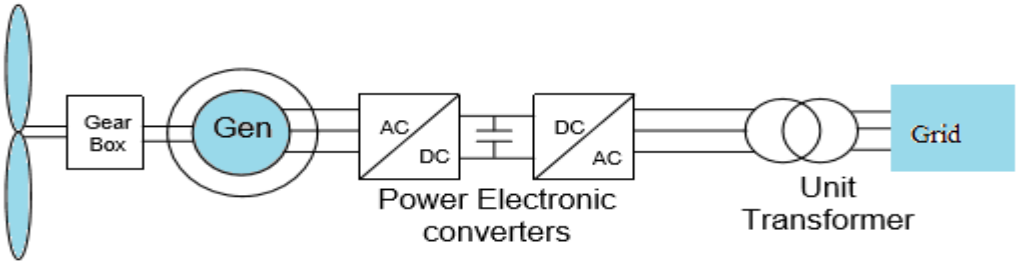

Figure 2.5: Full converter wind turbine

The converter is connected to the stator. This converter has to be able to convert full power from the generator. The gear box can be removed or simplified if a multi-pole synchronous generator is employed. The main advantages of this type of wind turbine are the most favorable dynamic behavior during disturbances, with minimum transients at fault occurrence and clearing. It has also the capability to enhance active and reactive power control and therefore the compatibility with grid code requirements can be satisfied [5].

"With the development of the doubly-fed induction generator (DFIG) technology, large scale DFIG wind power plants are integrating into power systems increasingly. The DFIG machines are collectively referred to as variable speed machines and they possess important advantages such as reactive power control capabilities, smaller and cheaper converter compared with a full size one (Rueda, J.L. and Shewarega, F. (2009))[2]"

Among those four types of wind turbine, a variable-speed wind turbine with Doubly-Fed Induction Generator (DFIG) has been explained in detail.

2.4 Modeling Control System of Doubly Fed Induction Generator

A DFIG system is basically a wound rotor induction generator with slip rings, with the stator directly connected to the grid and with the rotor interfaced through a back-to-back partial-scale power

converter. The converter consists of two conventional converters that is rotor-side converter and Line-side converter and a common DC bus, as illustrated in Figure 2.6. The DFIG is doubly fed, meaning that the voltage on the stator is applied from the grid and the voltage on the rotor is induced by the power converter. This system allows variable speed operation over a large but restricted range depending on the converter size. The voltage source converter supplies the rotor windings with variable voltage and frequency. In addition to the DFIG's ability to feed the rotor with power of variable frequency, a distinct aspect of the DFIG is that it has a fast current control. This means that the DFIG control can, within limits, hold the electrical power constant in spite of fluctuating wind, thus temporarily storing the rapid fluctuations in power as kinetic energy. The use of the partial-scale converter to the generator rotor makes this concept on one hand attractive from an economic point of view. On the other hand, this converter arrangement requires an advanced protection system, as it is very sensitive to disturbances on the grid. Without such protection, high transient currents induced in the rotor can damage the power converter device. [9]

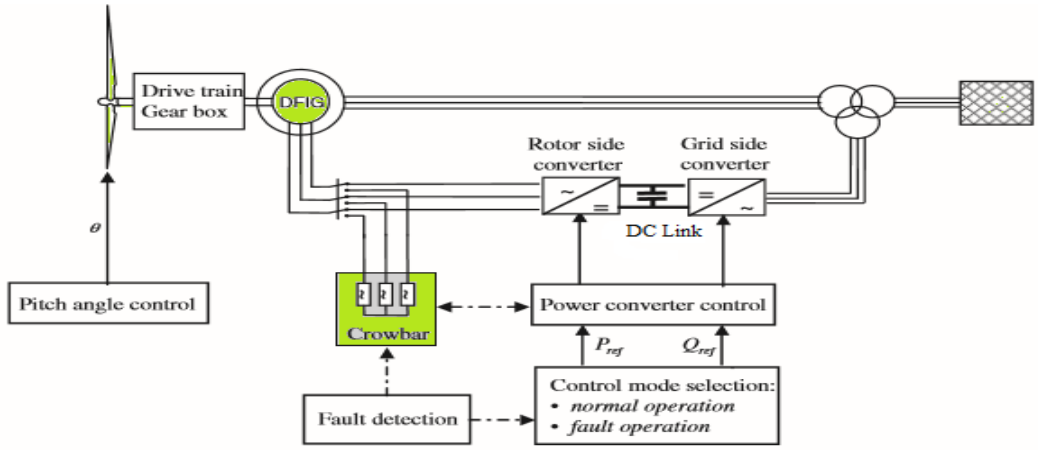

Figure 2.6: Model of Doubly fed induction generator and its main components of the controls

Many large modern wind power plants apply doubly-fed induction generators (DFIGs) since they possess important advantages such as reactive power control capabilities, smaller and cheaper converter compared with a full size one. Furthermore, the voltage control of the DFIG wind turbine could reinforce the system voltage and dynamic stability (Rueda, J.L. and Shewarega, F. (2009.These machines are collectively referred to as variable speed machines .This thesis focuses on Adama II wind farm that uses DFIG type of generators so their impacts on power system static and dynamic behavior must be analyzed.

Electrical System Control of DFIG Wind Turbine

Frequency Converter Model

Frequency converters are power electronic devices, which can connect two systems with different frequency and voltage. The frequency converter of a DFIG is connected in the rotor circuit of the generator. Since the converter has to guarantee a bi-directional power flow it must consist of active elements. "The model uses an IGBT back-to-back voltage source converter as illustrated in Figure 2.7. With the emerging technology of wind turbines, frequency converters are popularly used in wind energy conversion systems. In fixed-speed wind turbines, converters are used to reduce inrush current and torque oscillations during the system start-up, whereas in variable-speed wind turbines they are employed to control the speed/torque of the generator and also the active/reactive power to the grid [C. Feltes, 2012]."[4]

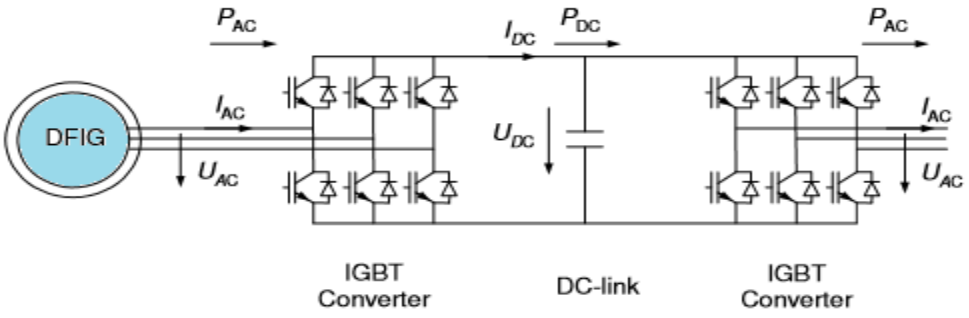

Figure2.7: IGBT back-to-back voltage source converter circuit in the rotor of the DFIG

The converter is modeled by a fundamental frequency approach, which is appropriate and sufficient for power system analysis. The relation between AC- and DC-voltages, which result from the PWM-converter, can be achieved with the following equations:

$$U_{Ac,r} = K_0 PWM_r . U_{DC} \quad (2.33)$$

$$U_{Ac,i} = K_0 PWM_i . U_{DC} \quad (2.34)$$

The equations (2.33) and (2.34) is real and imaginary part of AC voltage U_{Ac}. The PWM factors, separated into real and imaginary part PWMr and PWMi, are limited to 1 and –1 in order to avoid saturation effects. The factor K_0 depends on the modulation method, e.g. rectangular or sinusoidal modulation. In case of sinusoidal modulation the factor K_0 is defined as:

$$K_0 = \frac{\sqrt{3}}{2\sqrt{2}} \quad (2.35)$$

If a loss-less power conversion in the IGBT converter is assumed, the power at the AC side PAC and the power at the DC side PDC are equal; this is expressed by means of equation (2.36):

$$P_{AC} = \Re\{U_{AC}.I^*_{AC}\} = I_{DC}.U_{DC} = P_{DC} \quad (2.36)$$

Equation (2.36) can then be solved to determine the converter currents. Nevertheless, losses can be modeled by specifying a series resistance to the converter. Moreover, as PWM converters are generally grid connected to the AC system through a reactance, the power, which is transmitted via the converter, can be approximated by:

$$P_r = -s.P_s \quad (2.37)$$

This means, that the size of the frequency converter decides about the speed range of the DFIG wind turbine. The larger the converter size, the more power can be transmitted via the converter and the larger the slip, which can be provided. However, a larger converter size means higher costs. Thus, there is a trade-off between financial benefits using a cheaper, smaller converter and the speed range, which can be provided. Generally, the DFIG converter size is designed for approximately 1/3 of the generator power, which results in a speed range of ±30 % around synchronous speed. [6]

Frequency Converter Control Strategies and Performance of DFIG

The grid-side converter operates at a network frequency and controls the voltage level in the dc link circuit. If required, it is possible assign the grid-side converter to deliver reactive power to the grid. The rotor-side converter operates at different frequencies (slip frequency), depending on the rotor speed, and controls the flux of the DFIG and thus the active and reactive power [6].

The rotor-side converter has an over-current protection called crowbar. The crowbar protects the rotor-side converter, as well as the rotor circuit of the DFIG, against high currents during grid disturbances. The location of crowbar resistor is shown in Figure 2.12, where RSC is the rotor-side converter, LSC is the line-side converter or GSC (grid-side converter), CH is the chopper circuit and CR is the crow bar circuit.

The rotor side converter is used to control the real and reactive power outputs of the machine. The power rating of the rotor-side converter is determined according to the maximum slip power and

reactive power control capability. The rotor-side converter can be simplified as a current-controlled voltage source converter.

The extraction of maximum energy from the wind necessitates the adjustment of the rotor speed to correspond to the changing wind speed. The reference rotor speed is obtained from power-speed characteristic curve as shown in Figure 2.8.The rotor speed is then used as an input for a PI controller to get the stator active power reference. The rotor reference current in dq reference frame is then calculated by the following expression [3].

$$i_{rd}{}^{ref} = -\frac{L_s.P_s^{ref}}{L_m.u_{sd}} \quad (2.38)$$

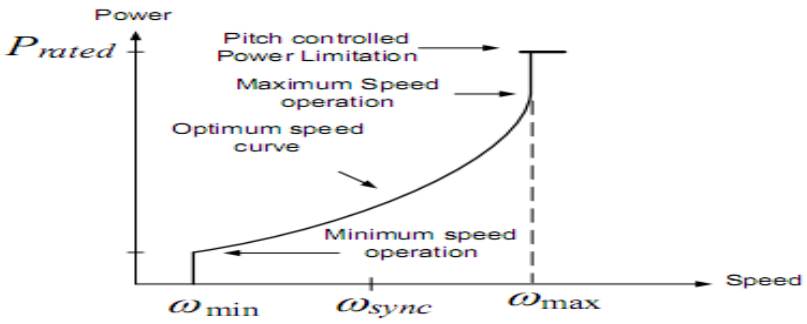

Figure2.8: Power-speed curve

It can be found from above equation that the stator active power is controlled by controlling the rotor current in d direction. The magnitude of reference rotor current in q direction is calculated as:

$$i_{rd}{}^{ref} = -\frac{\omega_1 L_s i_{sq} + u_{sd}}{L_m \omega_1} \quad (2.39)$$

The control diagram for active and reactive power controls is shown in Figure 2.9.

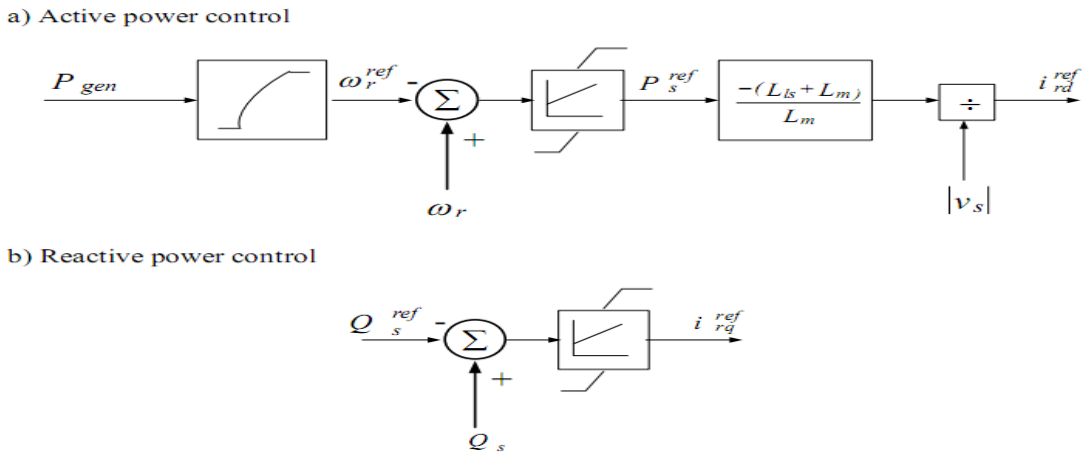

Figure 2.9: Rotor current controller: (a) active and (b) reactive power control

The grid and rotor side converters are linked through a DC circuit comprising of capacitances. If the DC voltage is assumed not to exceed certain limits, which otherwise would impose limitations on the capability of the controllers or initiate action by the protection system, an explicit representation of the DC circuit can be omitted for stability kind of power system simulations.

The converter can also be utilized to support grid reactive power during a fault and it can also be used to enhance grid power quality. However, these abilities are seldom utilized since they require a larger converter rating [5].

Mechanical System Control of DFIG

It is essential to use realistic models for the electrical system as well as for the mechanical part of the wind turbine to develop advanced control strategies for variable speed wind turbines and to investigate their interaction with the power system especially during grid faults. Moreover, a control of the mechanical system, i.e. the blade angle control, must be designed and coordinated with the control of the electrical system.

The mechanical part of the wind turbine includes wind speed model, the aerodynamic model, the blade pitching mechanism and the drive train with gearbox. The mechanical model of a DFIG wind turbine and its control in dynamic studies of power system are presented in Figure 2.10.

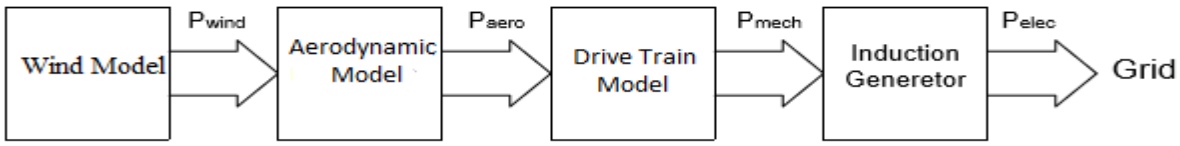

Figure2.10: Modeling scheme of mechanical system of DFIG

Turbine Speed Control Model

The basic strategy for the wind turbine control system is to get the maximum power from the wind. The limiting factor that affects the amount of energy from wind is the equipment power ratings. Accordingly, the mechanical input power has to be limited when the input power from wind is higher than the equipment power ratings. Otherwise, it may destroy the mechanical parts. To reduce the amount of input mechanical power the turbine blades must be turned. This ability of controlling the mechanical input power is called pitch control of turbine blades. The dynamics of the pitch control are moderately fast, and can have significant impact on dynamic simulation results.

On the hand if the available wind power is less than the equipment ratings, the blades is set at a certain pitch angle to get maximum power from wind. The turbine control model sends a power order to the electrical control according to the available wind speed, requesting the converter to deliver this amount of power to the grid.

Aerodynamic and Pitch Control Model

For a power system simulation involving grid disturbances and fault-ride through capability, it is important to include the aerodynamic model. The aerodynamic of the rotor is sufficiently modeled by means of a quasistatic aerodynamic model based on the aerodynamical equation (2.40). In this model, the mechanical power to the turbine is a function of wind speed, blade pitch angle and shaft speed.

$$P_{rot} = {}^{1}/_{2}\,\rho A_r V_w^3 C_p(\lambda,\theta) \quad (2.40)$$

P_{rot} is the aerodynamic power from the wind, ρ is the air density [kg/m^3], A_r is the area swept by the rotor blades [m^2] or $A = \pi r^2, V_w$ is the wind speed [m/sec], and C_p is the is aerodynamic power efficiency, which is a function of λ and θ. λ is the ratio of the rotor blade tip speed and the wind speed (v tip/V_w), θ is the blade pitch angle in degrees.

In this wind turbine model the aerodynamic power efficiency C_p depends on the actual pitch angle θ and the tip speed ratio λ .

The relationship between blade tip speed and generator rotor speed is a constant (λ) and it is defined as

$$\lambda = \frac{r*\omega}{V_w} \quad (2.41)$$

Where r is the rotor blade radius; ω is turbine angular speed; and is wind speed.

The pitch angle controller is shown in Figure 2.11 including the pitch control and pitch compensation. The block diagram to control of active power is also illustrated in Figure 2.11. The pitch controller, pitch compensator and drive train models are included in the block diagram.

In the diagram the voltage measured at the terminal of wind turbine, is the current injected from the wind turbine to the grid, is the wind turbine rotating shaft speed, is the wind speed, is the output electrical power measured at the terminal of wind turbine, is mechanical input power to the shaft, is the command power and is the pitch angle.

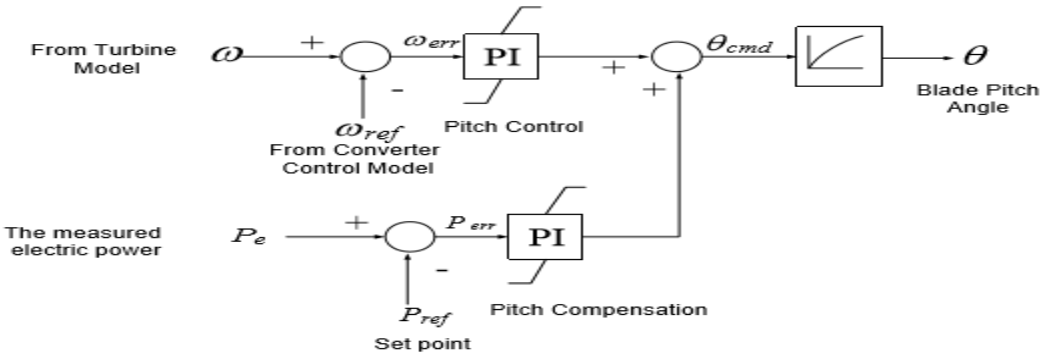

Figure 2.11: Pitch control and pitch compensation block diagram

Drive Train Model

In stability analysis, when the system response to heavy disturbances is analyzed, the drive train system must be approximated by at least a two-mass spring and damper model. This yields a more accurate response of the wind turbines dynamic behavior during fluctuating wind conditions or during grid faults.

The idea of using a two-mass mechanical model is to get more accurate response from the generator and the power converter during grid faults and to have a more accurate prediction of the impact on the power systems. The RSC and GSC reactive power controllers comprise of two control schemes: a slow controller and fast current controller. In terms of the GSC an additional droop is implemented within the slow controller, since both controllers control the reactive power at the point of common coupling (PCC).[10]

2.4.1 Wind Power Plant Voltage Control

Since the wind energy is renewable and environmental natural resource, the utilization of wind power plant increased quickly. Wind power constitutes the renewable generation technology which has experienced the fastest growing among all types of renewable generation technologies currently investigated (Erlich, I. Winter, W. and Dittrich, A. (2006), Rueda, J.L. and Shewarega, F. (2009).Since integration of large DFIG wind power plant is the concern of this thesis, its characteristics must be considered here. The basic structure of DFIG is shown in Figure 2.12.

According to Grid Codes, active power (P) and reactive power (Q) should be controlled at the point of common coupling (PCC), which is usually located at medium or high voltage side of the wind power

plant transformer. Therefore the wind power plant controller can be installed at the PCC, as shown in Fig. 2.12 (Bluhm, R. and Fortmann, J. (2010)). [17]

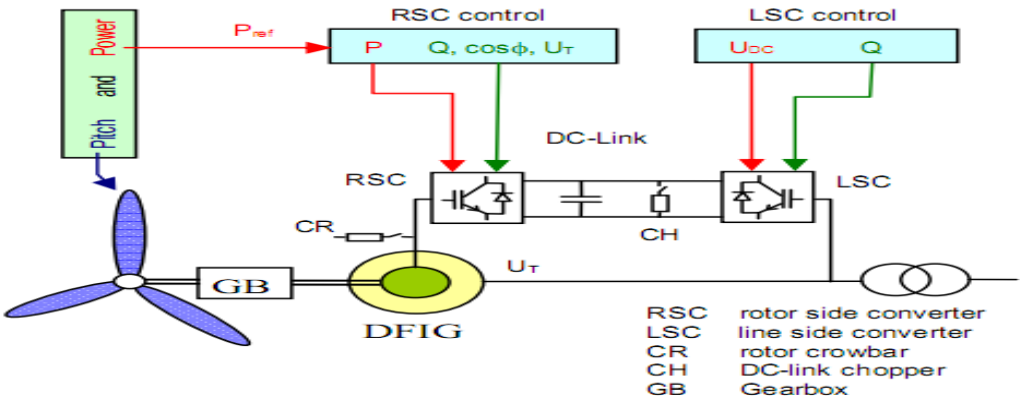

Figure 2.12: Typical layout of a DFIG [10]

2.5 Wind Power Generation and Power System Stability

In most countries, the amount of wind power generation integrated into large-scale electrical power systems is only a small part of the total power system load. However, the amount of electricity generated by wind turbines (WTs) is continuously increasing. Therefore, wind power penetration in electrical power systems will increase in future and will start to replace the output of conventional synchronous generators. As a result, it may also begin to influence overall power system behavior. WTs use generators, such as squirrel-cage induction generators (IGs) or generators that are grid-coupled via power electronic converters. The interactions of these generator types with the power system are different from that of a conventional synchronous generator. As a consequence, WTs affect the dynamic behavior of a power system in a way that might be different from that of synchronous generators. Therefore, the impact of wind power on the dynamics of power systems should be studied thoroughly in order to identify potential problems and to develop measures to mitigate those problems.

In grid impact studies of wind power integration, voltage stability is one of the power system stability problems that is the main interest of this thesis. Voltage stability deterioration is mainly due to the large amount of reactive power absorbed by the WTs during their continuous operation and system contingencies. The various WT types presently in use behave differently during grid disturbances. Induction generators consume reactive power and behave similarly to induction motors for the duration of system contingency and will deteriorate the local grid voltage stability. Also, variable-speed wind turbines (VSWTs) equipped with doubly fed induction generators (DFIGs) are becoming more widely

used for their advanced reactive power and voltage control capability. DFIGs make use of power electronic converters and are, thus, able to regulate their own reactive power so as to operate ata given power factor or to control grid voltage. But, because of the limited capacity of a pulse-width modulation (PWM) converter [11], the voltage control capability of a DFIG cannot match with that of a synchronous generator. When the voltage control requirement is beyond the capability of a DFIG, the voltage stability of the grid is also affected[12].The penetration of wind farm to electrical power systems also influences the system operation point, the load flow of real and reactive power, nodal voltages and power losses.

Voltage stability is concerned with the ability of a power system to maintain acceptable voltages at all buses in the system under normal conditions and after being subjected to a disturbance. A power system is said to have entered a state of voltage instability when a disturbance increase in load demand, or when change in system condition causes a progressive and uncontrollable drop in voltage. The main factor causing instability is the inability of the power system to meet the demand for reactive power. [13]

Many of power system faults are cleared by the relay protection of the transmission system either by disconnection or by disconnection and fast reclosure. In all the situations the result is a short period with low or no voltage followed by a period when the voltage returns. A wind farm nearby will see this event. In early days of the development of wind energy, only a few wind turbines were connected to the grid. In this situation, when a fault somewhere in the lines caused the voltage at the wind turbine to drop, the wind turbine was simply disconnected from the grid and was reconnected when the fault was cleared and the voltage returned to normal. Because the penetration of wind power in the early days was low, the sudden disconnection of a wind turbine or even a wind farm from the grid did not cause a significant impact on the stability of the power system. With the increasing penetration of wind energy, the contribution of power generated by a wind farm can be significant. If the entire wind farm is suddenly disconnected at full generation, the system will loss further production capability. Unless the remaining operating power plants have enough "spinning reserve, to replace the loss within very short time, a large frequency and voltage drop will occur and possibly followed by complete loss of power. Therefore, the new generation of wind turbines is required to be able to "ride through" during disturbances and faults to avoid total disconnection from the grid. In order to keep system stability, it is necessary to ensure that the wind turbine restores normal operation in an appropriate way and within

appropriate time. This could have different focuses in different types of wind turbine technologies, and may include supporting the system voltage with reactive power compensation devices, such as interface power electronics, SVC, STATCOM and keeping the generator at appropriate speed by regulating the power etc.[11],[14].

One of the challenges which has gained significant importance within the field of electrical power systems over the last years is reactive power control and voltage support from wind farms. Previously the voltage control in the transmission systems was mainly carried out by adjusting the reactive power production or absorption of central power plants, but as the amount of wind power is growing, the requirements for system services including voltage control delivered by wind turbines, and large wind farms in particular, are rising. So far reactive power control by wind farms has mainly been carried out by utilizing the reactive power capabilities of the wind turbines, but this strategy may not be the most feasible solution when taking into account the new grid code requirements. The optimal reactive power control strategy is influenced by factors like the reactive power capabilities of the wind farm, the on load tap changers of transformers and possible implementation of compensating devices. [15], [16].

2.6 Wind Power Integration and Grid Connection Requirements

Integrating a wind farm in an electrical network poses a significant challenge to the grid. Until some years ago, wind farms were allowed to disconnect from the grid during a disturbance in the grid since, most grid codes did not require wind turbines to support the power system during a grid disturbance. This has changed significantly, due to the addition of large amounts of installed wind power capacity. The impact varies with the strength of the grid and the size of the wind farm. As the wind farm capacity grows, grid integration issues may arise, as increasingly large amounts of electricity are fed into networks, either in distribution or transmission systems.

The disconnection of a large wind farm would result in a significant loss of generation that could cause some stability problems to the network. Nowadays, transmission system operators require for wind farms to stay connected under certain disturbances in the grid. As established in most grid codes, only under certain circumstances shall wind farms be disconnected from the grid following a grid fault, remaining otherwise connected in order to assist in the stabilization of the grid frequency or the voltage during fault, providing voltage back-up[7].The attention in these requirements is drawn to both the wind turbine fault ride-through capability and the wind turbine grid support capability, i.e.

their capability to assist the power system by supplying ancillary services are generally regulated in grid codes. The ancillary services represent a number of services required by the power system operators, such as voltage control, in order to secure safe and reliable grid operation. Fault ride-through capability addresses primarily the design of the wind turbine controller in such a way that the wind turbine is able to remain connected to the network during grid faults (e.g. short circuit faults). The effect of wind farm integration in the power system depends on both the power system design to which the wind farms are connected and the wind farm control ability to fulfill the grid requirements. This ability depends on the wind turbine/wind farm technology [9].

2.6.1 Performance Requirements of Wind Farms Connected to Ethiopian Grid

In the past the wind farms were disconnected from the grid following a grid fault and then there were no requirements for wind farms to contribute in voltage stability .Such wind farms usually had small power ratings. Recently, in Ethiopia wind turbines grow in size. Large wind farm like Adama II consisting several units of wind turbines are connected together to make wind farms with high power rating. As the wind farm power rating is higher disconnection of large wind farms from the grid during disturbance will lead to loss of large amount of power from the grid.

Therefore it is necessary to define the performance requirements in operation of wind farms connected to the Ethiopian grid which have or could have an impact on the reliability, security and adequacy of supply of the Eastern Africa Power Pool (EAPP) Interconnected Transmission System.

Wind turbine generating plants do not have the same characteristics as conventional generators and alternative provisions are required. Grid codes, determining the requirements about grid connection of wind farms, have been developed to fulfill one of the objectives of this thesis.

The most common grid code (international grid code) requirement encountered in the majority of new grid codes concerning wind farm integration are briefly described below:

Voltage and Reactive Power Regulation

Voltage regulation is essential for reliable system operation and requires some reactive capability in order to perform. Voltage regulation and reactive power performance of a WF will be assessed at the low voltage side of the transmission step-up transformers, which is the same as the collector buses at a WF. All reactive power requirements are based on the rated collector buses voltage. The WF must be able to regulate the system voltage both under normal and system disturbance conditions.

Active Power Regulation

Active power regulation is the ability of wind turbines to regulate their active power outputaccording to system requirements. Active power regulation in the grid codes include activepower control modes, which limit the maximum active power, balance the active power output, and define the ramp rates in the upward or downward direction. The rate at which the power is ramped should not cause significant power surges. Furthermore, it is required from wind farms to regulate their active power output in accordance with the frequency deviations. Although the power output of wind turbines fed into the grid is independent of the frequency of the grid, the active power controller must take the requirement of the grid into account. [4]

According to the [4, 20] and also on the basis of the experiences of other countries, the following active power control requirement may be adopted for the Ethiopian wind farm.

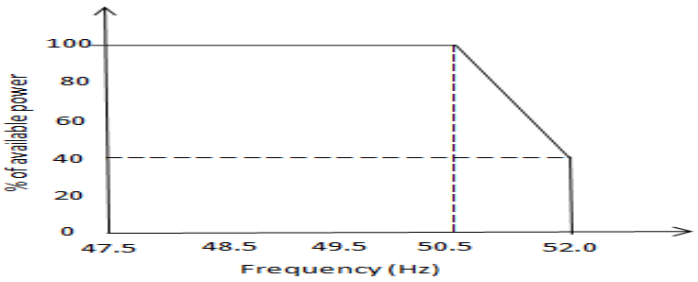

Figure 2.13: Active power output variation of wind farms with respect to frequency

“The power control mainly concerns the top right part of the curve in Figure 2.13 when the frequency increases above 50.5 Hz. The reason is that the active power response of wind farms to frequency should be such that the power injection in to the grid is limited to frequencies above nominal. Furthermore in order to avoid extreme increase in active power within a short period of time the active power gradient must be constrained. For example, the German grid code imposes the reduction of active power of wind farms when frequency exceeds the value 50.2 Hz with a gradient of 40% of the available power of the wind turbines/ Hz. The same can be adopted for the Ethiopian wind farms but with the reduction of active power of wind farms when frequency exceeds the value 50.5 Hz and the reduction of active power with a gradient of 33.3%. [4]”

Fault Ride Through Capability

Fault ride-through (FRT) capability is one of grid code requirements for an integrated wind farm that refers to the ability of a generating plant to remain connected during system voltage disturbance. i.e. the requirement for the wind farm to stay connected to the grid during the disturbance, thus contributing to

the reestablishment of the normal operation. The fault ride through capability of the wind turbines in the wind farm is guaranteed by the under/over voltage disconnection relays of the wind turbine generators. These devices allow the operation of the wind turbines even when the terminal voltage decreases. This capacity of "riding through" a fault is limited to defined voltage dips and fault durations. So, and according to fault ride through characteristic (as defined in Figures 2.14), the wind turbine will only trip if the fault that occurs across the terminals of the machine are outside the defined limits.

A typical FRT limiting curve is shown in Figure 2.14. During dips above the limit line wind turbines must remain in operation, but they can disconnect in the event of dips below the limit line. [4]

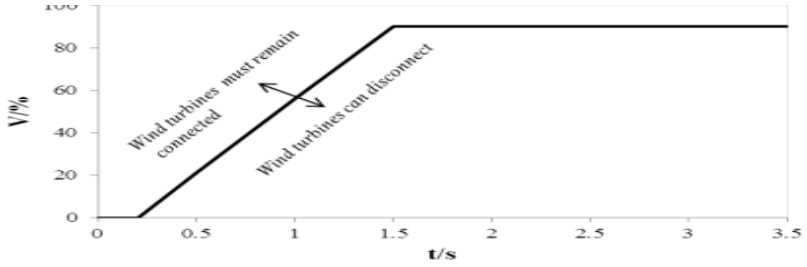

Figure 2. 14: Typical limit curve for fault ride-through requirements

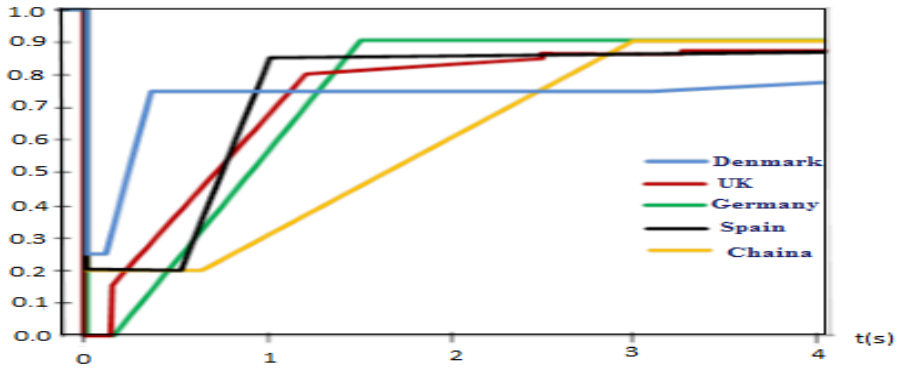

Figure 2. 15: Fault ride-through requirements of various grid codes

Figure 2.15 presents FRT requirements of different countries in a single graph.Many countries are defining FRT requirements not only for the period of voltage dip but also for the time of voltage support by reactive power injection during recovery period. Table 2.1 presents a clear view of the main characteristics of the curves of Figure 2.15.

Table 2. 1: Characteristics of fault ride-through curves in various grid codes

Grid Code	Fault duration (ms)	Fault duration (cycles)	Voltage restoration (s)	Voltage restoration (s)	Min voltage level (% of V_{nom})
German (Eon.Netz)		150	1.5	1.5	7.5
UK	140	7	1.2	1.2	0
Denmark (<100 kV)	140	7	0.75	0.75	25
Denmark (>100 kV)	100	5	10	10	0
Spain	500	25	1	1	20
China	600	30			

Frequency Requirement

Increasing penetration of wind generation, and to a limited extent other RPPs, can increase the need for various kinds of reserves. The variability of their output requires higher levels of both planning and operating reserves to offset the greater chance of being or going off-line when needed. They also contribute little or no inertia to the system, increasing the need for frequency regulation, which may lead to a need for higher levels of regulating and spinning reserve. These factors shall be taken into account in establishing both planning and operating reserve requirements.

According to [20] which are in agreement with different country experiences the following frequency range in Table 2.2 is frequency limits in the Ethiopia Electric Transmission System (ETS) for Ethiopian wind farms.

Table 2. 2: Frequency ranges for Ethiopian wind farms

Operating conditions	Frequency Limits
Under normal operation	49.50HZ to 50.50HZ
Under system disturbance	49.00HZ to 51.00HZ
Maximum band under system fault	48.75HZ to 51.25HZ
Under extreme system operation or fault conditions	f<47.50 HZ or f> 51.50 HZ for upto 20 seconds

According to the frequency requirement in the Table 2.2, wind farms are required to be capable of continuous operation between 47.5 Hz and 51.5 Hz. Time limit is set for frequency ranges between 47.0 Hz to 47.5 Hz and 51.5 to 52.0 Hz. For frequency ranges lower than 47.0 (inclusive) and greater than 52.0 Hz (exclusive) fast automatic disconnection is imposed. The consequence of operation outside these limits may result in total black-out of the wind farms and even may damage wind turbines because any further deviation in frequency limits may initiate the load shedding relays to trip and

generation capacity would be lost. The loss of generation leads to further frequency deviation (decrease) which may end up with black-out. [4].

Frequency response can be achieved through decreasing RPP power output when frequency exceeds the upper bound of a specified acceptable frequency range, and by increasing RPP power output when frequency falls below the lower bound of the specified range. Thus, an RPP must operate at a level below its instantaneous available capacity, if it is to provide both upward and downward frequency regulation capability.

For frequencies below 47.00 Hz, a generating plant shall be capable of operating for at least 200 ms. The RPPs shall remain connected to the Ethiopia ETS during rate of change of frequency of values and including 1.0 Hz per second. For frequencies above 52.00 Hz, a generating plant must disconnect as indicated in Table 2.3.

Table 2.3: Frequency Limits in the Ethiopia Electric Transmission System

Frequency Limits	Duration
49.50 Hz to 50.50 Hz	Continuous operation (normal)
49.00 Hz to 51.00 Hz	For duration of at least 60 minutes
48.00 Hz to 51.50 Hz	For duration of at least 30 minutes
47.50 Hz to 51.50 Hz	For duration of at least 3 minutes
<47.50 Hz or >51.50 Hz	For duration of at least 20 seconds
<47.00 Hz for more than 0.2 sec	May disconnect
>52.00 for more than 4 sec	Must disconnect

The requirements for remaining connected during a frequency disturbance apply when the rate of change of frequency is within certain limits. Outside these limits, the unit is not obliged to remain connected. [20]

2.7 Reliability of Operation of the WF on System Weak Points

Generally the strength of a power system at a certain point is determined by the short circuit ratio which is directly proportional to the fault level. The fault level is inversely proportional to the impedance between source and load. The magnitude of the impedance will therefore determine whether the system is strong or weak. In weak power systems voltage fluctuations will easily take place and it will be severe in case of the integration of large wind farms. Therefore the continuous operating voltage range for each nominal network voltage level must be specified for safe connection of wind farms.[4]Therefore the voltages on the EAPP Interconnected Transmission System shall normally be maintained within the limits set out below:

1. Operating voltage range of 0.95 to 1.05 per unit in steady state normal conditions for nominal voltages used in the EAPP Interconnected Transmission System namely 500 kV, 400 kV, 230 KV, 220 kV, 132 kV, 110 kV and 66 kV,
2. Operating voltage range of 0.90 to 1.10 per unit after any single contingency, and
3. Operating voltage range of 0.85 to 1.20 per unit after any multiple contingency or severe system stress as indicated in Table 2.4.

Table 2. 4: Voltage Range/Limits

Operating Conditions	Voltage Limits
Normal	0.95 - 1.05
Contingency (N-1)	0.90 – 1.10
Multiple Contingency	0.85 – 1.20

Generally, the voltage range varies from country to country depending on the strength of the transmission system and the level of the voltage.

Based on the above facts as well as other countries experiences the Ethiopian wind farms shall be able to deliver their rated power when the voltage at the grid connection point continuously remains within following ranges: [4]

2.8 Steady State and Dynamic Reactive Power Capability

The intent of voltage regulation requirements is to achieve reasonable response to disturbances as well as a steady-state regulation of +/- 0.5% of the controlled voltage. Figure 4.5 illustrates the reactive power requirements for a WPF[21].

Available Reactive Power for Voltage Support

Voltage regulation and reactive power capability from a WPF(Wind Power Farm) can vary with technology. Some WPFs may utilize reactive capability from the WTGs, other WPFs may use dynamic var devices, and some WPFs may be aggregated with synchronous generators. Some WPFs may wish to connect to a common transmission substation and may wish to consider aggregating voltage regulation and reactive power from a single source for multiple WPFs .

As voltage regulation requires some reactive power capability these two (2) requirements (voltage regulation and reactive power) are specified in this section. [21]

The maximum and minimum active and reactive power limits(Max and min limit in voltage regulator) according to the capability curve of generators are among the most important input data that must be specified during data preparation[Appendix D].The capability curve for a 1.5 MW GE wind turbine generator is shown in Figure 2.16.

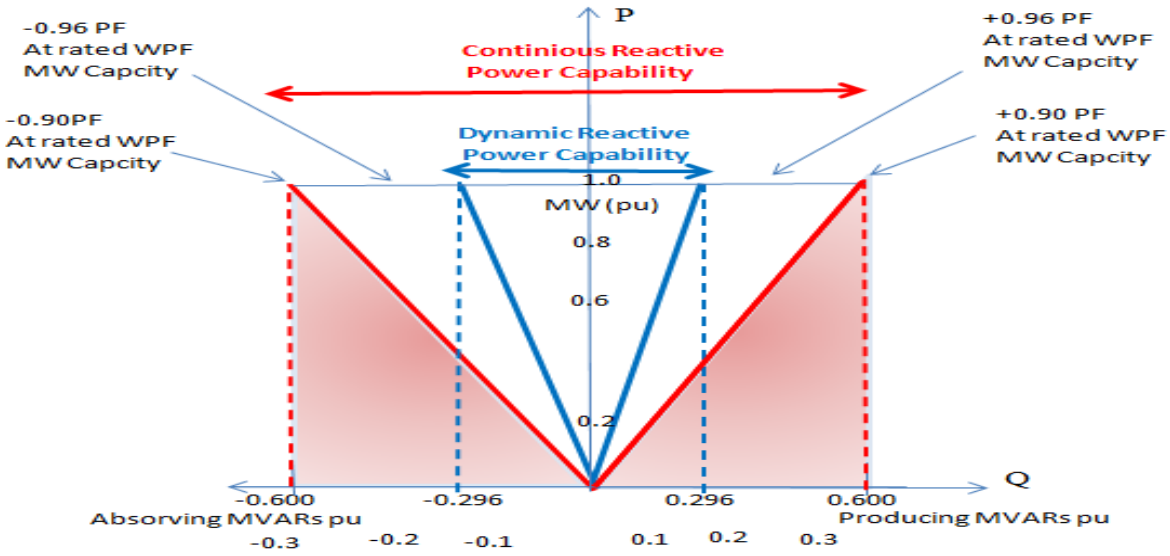

Figure 2.16: Reactive Power Capability Curves for a 1.5 MW GE wind turbine generator

From Figure 2.16,it can be observed that a WPF reactive capability shall meet or exceed +0.90 Power Factor (PF) to -0.90 PF based on the WPF aggregated MW Output.The steadystate range is 1.8.Therefore continuous reactive power capability can be aggregated to satisfy the +0.90 PF and the -0.90 PF requirement.[21]

Dynamic Reactive Power Capability

From Figure 2.16it can be observed also that a WPF's dynamic reactive power capability shall meet or exceed +0.96 Power Factor (PF) to -0.96 PF based on the WPF Aggregated MW Output. The dynamic range (PF range) is 1.92 so Dynamic range exceed the steady-state range.

Reactive Power Capability without Wind Generation

Manufacturers offer different options for var generation by DFIG based wind turbines in steady state. Figure2.17shows that the reactive power generation range by a better utilization of the reactive power capability of the DFIG .This indicates that,the DFIG based wind turbines can supply reactive power duringall the time when active power is avilable.

Voltage support continues without active power generation even following trips that isreactive power even without wind,when the WPF VRS must be in service at any time the WF is electricallyconnectedto the TS regardless of MW output from the WPF.

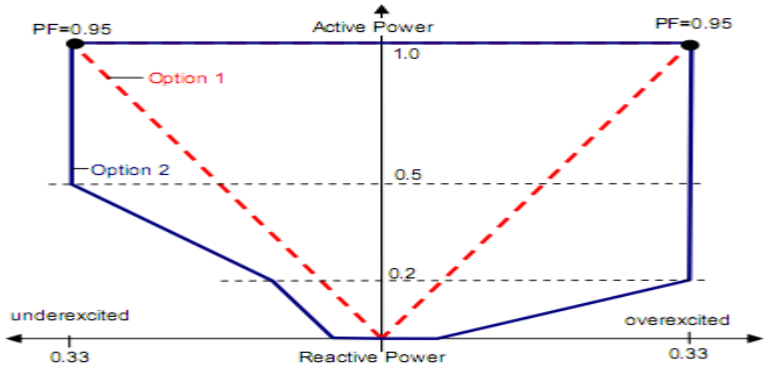

Figure 2. 17: Reactive power characteristics of DFIG base wind turbines [22]

2.9 PF Requirements and Reactive Power Capability

In steady-state, Type-1 and Type-2 WTGs are induction generators, and as such, the steady-state power factor is approximately 0.9 leading (absorbing VARs). Capacitors are added at the generator terminals to correct the power factor. Several capacitor stages are used to maintain steady-state power factor close to unity over the range of output of the WTG. However, these WTGs do not have the ability tocontrol reactive power dynamically. STATCOMS or SVCs are usually needed for Type-1and Type-2 WPPs to compensate for reactive power losses in the collector system lines and transformers, and meet reactive control requirements at the point of connection. Type-3 and Type-4 WTGs, on the other hand, have the capability of absorbing or sourcing reactive power. In actual implementation, each Type-3 or Type-4 WTGs follow a power factor reference that can be adjusted by a plant-level supervisory controller, possibly dynamically, to achieve control objective at the point of connection (voltage or reactive power control). Faster-acting controls local to the WTG can override the power factor reference to avoid exceeding converter current and terminalvoltagelimits. Depending on the plant design, additional reactive power support equipment may be added to meet connection reactive control and voltage ride-through requirements. This is especially true in weak interconnections.[23].Therefore, PFrequirements primarily met by turbine reactive power capability or it is augmented by mechanicallyswitched shunt devices.

Depending on the structure of the grid, transmission system operators (TSO) change the desired power factor range for different voltages.

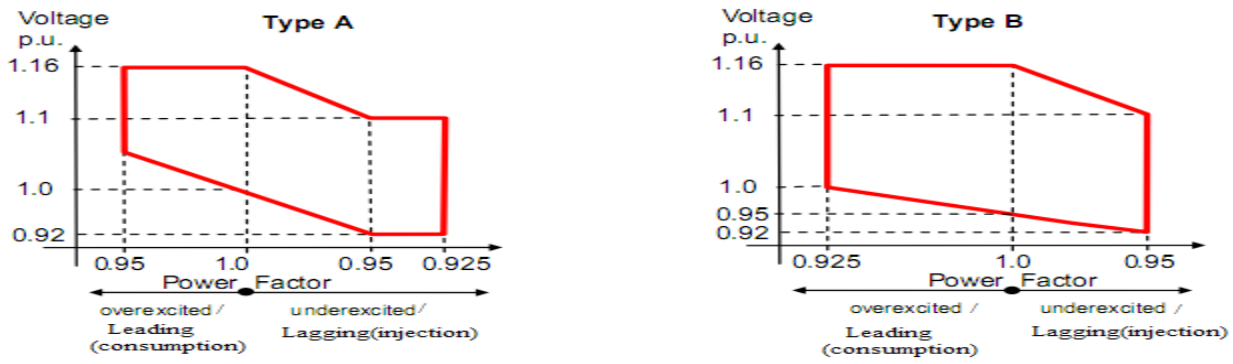

Figure 2.18: Power-factor requirements of two different TSOs for generating units connected to the high voltage grid.

The requirements have to be fulfilled at the PCC, which offers several options to provide the desired power factor. “The transmission system operator shall adjust the voltage by signaling a voltage set point for the voltage at the connection point. The voltage regulation system shall act to regulate the voltage at this point by continuous modulation of the reactive power output within its reactive power range,and without violating the voltage step changes [24]”

Therefore,the operation according to Figure 2.18enables wind farms to consume large reactive power during lower voltage and inject large reactive power during higher system voltage. When system voltage is lower higher leading power factor is required but, lower lagging power factor is required during higher system voltage.[4]

2.10 Operating Mode and Operation Control of Wind Power Plants

The controllability demands on future large WPPs will likely be higher than for conventional units today. If the power system has a large proportion of stochastically generating units such as wind power, this might decrease system stability.

Considerations due to the impact on the transmission network lead to more specific requirements towards the wind turbine manufacturers, operators and utilities. It is not only the functions within the WPP that will be affected when the impact on transmission network must be better controlled.Or else,the safety margins and reliability for existing power systems decrease as a consequence of the increasing the share of installed WPPs.[25]

Voltage, Var and PF Control Modes of Operation

Modern wind power plants have good ability to quickly control reactive power. The reactive power capability of a wind turbine with full scale power converter is limited by the maximum converter current and will therefore depend on the instantaneous values of the local voltage and the active power produced. In a DFIG, the reactive capability will also depend on the actual turbine speed.

Some wind power plants will have separate equipment, e.g., FACTS devices, for reactive power compensation that can add to the capability. The reactive consumption or production of the collection grid must be taken in to account.

There are several modes for reactive power control:

- Reactive power set point, the desired reactive power is given directly.
- Power factor control, the desired ratio between active and reactive power are given.
- Voltage control, the wind power plant tries, by adjusting the reactive power, to keep the voltage at an arbitrarily chosen point in the system, normally the local voltage close to a given set point.

Traditionally voltage control has been avoided in wind power plants since it increases the probability that an unintended island situation will be stable.

The steady-state and dynamic characteristics of DFIG WTGs are dominated by the power converter. The converters allow the machine to operate over a wider range of speed, and control active and reactive power independently. This means that DFIG has the capability to participate in steady-state and dynamic volt/var control. [23]

The operational mode of the WF in the grid model used for this thesis work is voltage control mode" (PF is not unity).

2.11 Coordinated Wind Turbine and Wind Plant Supervisory Control Structure

The technology that is applicable in operation control of integrated WFs is WindSCADA system provides a broad set of intuitive tools for operation and maintenance of the wind power plant. One of the tools is Operator/Technician Maintenance Tools:uses the WindSCADA viewer application used for operation and maintenance of the equipment. This viewer is accessible from any wind turbine as well as from the operations and maintenance building. It also can be used remotely with a secure internet connection or a telephone line.[26]

2.11.1 Regulation of Wind Power Plant Reactive Power

The supervisory control will instruct individual machines to adjust their reactive power output in order to regulate system voltage; normally at the point-of-interconnection or at PCC.

According to Grid Codes, active and reactive power should be controlled at the point of common coupling (PCC). Therefore the wind power plant controller can be installed at the PCC, as shown in Figure 2.19 (Bluhm, R. and Fortmann, J. (2010))[17].Hence,the total wind plant reactive power can be regulated through control of individual turbines.

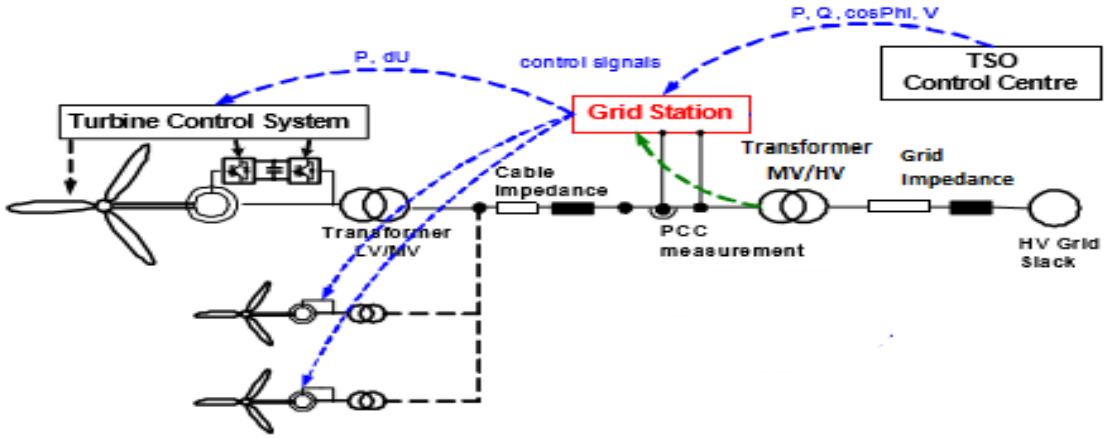

Figure 2.19: Wind power plant control.

“The wind power plant controller can receive active and reactive power set points from the control centre of the system operator. A classical control mode is a power factor set point at the PCC controlled by the wind power plant controller sending reactive power set points to all turbines of inside the plant. In case of voltage control, there is a voltage set point at the PCC. (Bluhm, R. and Fortmann, J. (2010)). Optionally, external reactive power compensation can be connected to the PCC and can be controlled by the wind power plant controller. This is only necessary, if the reactive power range of the wind turbine is not sufficient to fulfill the requirements at the PCC.

The basic function of a voltage controller is to calculate the set point for reactive power depending on the voltage. A general block diagram for a proportional characteristic is shown in Figure 2.20. The voltage measurement (U_meas) is subtracted from the voltage set point (U_set) to calculate the voltage deviation (ΔU). This deviation is multiplied by the proportional control factor KVC to calculate the reactive power set point (Q_set). Depending on the desired control characteristic, a reactive current set point (Iq_set) can also be used (Bluhm, R. and Fortmann, J. (2010)).

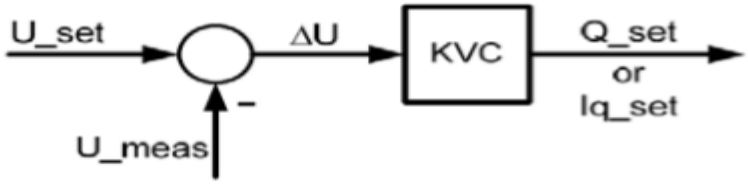

Figure 2.20: Proportional voltage control block diagram

The voltage control can be implemented in both turbine level (local) and the wind power plant level (central) and the detailed description can be found in (Bluhm, R. and Fortmann, J. (2010)). A combination of the central and local voltage control can combine their favorable characteristics with benefit for grid stability. The continuous voltage control at the turbine level delivers a very fastresponse to deep voltage drops and also to small voltage deviations inside the standard operation range (Bluhm, R. and Fortmann, J. (2010)). The combination with voltage control at the wind power plant level ensures an exact adjustment of the required reactive power value at the grid connection point. A stable control of the combined controller can be guaranteed because the time constant of the subordinate local control is more than 10 times faster than the time constant of the wind power plant controller (slower plant control). Settings such as slope or response time of the combined voltage control can be easily adapted to achieve the desired characteristics required at different connection points or in different countries (Bluhm, R. and Fortmann, J. (2010))."[17]

2.12 Operating Principle of DFIG Control

2.12.1 DFIG Control in Normal Operation

The DFIG control structure, illustrated in Figure2.21, contains the electrical control of the power converters, which is essential for the DFIG wind turbine behavior both in normal operation and during fault conditions. Power converters are usually controlled utilizing vector control techniques [9], which allow decoupled control of both active and reactive power. In normal operation the aim of the RSC is to control independently the active and reactive power on the grid, while the GSC has to maintain the DC link capacitor voltage at a set value regardless of the magnitude and direction of the rotor power and to guarantee converter operation with unity power factor (zero reactive power).

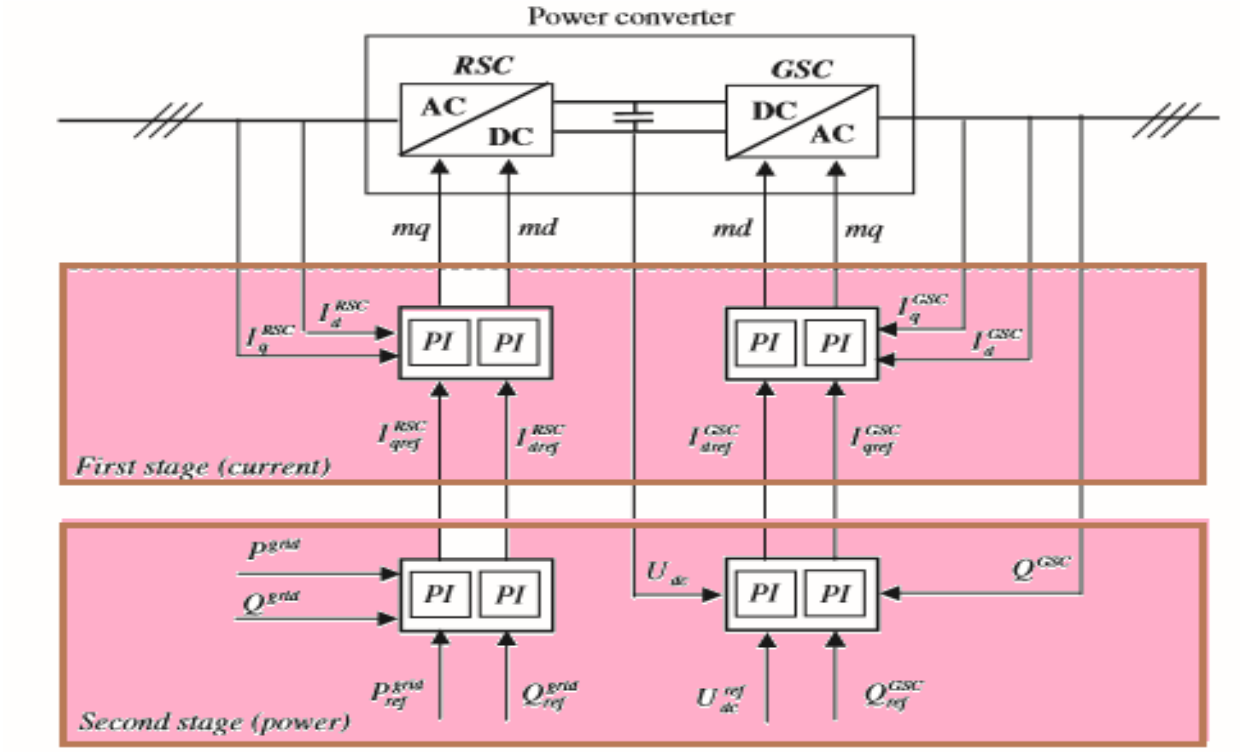

Figure 2.21: DFIG control structure – normal operation.

As illustrated in Figure 2.21, both RSC and GSC are controlled by a two stage controller. The first stage consists of very fast current controllers regulating the rotor currents to reference values that are specified by a slower power controller (second stage). The control performance of the DFIG is very good in normal grid conditions. DFIG control can, within limits, hold the electrical power constant in spite of fluctuating wind, storing thus temporarily the rapid fluctuations in power as kinetic energy.

2.12.2 DFIG Control under Grid Faults

The technical specifications defined by the power system operator require that the wind turbines remain connected to the grid during a grid fault. The wind turbines have to behave as active components and thus support the grid during the fault. The voltage grid support capacity of a DFIG depends on the quantity of reactive power injection but also on the transmission line characteristic from the generator to the connection point with the power system.

During a grid fault the tasks of the rotor-side and grid-side converters can be changed depending on whether the protection system (i.e. crowbar) is triggered or not. In the case of less severe grid faults or reactive power unbalance in the system, and when the crowbar is not triggered, the rotor-side converter and the grid-side converter have the same tasks as in normal operation. In such situations the rotor-side

converter is not blocked and therefore can still independently supply active and reactive power to the grid. On the other hand, in the case of a severe fault, when the crowbar is triggered, the rotor-side converter is blocked, its controllability is lost and therefore its task to support the grid with reactive power is taken over by the grid-side converter. The grid-side converter does not block at a grid fault but continues its operation as a STATCOM as long as the rotor-side converter is blocked. When the crowbar is removed, the rotor-side converter starts to operate and the grid-side converter is set again to be reactive neutral. At a severe grid fault, if the generator is not tripped, the DFIG wind turbine has to continue its operation with a short-circuited generator, trying to sustain grid connection. Over speeding of the wind turbine is prevented by the pitch control. [9]

The third control stage is added to the normal operation control structure consisting of two control stages (i.e. current and power control stages) as illustrated in Figure 2.22. This third (voltage) control stage provides the reference signals for the second-stage controllers in the case of fault operation. This control stage contains three additional controllers, namely a damping controller, a rotor-side converter (RSC) voltage controller and a grid-side converter (GSC) reactive power boosting. It has as its task to improve the controllability of the DFIG for grid voltage support in uninterrupted operation during a grid fault. The damping controller and the RSC voltage controller provide the active power Pgrid ref and reactive power Qgrid ref references for the rotor-side converter respectively, while the GSC reactive power boosting defines the reactive power reference for the grid-side converter.

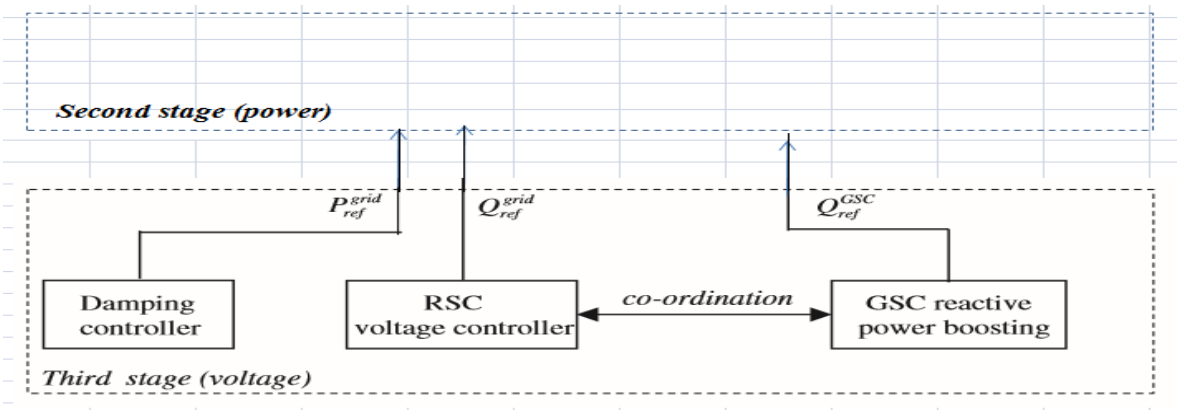

Figure 2.22: DFIG control structure – Under Grid Faults

The damping controller has as its task to damp the torsional excitations that are excited in the drive train owing to the grid fault. Different control schemes can be applied to damp these oscillations. The rotor-side converter is blocked at the moment when the crowbar is triggered by either an over current in the rotor circuit or an overvoltage in the DC link. In such a situation, its controllability is lost and

therefore its task to support the grid with reactive power is taken over by the grid-side converter. The grid-side converter does not block at a grid fault but continues its operation as a STATCOM as long as the rotor-side converter is blocked. Its capability to control independently the active and reactive power is lost when it is actually most needed, namely during and shortly after the fault.

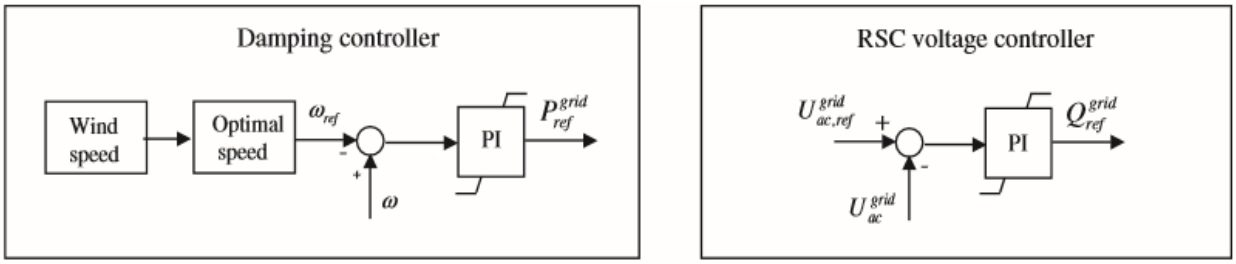

Figure2.23: Damping controller and RSC voltage controller

As illustrated in Figure 2.23, the PI damping controller produces the active power reference signal Pgrid ref for the rotor-side converter control based on the deviation between the actual generator speed and its reference. The speed reference is defined by the optimal speed curve at the incoming wind. The damping controller is tuned to actively damp the torsional oscillations excited at a grid fault in the drive train system. [8, 9]

"[(Akhmatov V, 2002)]shows that absence or insufficient tuning of this PI controller may lead to self-excitation of the drive train system and to a risk of grid power tripping as protection against vibrations in the mechanical construction. The pitch control system is not able to damp the torsion oscillations, because of several delay mechanisms in the pitch. The pitch control damps the slow frequency variations in the generator speed, while a damping controller has to damp the fast oscillations in the generator speed."[8]

The RSC voltage controller provides the reactive power reference signal Qgrid ref for the rotor-side converter when the protection system is not triggered. As illustrated in Figure 2.23, the RSC voltage controller controls the grid voltage at the point of common coupling as long as the rotor-side converter is not blocked.

As illustrated in Figure 2.22, a reactive power boosting added to the cascaded control loops of the grid-side converter generates a reactive power reference signal QGSC ref for the reactive power control loop of the grid-side converter. The implemented reactive power boosting provides a zero reactive power reference when the rotor side converter is active and a maximum reactive power of the grid-side converter (1p.u) as reference value when the rotor-side converter is blocked. This means that the grid-

side converter contributes with its maximum reactive power capacity for grid support under severe grid faults. When such supplementary reactive power control by the grid-side converter is applied, a co-ordination control between the rotor-side and grid-side converters is needed. During the grid fault, some of the controllers have to be disabled, while others are enabled. Controller start-up must be treated with some care to avoid discontinuities and to minimize the loads on the wind turbine. Such discontinuities could eventually lead to prolonged transients and, implicitly, to subsequent operations of the crowbar protection. [8,9].

2.12.3 DFIG Protection Schemes

For wind power generation systems, the doubly-fed induction generator (DFIG) currently dominates with its variable wind speed tracking ability and relatively low cost compared to full-rated converter systems. Significant disadvantage of the DFIG is its vulnerability to grid disturbances because the stator windings are connected to the grid through a transformer and switchgear with only the rotor-side buffered from the grid via a partially rated converter. Therefore, to protect the wind farm from interruptions due to grid and WF faults, a crowbar protects the induction generator and associated power electronic devices. This protection system is widely used in industrial applications. [10]

Over-Current Protection (Crowbar)

The wind farm should have fault-ride-through capability. However, riding through grid faults with DFIG will lead to high peak currents in the rotor and high power into the DC circuit. Thus the rotor and rotor-side converter need to be protected against over-current and over voltage. In order to protect against over current and over voltage, a DC-chopper parallel with DC-link and an AC-crowbar installed in the rotor circuit are used.

When there is a short circuit in the grid, the voltage at the terminal of DFIG goes down almost immediately and it will cause high transient rotor current. One possible solution to avoid over-current is to use a rotor over-current protection, a so-called crowbar. The crowbar is connected in parallel with the rotor-side converter as shown in Figure 2.5. The crowbar deactivates the rotor-side converter and short-circuits the rotor winding, whenever the rotor current exceeds the maximum limit value. When the grid fault is cleared, the rotor-side converter is restarted.

The crowbar protection is specific to doubly fed induction generators and, as illustrated in Figure 2.6, is external rotor impedance. It is coupled via the slip rings to the generator rotor instead of to the converter and has a rotor current-limiting function. When the crowbar is triggered and the rotor is short

circuited over the crowbar impedance, the DFIG behaves as a squirrel cage induction generator (SCIG) with an increased rotor resistance. In this case, as the rotor-side converter is deactivated and bypassed, the controllability of active and reactive power gets lost during fault detection. This implies that the magnetization of the generator, which in normal operation is done over the rotor circuit by the rotor-side converter, must in the case of a fault be done over the stator. Since the grid-side converter is not directly coupled to the generator windings, there is no need to disable this converter too. The grid-side converter can therefore be used as a STATCOM to produce reactive power (limited, however, by its rating) during faults. Note that the connection of the external impedance improves the torque characteristic and thus the dynamic stability of the induction generator during grid faults. [2, 10]

DC-chopper

A braking resistor (DC-chopper) is connected in parallel with the DC-link capacitor to limit the overcharge during low grid voltage. This protects the IGBT from over-voltage and can dissipate energy, but this has no effect on the rotor current. [10]

2.12.4 Voltage Control of DFIG Wind Turbines

In general, different possible voltage control strategies exist for regulating voltage at the terminals of the DFIG. The voltage can in principle be controlled by either the rotor-side converter or the grid-side converter or by both of them. The objective is to enhance the DFIG wind turbine capability for uninterrupted operation during grid faults. A co-ordinated voltage control of the DFIG wind turbine for uninterrupted operation during a fault is implemented. It is based on a strategy whereby both DFIG converters, i.e. rotor-side converter (RSC) and grid-side converter (GSC), are used in a co-ordinated manner. The idea is that the RSC is used as the default reactive power source, while the GSC is used as a supplementary reactive power source when the protection system is triggered and, as a result, the RSC is blocked. During a grid fault the tasks of the rotor-side and grid-side converters can be changed depending on whether the protection system (i.e. crowbar) is triggered or not.

The control performance of the DFIG is excellent under normal grid conditions, allowing active and reactive power changes in the range of few milliseconds owing to the presence of power electronics. However, since the stator in a DFIG is directly connected to the grid, and the rotor interfaces through a partial-scale power converter, this concept is more sensitive to grid disturbances compared with the full-scale power converter concept.

The concern with the DFIG is usually the fact that large disturbances lead to large fault currents in the stator due to the stator's direct connection to the grid. Because of the magnetic coupling between stator and rotor and the laws of flux conservation, the stator disturbance is further transmitted to the rotor. High voltages are thus induced in the rotor windings that in turn cause excessive currents in the rotor as well. High stator currents may be advantageous for the co-ordination of the protection in the grid. They guarantee that the fault current level is high enough to trip circuit breakers in the faulty part of the grid and thus disconnect the turbine. However, as the stator is directly connected to the grid, the converter has only partial control over the generator during grid faults. It reaches its limits quickly and as a consequence loses the control of the generator. The results are both high rotor currents and voltages during grid faults. Furthermore, the surge following a fault includes a 'rush 'of power from the rotor terminals towards the converter. As the grid voltage drops at the fault moment, the grid-side converter is not able to transfer the power from the rotor-side converter further to the grid; instead, the additional energy goes into charging the DC bus capacitor and thus the DC bus voltage rises rapidly. A suitable protection system for the DFIG converter is therefore necessary to break the high currents and the uncontrollable energy flow through the rotor-side converter to the DC link and thus to minimize the effects of possible abnormal operating conditions. The protection system monitors different signals such as the rotor current and the DC link voltage; when at least one of the monitored signals exceeds its respective relay settings, the protection is activated. A simple protection method is to short circuit the rotor through a device called a crowbar and disables the rotor converter control. Without such protection a DFIG wind turbine is not able to stay grid connected during a grid fault, as high transient currents can damage the power converter device. [9]

2.13 Performance of the Wind Farm in Steady State Operation

In steady state operation large wind farms have to fulfill the same requirements as existing large conventional power plants. These requirements are defined in grid codes, which every grid utility can modify individually.

When large-scale wind farms are connected to the transmission network ,these can affect the power flows and hence the node voltages,in the transmission network. Voltages are controlled mainly by large-scale conventional power plants. If their capability to control voltages within the transmission network is not sufficient to compensate the impact of the wind farm on the node voltages, again, the

voltage at some nodes can no longer be kept within the allowable deviation from its nominal value and appropriate measures have to be taken. [7]

It is mainly due to the fact that the wind farm creates a new capability to control the voltage at the vicinity of the PCC byinjecting or absorbing reactive power. This will of course depend on the wind speed situation. When there is enough wind, the real power will have priority and the reactive power needs to be curbed, which limits the operational flexibility. However, the long transmission line and the weakness of the link to the wider network restrict this benefit to the part of the network around the wind farm. [4]

2.13.1 Voltage and Reactive Power at POI in comparison with Conventional Power Plant

As a promising renewable alternative, the wind power is highly expected to contribute a significant part of generation in power systems in the future, but this also bring new integration related power quality issues, which mainly consist of voltage regulation and reactive power compensation. Wind power, as a rule, does not contribute to voltage regulation in the system. Induction machines are mostly used as generators in wind power based generations. Induction generators draw reactive power from the system to which they are connected. If system disturbances make voltage fluctuating, the point of interconnection (POI) is selected as a voltage control point and steady-state voltage without disturbances is selected as control object. Then reactive power output of wind farm is regulated dynamically to maintain voltage level at POI strategy for reactive power control of wind farm for improving voltage stability in wind power integrated region.

2.13.2 Voltage Fluctuation at POI as Wind Speed Varies

If the wind speed becomes either too low or too high, the wind turbine will stopautomatically. In the first case the turbine will be stopped in order to avoid a negativepower flow. In the next time, it will be stopped to avoid high mechanical loads. At lowwind speeds (3–4m/s) the active power is almost zero. The stop will be rather soft andthe impact on the voltage at the PCC will be small at such low wind speeds. The impactmay be larger at high wind speeds (greater than 25m/s) since the turbine produces atrated power on these occasions. If the turbine is stopped and the power decreases fromrated power to zero production, the voltage at the PCC will be affected.[7]

2.14 Performance of the Wind Farm in Weak Grid

The term ‘weak grid’ in a general context with or without wind turbines implies that the voltage at the point of common coupling (PCC) is not “stiffly” constant. The defining feature of a weak grid therefore is the poor voltage regulation at the PCC. Weak grids are found in remote places where the feeders are long, and are typically operated at medium voltage level.

In wind farms operating on weak grids are typically connected through dedicated medium voltage over headlines specifically dimensioned for the transport of the wind farm output. To compensate for the voltage drop on the impedance of the feeder linking up the wind turbine to the grid, the voltage at the terminals of the wind farm can be raised to a certain degree. But when the upper limit is reached, the excessive voltage can have a limiting effect on the power from the wind farm being absorbed by the grid at PCC. When wind farm is operated on weak grid, the poor voltage regulation at the PCC in combination with the fluctuating nature of wind power and stochastically changing system load can produce a voltage profile at the PCC and beyond, which can adversely affect the overall power quality in the system. One can consider control measures in the wind farm or compensation techniques at the PCC to improve the situation. [4]

CHAPTER 3

3 Mathematical Modeling and Analysis of Adama II Wind Farm

3.1 Introduction

The development of aggregated models of wind farms is also an important issue because, as the sizes and numbers of turbines on wind farms increase, representing wind farms as individual turbines increases complexity and leads to a time-consuming simulation which is not beneficial for stability studies of large power systems. For the aggregation of WTs, the models of several identical WTs (even in the incoming wind) are combined in a single turbine model with a higher rating. This aggregated model reduces computation and simulation times in comparison with those of a detailed model with different representations of tens or hundreds of turbines and their interconnections. [12]

“Within a wind power plant, there are a lot of diversities in the line feeder and the wind speed at each turbine. Line impedance in the line feeder connecting each wind turbine to the point of interconnection differs from each other. The wind speed experienced by one turbine can be significantly different from another turbine located at another part of the wind power plant. In new wind power plants, the wind turbines used is generally of the same type and supplied by the same manufacturer. Generally, a full system representation (FSR, where all turbines are represented) of a wind power plant shows the same behavior at the point of interconnection (POI) as wind power plant with a single turbine representation (STR) [27]”[30].

3.2 Wind Farm Aggregation

The collective behavior of a wind farm can be represented by single turbine representation (STR). Most frequently, the collector system is connected to a medium voltage of 12 kV-34.3 kV voltage level, where the wind turbines are connected to each other in a string (cluster) using underground cables. Each cluster may contain one or more groups of wind turbines. Each wind turbine is electrically attached to a unit transformer that steps up the generated terminal voltage to a medium voltage collector system. Then, the collector system is connected to a central substation transformer which in turn steps up the medium voltage to the transmission voltage level [27].

In the following derivations, it is based on equivalent circuit on the apparent power loss (i.e. real power loss and reactive power loss).In [27] equivalent circuit for the collector system the following assumptions are going to be considered,

1. The current injection from all wind turbines is assumed to be identical in magnitude and angle.
2. Reactive power generated by the line capacitive shunt is based on the assumption that the voltage at the buses is one per unit (1p.u).

Steps for Wind Farm Aggregation

Step 1: Equivalent Wind Turbine

According to [30], "reducing n number of wind turbines to a single wind turbine, the parameters from the equivalent machine is active power *Peq* in MW, the reactive power *Qeq* in MVAr and the apparent power *Seq* in MVA [28].The parameters are given by:

$Peq = n * P\text{MW}$ (3.1)

$Qeq = n * Q\text{MVar}$ (3.2)

$Seq = n * S\text{MVA}$ (3.3)

Where *n* is the total number of wind turbines in the wind farm."

Step 2: Equivalent Pad Mount Transformer

"The equivalence of unit transformer connected to turbine generator is made using the loss formula."[30].Consider the system given in Figure 3.1a which have three turbines and three unit transformers, to derive the equivalent impedance of pad mount transformer.

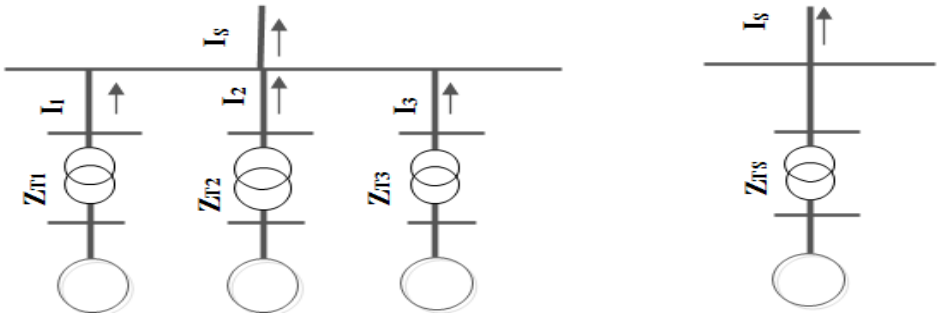

Figure 3.1 a. Three turbine system and b. Single turbine representation

From Figure 3.1a the voltage drop in each unit transformer becomes;

$$\Delta V_{T1} = I_1 Z_{T1} = \left(\frac{S_1}{V}\right) Z_{T1} = \left(\frac{P_1}{V}\right) Z_{T1} \quad (3.4)$$

$$\Delta V_{T2} = I_2 Z_{T2} = \left(\frac{S_2}{V}\right) Z_{T2} = \left(\frac{P_2}{V}\right) Z_{T2} \quad (3.5)$$

$$\Delta V_{T3} = I_3 Z_{T3} = \left(\frac{S_3}{V}\right) Z_{T3} = \left(\frac{P_3}{V}\right) Z_{T3} \quad (3.6)$$

From equation (3.1) to (3.3) the power losses in the individual pad mount transformer becomes:

$$S_{ZT1} = \Delta V_{Z\,T1} I_1^* = \left(\frac{P_1}{V}\right) Z_{T1} \left(\frac{P_1}{V}\right)^* = \left(\frac{P_1}{V}\right)^2 Z_{T1} \quad (3.7)$$

$$S_{ZT2} = \Delta V_{Z\,T2} I_2^* = \left(\frac{P_2}{V}\right) Z_{T2} \left(\frac{P_2}{V}\right)^* = \left(\frac{P_2}{V}\right)^2 Z_{T2} \quad (3.8)$$

$$S_{ZT3} = \Delta V_{Z\,T3} I_3^* = \left(\frac{P_3}{V}\right) Z_{T3} \left(\frac{P_3}{V}\right)^* = \left(\frac{P_3}{V}\right)^2 Z_{T3} \quad (3.9)$$

From Figure 3.1bthe voltage drop across the equivalent impendence becomes;

$$\Delta V_{Z_{TS}} = I_S Z_{TS} = (I_1 + I_2 + I_3) Z_{TS} = \left(\frac{P_1}{V} + \frac{P_2}{V} + \frac{P_3}{V}\right) Z_{TS}$$

$$\Delta V_{Z_{TS}} = \left(\frac{P_{Total}}{V}\right) Z_{TS} \quad (3.10)$$

Where,Z_{TS} is the equivalent impedance of the unit transformers in a group.

The total loss is in the equivalent impendence becomes;

$$S_{ZTS} = S_{ZT1} + S_{ZT2} + S_{ZT3} \quad (3.11)$$

After rearranging parameters and substituting values from (3.7) to (3.9) into (3.11) becomes;

$$\left(\frac{P_{Total}}{V}\right)^2 Z_{TS} = \left(\frac{P_1^2 Z_{T1} + P_2^2 Z_{T2} + P_3^2 Z_{T3}}{V^2}\right) \quad (3.12)$$

$$Z_{Ts} = \frac{\sum_{m=1}^{n} P_m^2 Z_m}{(\sum_{m=1}^{n} P_m)^2} \quad (3.13)$$

Step 3: Equivalence of Shunt Impedances

The equivalent circuit of a transmission line given in Figure 3.2 has been considered, and due to the nature of a capacitor generating reactive power that is proportional to the square of the voltage across them, and also considering that the bus voltage is close to unity under normal conditions, the representations of the shunt parameter can be considered as the sum of all the shunts in the power system network [27].By these given assumptions, the total shunt capacitance within the wind farm can be computed as follow;

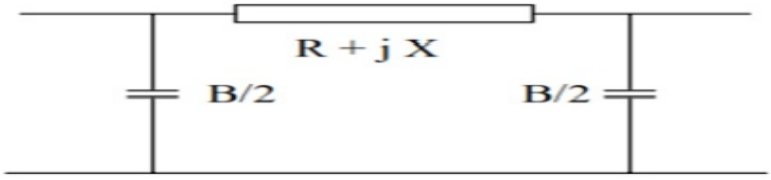

Figure 3.2: Equivalent circuit of a transmission line [27]

$$B_{Total} = \sum_{m=1}^{n} B_m \quad (3.14)$$

Step 4: Equivalence of Collector Circuit

Modeling procedure for collector circuit impedance can be demonstrated considering a cluster which contains only one group with three wind turbine connected as shown in Figure 3.3.The voltage drops across the line impedances Z_1 can be written as: [29].

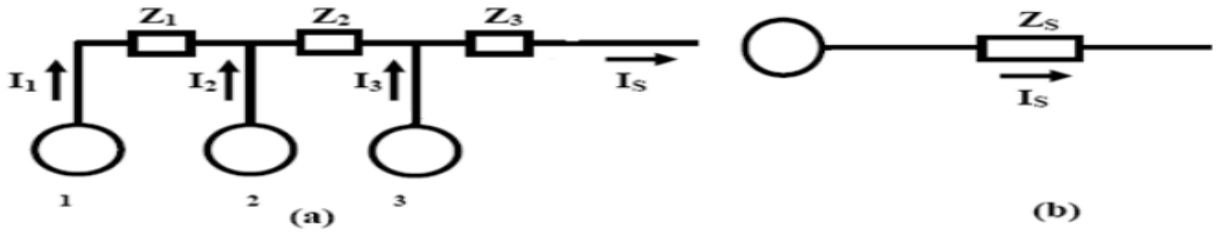

Figure3.3:a.Wind turbines generators with collector impedance; b. Equivalent circuit [29].

$$\Delta V_1 = I_1 Z_1 = \left(\frac{S_1}{V}\right) Z_1 = \left(\frac{P_1}{V}\right) Z_1 \quad (3.15)$$

The apparent power S_1 can be substituted by active power P_1 assuming that each wind turbine is compensated and have a very close unity power factor. So that, the current injected by wind generator one is given by $I_1=S_1/V$ (where $S_1$is the rated apparent power of wind turbine one). The voltages drop across each line impedance Z_2 though Z_3 can also be written as:

$$\Delta V_2 = (I_1 + I_2)Z_2 = \left(\frac{S_1}{V} + \frac{S_2}{V}\right) Z_2 = \left(\frac{P_1}{V} + \frac{P_2}{V}\right) Z_2 \quad (3.16)$$

$$\Delta V_3 = (I_1 + I_2 + I_3)Z_3 = \left(\frac{S_1}{V} + \frac{S_2}{V} + \frac{S_3}{V}\right) Z_3 = \left(\frac{P_1}{V} + \frac{P_2}{V} + \frac{P_3}{V}\right) Z_3 \quad (3.17)$$

The power flow on the line segment Zi be P_{Zi}(i=1, 2, 3) then the total power flow in the line segment will be

$$S_{LossZ1} = \Delta V_{Z1} I_1^* = \left(\frac{P_1}{V}\right) Z_1 \left(\frac{P_1}{V}\right)^* = \left(\frac{P_1}{V}\right)^2 Z_1 = \left(\frac{P_{z1}}{V}\right)^2 Z_1 \quad (3.18)$$

$$S_{LossZ2} = \Delta V_{Z2} I_2^* = \left(\frac{P_1}{V} + \frac{P_2}{V}\right)\left(\frac{P_1}{V} + \frac{P_2}{V}\right) Z_2 = \left(\frac{P_1}{V} + \frac{P_2}{V}\right)^2 Z_1 = \left(\frac{P_{z2}}{V}\right)^2 Z_1 \quad (3.19)$$

$$S_{LossZ3} = \Delta V_{Z3} I_3^* = \left(\frac{P_1}{V} + \frac{P_2}{V} + \frac{P_3}{V}\right)\left(\frac{P_1}{V} + \frac{P_2}{V} + \frac{P_3}{V}\right) Z_3 = \left(\frac{P_1}{V} + \frac{P_2}{V} + \frac{P_3}{V}\right)^2 Z_3 = \left(\frac{P_{z3}}{V}\right)^2 Z_1 \quad (3.20)$$

Note that Z3 is the last line segment in the daisy chain branch. The total loss can be computed as:

$$S_{TotalLoss} = \left(\frac{P_{z1}}{V}\right)^2 Z_1 + \left(\frac{P_{z2}}{V}\right)^2 Z_2 + \left(\frac{P_{z3}}{V}\right)^2 Z_3 \quad (3.21)$$

From Figure 3.3b, we can compute the voltage drop across the equivalent impedance as:

$$\Delta V_3 = I_S Z_S \quad (3.22)$$

Where

$$I_S = \frac{P_1}{V} + \frac{P_2}{V} + \frac{P_3}{V} \quad (3.23)$$

The total loss in the equivalent impedance can be computed as:

$$S_{Loss\,Z_S} = \Delta V_{Z_S} I_S^* = \left(\frac{P_1}{V} + \frac{P_2}{V} + \frac{P_3}{V}\right)\left(\frac{P_1}{V} + \frac{P_2}{V} + \frac{P_3}{V}\right)^* Z_S = \frac{P_{Z3}^2 Z_S}{V^2} \quad (3.24)$$

Equating the two-loss equation

$$S_{TotalLoss} = S_{Loss\,Z_S} \quad (3.25)$$

$$\frac{P_{Z3}^2 Z_S}{V^2} = \frac{P_{z1}^2}{V} Z_1 + \frac{P_{z2}^2}{V} Z_2 + \frac{P_{z3}^2}{V} Z_3 \quad (3.26)$$

Then, after rearranging terms the general expression for the impedance of the collector circuit can be calculated from (3.26);

$$z_S = \frac{\sum_{m=1}^{n} P_{z_m}^{\,2} z_m}{\left(\sum_{m=1}^{n} P_{z_m}\right)^2} \quad (3.27)$$

Step 5: Model Validation

The load flow analysis has been done using PSS/E simulation software after the aggregation process is completed; so that the aggregated system will have identical output as that of the complete system output. For validating the equivalence of full turbine representation (FTR) and its single turbine representation (STR), testing has been carried out using the software. Therefore a power flow

simulation has been performed under normal conditions for FTR and STR. The active power flow per total active power transferred and reactive power flow per the total reactive power transferred would be compared on the two representations. The active /reactive power flow is the difference between FTR and STR active /reactive power correspondingly.

3.3 Modeling the Wind Farm and Grid System using PSS/E

The simulations presented in this thesis have been carried out using the software tool Power System Simulator for Engineering (PSS/E) version 33, which is mainly used for power system studies.

The application software, PSS/E is applied for the steady-state and dynamic analyses of the electrical transmission network model and also for aggregation of the wind farm. It is used to perform the static load-flow calculations and the switching (dynamic) studies. The Full Newton-Raphson method is employed to solve the power-flow calculations. Many wind turbine manufacturers provide PSS/E models that are used for verification of grid codes however most of them are bound with non-disclosure agreements.PSS/E is developed by Siemens Power Technologies International (PTI).

The model consists of three simulation data files: power flow data, dynamic data and sequence data. PSS/E can be utilized to facilitate calculations for a variety of analyses, including: Power flow and related network functions, optimal power flow, balanced and unbalanced faults, network equivalent construction, dynamic simulation.

3.4 Modeling of Adama II Wind Farm

The power system modeling, Adama II wind farm, for steady state analysis in PSS/E has been selected as a case study. The installed capacity of the wind farm is 153MWand individual wind turbine generates 1.5 MW. It has 102 turbines and grouped into eight clusters. Each individual wind turbine generator (WTG) is connected to a 690 V bus, and the WTGs are connected to the wind farm internal grid through their 0.69/33 kV step-up transformers. The wind turbines are connected through 33kV underground cables and overhead transmission line of different lengths and capacities depending on the location of each unit and the distance to the 33 kV collector bus.

The aggregation is developed then a WPP with 102 wind turbines into a single turbine representation has been made and the model has been verified with load flow analysis.

The power flow modeling data for the wind farm are given in Tables 3.1andtechnical data for the cable and overhead line are indicated on Appendix B. Specifications of Adama II wind power plant turbine

generator, unit transformer and main transformer which has been used for aggregation of the farm are indicated on Appendix E.

3.4.1 Site Description

Adama II wind farm is located in the middle of Ethiopia as shown in Figure4.4, approximately 90km east of capital city, Addis Ababa and 3km North West of Adama city at elevation of 1741~2173m. According to the feasibility study, the central geographical position of the wind park is 39° 12' 10"E, 8° 34' 18" N and the average wind speed in the area is 8 – 9m/s. The farm has been used doubly fed induction generator (DFIG) type.

Figure 3.4: Location of AdamaII Wind Farm [Google earth]

3.4.2 Layout of Adama II Wind Farm

The Adama II wind farm has 102 turbines. Each turbine is attached to a unit transformer that steps up the generator voltage (690 V) in to a medium voltage level of 33 kV and all are grouped into eight

clusters (cluster A to cluster H). Except one of the clusters that have eleven turbines, while the remaining seven clusters have thirteen turbines each, grouped together and a 33 kV overhead line connect each clusters to the main substation. The main substation has two transformers with the capacity of 90 MVA with voltage level 33/230 kV. The high voltage terminal side is connected to Koka substation with single 230 kV overhead transmission line. The layout of Adama II wind farm is shown in Figure 3.5.

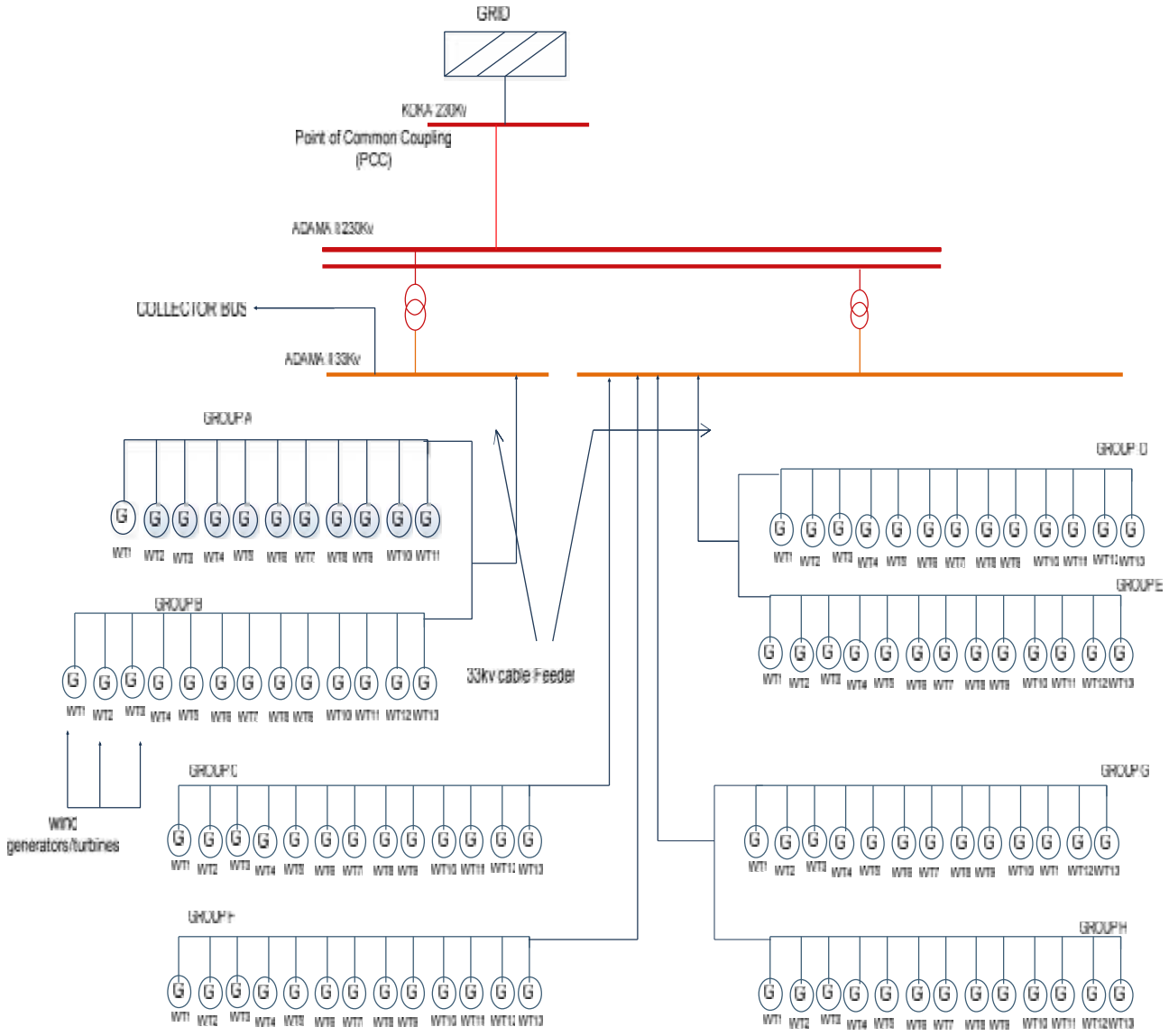

Figure 3. 5: Lay out of the Adama II wind farm

Table 3. 1: Power flow modeling data input for the Adama II wind farm

Parameter (symbol)	Value(Unit)
A. Wind turbine generator data	
Sn	1.6 MVA
Qmax (Qmin)	0.9 (−0.8)MVAr
Z source	0 + j 0.8 pu.
Pmax (Pmin)	1.5(0.0) MW
M base	1.6 MVA
B. Wind turbine transformer data	
Sn	1.6 MVA
Unp/Uns	0.69/33 KV/KV
Ztr	0.0012 + j 0.0057 p.u
M base	1.6 MVA
C. Substation transformer data	
Sn	90 MVA
Unp/Uns	33/230 KV/KV
Ztr	0.00361+j0.129950 p.u
Ytr	0.0005 − j 0.00149p.u
M base	100MVA

The steps that useful for aggregation of Adama II wind farm:

Step 1: Equivalent Wind Turbine

The large wind farm is composed of 102 GE DFIGs, each delivering 1.5 MW of active power. Thus, according to equation (3.1):

$$Peq = 102 * 1{:}5\text{MW} = 153\text{MW}$$

Step 2: Equivalent Pad Mount Transformer

The resistive and reactive component of a single transformer can be given as

$Z_{TS} = R_{TS} + X_{TS}$

But

$$R_{TS} = \frac{U_{Rr} * U_{rt}^2}{100 S_{rt}} \quad (3.28)$$

$$X_{TS} = \frac{U_{Xr} * U_{rt}^2}{100 S_{rt}} \quad (3.29)$$

Where

U_{Rr} is rated, resistive voltage drop (%) = 1.3%

U_{Xr} is rated reactive voltage drop (%) = $\sqrt{U_{kr}^2 - U_{Rr}{}^2}$

U_{rt} is transformer primary voltage (0.69 kV)

S_{rt} is transformer apparent power (1.6 MVA)

U_{kr}^2 is transformer short circuit impedance (%)=6.5%

Therefore,

$U_{Xr} = \sqrt{U_{kr}^2 - U_{Rr}{}^2}$

$U_{Xr} = \sqrt{6.5^2 - 1.3^2}$

$= 6.37\%$

Then, substituting the values into (3.28) and (3.29):

R_{TS} = 0.00387 Ω

X_{TS} = 0.0187 Ω

Z_{TS1} = (0.00387+ *j*0.0187) Ω

Modeling Unit Transformer (Group 1 of Cluster A)

Group one of Cluster A has four unit transformers connected in parallel as shown in the micro setting of the wind farm. Thus applying equation (3.13) we have

$$Z_{TS\_1} = \frac{P_1^2 Z_{TS1} + P_2^2 Z_{TS2} + P_3^2 Z_{TS3} + P_4^2 Z_{TS4}}{(P_1 + P_2 + P_3 + P_4)^2}$$

Where $Z_{TS1}=Z_{TS2}= Z_{TS3}= Z_{TS4}$ are transformer leakage reactance, and $P_1=P_2= P_3= P_4$ are the rated power from each wind turbine

Hence, the equation will be reduced to

$$Z_{TS\_1} = \frac{Z_{TS1}}{4}$$

i.e $Z_{TS\_1} = \frac{Z_{TS1}}{4}$

$$Z_{TS\_1} = \frac{Z_{TS\,1}}{n} \tag{3.30}$$

Where n is the total number of turbines in the group. Since group one has four wind turbines and substituting value for transformer leakage reactance in equation (3.30)

$$Z_{TS\_1} = \frac{(0.00387 + j\,0.0187)}{4}\,\Omega = (0.000968 + \text{j}0.00468)\Omega$$

In per units

$$Z_{TS\_1} = \frac{1.6}{(0.69)^2}\,(0.000968 + \text{j}0.00468) = 0.00325 + \ j0.0157\,p.u$$

Modeling Unit Transformer (Group 2 of Cluster A)

Group 2 of Cluster A has seven unit transformers connected in parallel. Similarly the equivalent impedance can be calculated using equation (3.30)

$$Z_{TS\_2} = \frac{(0.00387 + j0.0187)}{7} = (0.0005529 + j0.00267)\Omega$$

In per units

$$Z_{TS\_2} = \frac{1.6}{(0.69)^2}\,(0.0005529 + j0.00267) = 0.001858 + \ j0.008978\,p.u$$

Hence, the final equivalence impedance of cluster A pad mounted transformer is given by Z_{TsA} applying equation (3.13) as follows,

$$Z_{TsA} = \frac{\sum_{m=1}^{n} P_m^2 Z_{TS\_m}}{(\sum_{m=1}^{n} P_m)^2}$$

Where n is the number of groups in cluster A

$$Z_{TS}A = \frac{P^2 G_1 Z_{TS\_2} + P^2 G_2 Z_{T\_2}}{(P_1 + P_2)^2}$$

Where P^2G_1 and P^2G_2 are the total power transferred in group 1 and group 2 respectively.

$$P^2G_1 = P_1^2 + P_2^2 + P_3^2 + P_4^2$$

$$P^2G_2 = P_5^2 + P_6^2 + P_7^2 + P_8^2 + P_9^2 + P_{10}^2 + P_{11}^2$$

But $\text{P}_1 = \text{P}_2 = \text{P}_3 = \text{P}_4 = \text{P}_5 = \text{P}_6 = \text{P}_7 = \text{P}_8 = \text{P}_9 = \text{P}_{10} = \text{P}_{11} = 1.5$ MW

Therefore,

$$P^2G_1 = (4 * 1.5)^2 = (6)^2 \text{ MW}$$

$$P^2G_2 = (7 * 1.5)^2 = (10.5)^2 MW$$

$$Z_{TS}A = \frac{(6)^2 0.00325 + j0.0157 + (10.5)^2 0.001858 + j0.008978}{(6 + 10.5)^2}$$

$Z_{TS}A$ = 0.001182+ j.005712 p.u

Step 3: Equivalence of Shunt Impedances

The equivalency of shunt admittance is calculated using equation (3.14)

1. Group 1 of Cluster A shunt impedance

$$BG1 = 4 * 8.84\mu s = 35.36\ \mu s$$

2. Group two shunt impedance

$$BG2 = 7 * 8.84\mu s = 61.88\ \mu s$$

$$B_{Total} = \sum_{m=1}^{n} B_m$$

Step 4: Equivalence of Collector Circuit

Group 1 Collector Circuit Modeling

Group one has four wind turbines thus the equivalence can be calculated using equation (3.27)

$$z_s = \frac{\sum_{m=1}^{n} P_{z_m}^{\ 2} z_m}{\left(\sum_{m=1}^{n} P_{z_m}\right)^2}$$

$$Z_{CG1} = \frac{P_1^2 Z_1 + P_2^2 Z_2 + P_3^2 Z_3 + P_4^2 Z_4}{(P_1 + P_2 + P_3 + P_4)^2}$$

Where *Z1, Z2, Z3,* and *Z4* are the branch impedance between wind turbine *WTG14-WTG15, WTG15-WTG16, WTG16 -WTG17 and WTG17 -WTGCCG1* respectively as shown in the micro sitting of the wind farm *P1, P2, P3, and P4* are branch flows. Thus, substituting the values of branch impedance and power flow that are given in Appendix C.

$$Re(Z_{CG1}) = \frac{1.5^2 R_1 + 3^2 R_2 + 4.5^2 R_3 + 6^2 R_4}{(1.5 + 3 + 4.5 + 6)^2}$$

$$= \frac{1.5^2 * 0.01 + 3^2 * 0.0082 + 4.5^2 * 0.009 + 6^2 * 0.006}{(1.5 + 3 + 4.5 + 6)^2}$$

$Re(Z_{CG1})$ =0.04191 p.u

$$Im\,(Z_{CG1}) = \frac{1.5^2 X_1 + 3^2 X_2 + 4.5^2 X_3 + 6^2 X_4}{(1.5 + 3 + 4.5 + 6)^2}$$

$$= \frac{1.5^2 * 0.0067 + 3^2 * 0.0051 + 4.5^2 * 0.055 + 6^2 * 0.003}{(1.5 + 3 + 4.5 + 6)^2}$$

$$Im\,(Z_{CG1}) = 0.005701 \text{ p.u}$$

$$ZCG1 = 0.04191 + j0.005701 \text{ p.u}$$

Group Two Collector Circuit Modeling

Since group 2 has seven wind turbines using equation (3.27) and taking values from Appendix C:

$$Z_{CG2} = \frac{P_1^2 Z_5 + P_2^2 Z_6 + P_3^2 Z_7 + P_4^2 Z_8 + P_5^2 Z_9 + P_6^2 Z_{10} + P_7^2 Z_{11}}{(P_1 + P_2 + P_3 + P_4 + P_5 + P_6 + P_7)^2}$$

Where Z5,Z6,Z7,Z8,Z9,Z10 and *Z*11 are the branch impedance between wind turbine WTG18 - *WTGCCG1 ,WTG18-WTG19, WTG19-WTG20,WTG20 -WTG21, WTG21-WTG22,WTG22 -WTG23, and WTG23 -W24* respectively as shown in the micro sitting of the wind farm *P1,P2,P3, P4,P5,P6* and *P7* are branch flows. Thus, substituting the values of branch impedance and power flow given in Appendix C.

$$Re(Z_{CG2}) = \frac{1.5^2 * 0.015 + 3^2 * 0.008 + 4.5^2 * 0.007 + 6^2 * 0.008 + 7.5^2 * 0.018 + 9^2 * 0.007 + 10.5^2 * 0.007}{(1.5 + 3 + 4.5 + 6 + 7.5 + 9 + 10.5)^2}$$

$$Re(Z_{CG2}) = 0.00163 \text{ p.u}$$

$$Im\,(Z_{CG1}) = \frac{1.5^2 * 0.007 + 3^2 * 0.028 + 4.5^2 * 0.005 + 6^2 * 0.005 + 7.5^2 * 0.013 + 9^2 * 0.005 + 10.5^2 * 0.002}{(1.5 + 3 + 4.5 + 6 + 7.5 + 9 + 10.5)^2}$$

$$Im\,(Z_{CG1}) = 0.00108 \text{ p.u}$$

$$ZCG2 = 0.00163 + j0.00108 \text{ p.u}$$

Now to represent the cluster with single turbine system group one and two impedances has to be reduced. Then, the collector circuit of cluster A can be reduced as

$$Z_{CA} = \frac{P_{G1}^2 Z_{CG1} + P_{G2}^2 Z_{CG2}}{(P_{G1} + P_{G2})^2}$$

$$Z_{CA} = \frac{6^2 * (0.04191 + j0.005701) + 10.5^2 * (0.00163 + j0.00108)}{(6 + 10.5)^2}$$

$$Z_{CA} = 0.0062 + j0.00119\ p.u$$

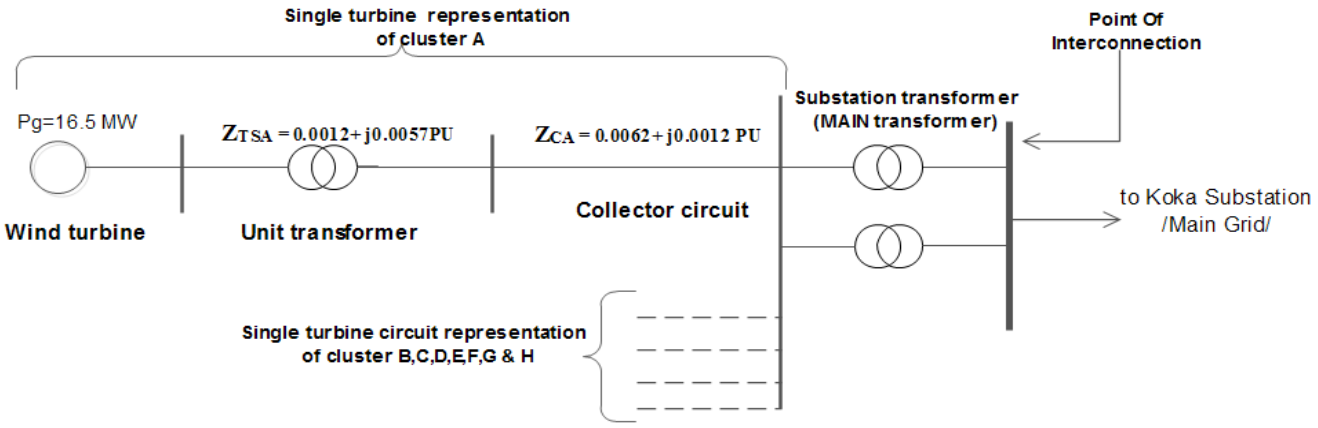

Figure 3. 6: Single turbine representation of cluster A of Adama II WPP

Similarly, the rest of the clusters are modeled with single turbine system and their respective equivalent unit transformer and collector circuit impedance are shown in Tables 3.2 and 3.3.

Table 3. 2: Summery of equivalent impedance of unit transformer for all clusters

Cluster	No. of Transformer	Total Power(MW)	Equivalent Transformer Impedance of each cluster	
			Req(pu)	*Xeq*(pu)
A	11	16.5	0.0012	0.0057
B	13	19.5	0.001	0.0048
C	13	19.5	0.001	0.0048
D	13	19.5	0.001	0.0048
E	13	19.5	0.001	0.0048
F	13	19.5	0.001	0.0048
G	13	19.5	0.001	0.0048
H	13	19.5	0.001	0.0048

Finally, STR parameters of Adama II wind farm has been determined with a base apparent power of *SB* = 100 MVA and base voltage of *VB* = 33 kV. Thus, the unit transformer equivalent impedance has been calculated using equation (3.27) by substituting values from Table 3.2.

Z_{TS} = 0.000127+ j0.0006156 p.u

Table 3. 3: Summary of equivalent impedances of all collector circuit for all clusters

Cluster	Length(km)	Total Power(MW)	Collector Impedance	
			Req(pu)	*Xeq*(pu)
A	1.4	16.5	0.0062	0.0057
B	3.57	19.5	0.1069	0.0145
C	0.15	19.5	0.0045	0.0006
D	5	19.5	0.1498	0.0204
E	5.61	19.5	0.1681	0.0228
F	5	19.5	0.1498	0.0204
G	5.45	19.5	0.1633	0.0222
H	5	19.5	0.1498	0.0204

Then, by substituting values from Table 3.3, the collector circuit equivalent impedance has been calculated using equation (3.27).

$$Z_{CC} = 0.000748 + j0.000125 \text{ p.u}$$

Step 5: Model Verification

From the above analysis, it can be seen, all 102 turbines/generators of Adama II WF has been reduced in to a single turbine/generator. For validating the equivalence of a large wind farm and its single turbine representation, testing has been carried out in PSS/E. Three cases are investigated. The aggregated system will have identical output as that of the complete system

3.5 Load Flow Analysis for Adama II Wind Farm Model Verification

A power flow simulation is solved under normal conditions for different wind farm representation. The flows of power in terms of total active power and reactive power will be compared on for three cases :

• Case 1: The large wind farm is composed of 102 GE (Generic models in PSSE) DFIGs, each delivering 1.5 MW of active power. The turbine voltage is 690 V. One hundred two pad mount transformers increase the terminal wind generator voltage from 690 V to medium voltage of 33 kV. The wind farm has 8 main 33 kV feeders, each of the seven feeders are connected with 13 wind turbines and the remaining one feeder is connected with 11 wind turbines as shown on Figure 3.7.

• Case 2: The large wind farm 102*1.5 MW is aggregated to 8 GE DFIGs, each delivering 19.5 MW of active power and the remaining one aggregated generator deliver an active power of 16.5 MW as shown on Figure 3.8.

• Case 3: The 8 GE DFIGs is further aggregated to one single wind turbine delivering an active power

of 153 MW with an equivalent medium voltage collector system as in Figure 3.9.

As can be seen from Figure 3.7, 3.8 and 3.9, the flow of active and reactive power at the common coupling can be observed that, 150.8 MW and 19.4 MVAR for case 1, 149.3 MW and 15.3 MVAR for case 2 and 150.9 MW and 19.4 MVAR for case 3. From this, it can be seen that there is 0.1 MW active power flow (which is 0.065% of total active power transferred) and 0.008 MVAR reactive power flow (which is 0.57% of the total reactive power transferred) difference between full turbine representation and single turbine representation of the power plant.

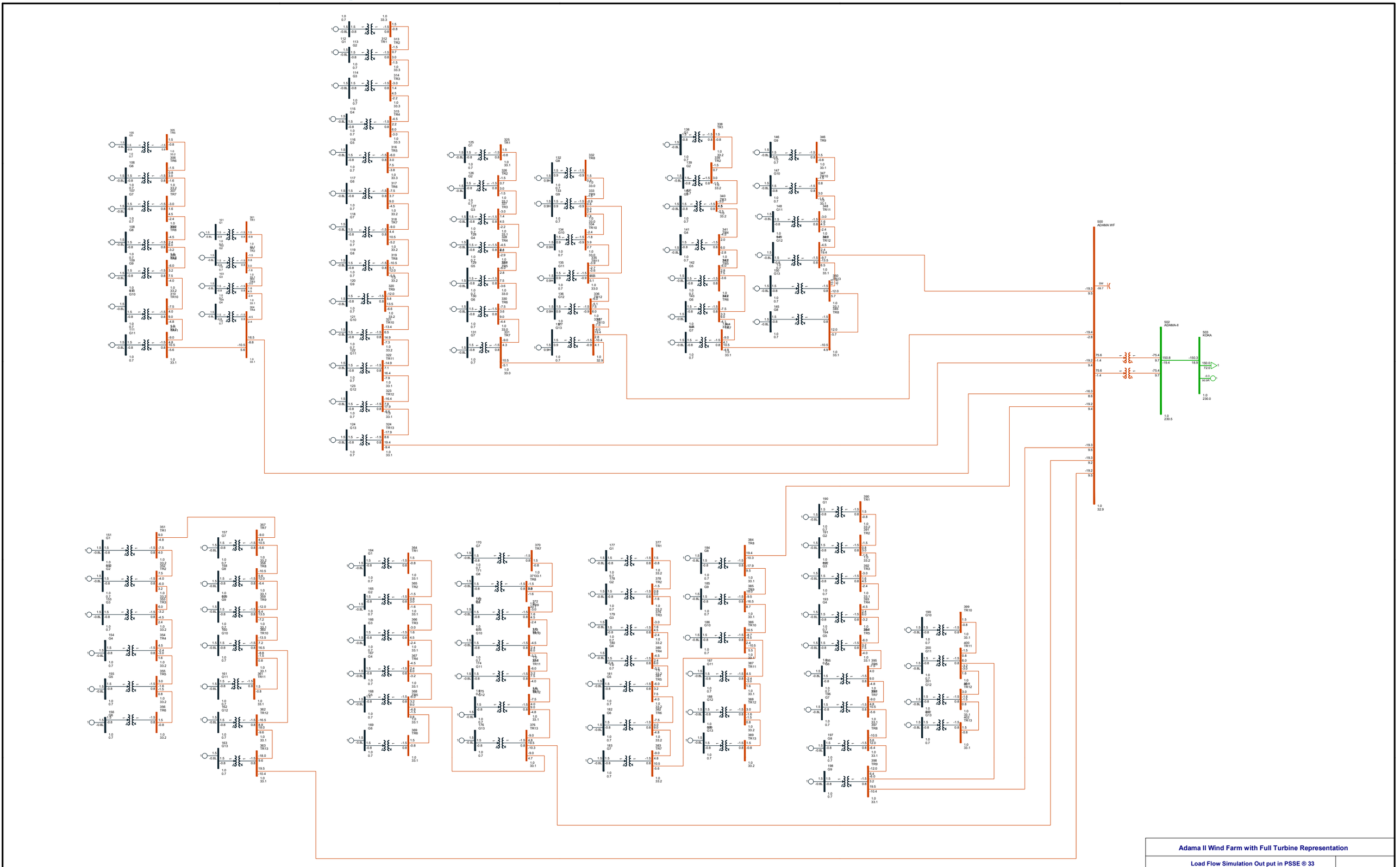

Fig 3.7: Full turbine representation of Adama II Wind Farm

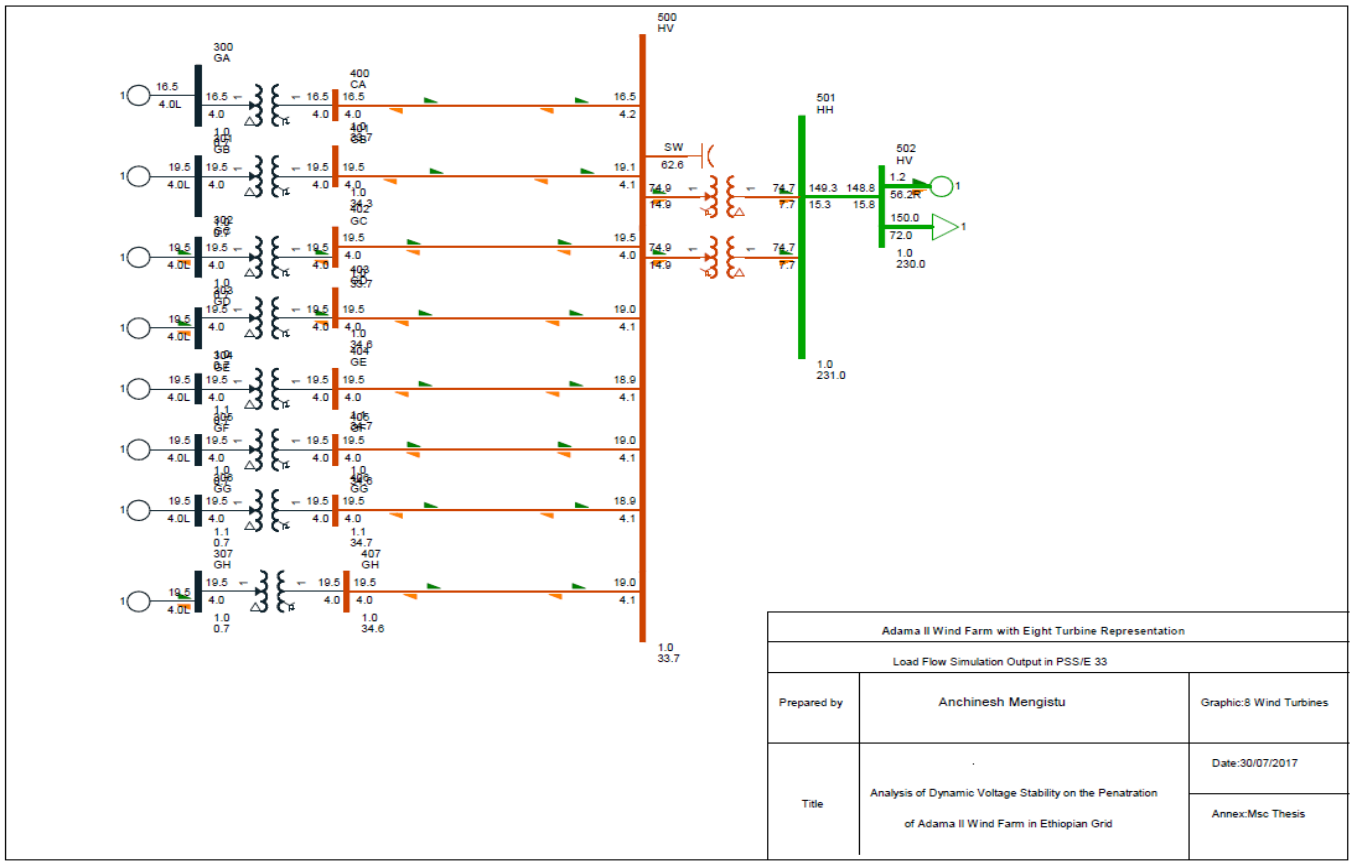

Figure 3. 8: Eight turbine representation of Adama II wind farm

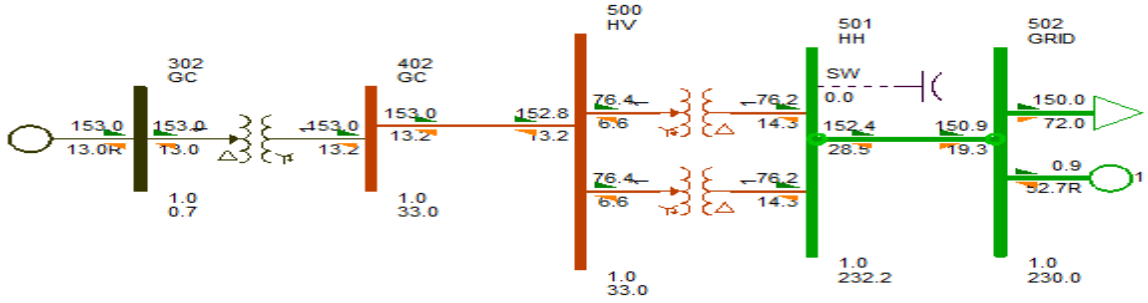

Figure 3. 9: Single machine/turbine representation of Adama II wind farm

Practically any system can't be 100% efficient, thus, Adama II wind power plant has a capacity of generating 153 MW of power (rated capacity) but in each of the models developed there is an active power loss. The FSR has a total active power loss of 2.2 MW, which is 1.43% of the rated capacity of the wind farm (153 MW). In the second case there is a total of 3.7 MW of active power loss which is 2.41% of the rated capacity of the farm. And the STR has a total active power loss of 2.1 MW which is 1.37 % of the rated capacity of the wind farm. Therefore, comparing the results obtained, the model developed is acceptable.

3.6 The Grid Model

In this section description of the grid model that is used for study and analysis the voltage stability of the grid is presented. The grid is modeled using the software tool PSS®E 33(PSS®E University 33). Mainly it consists of the eastern and central part of transmission line system of, the Ethiopian National Grid with the aggregated Adama II wind farm and a representation of a part of the remaining grid.

In Figure 3.10, a single line diagram of the model with the approximation of the high voltage (400 kV and 230 kV) transmission lines grid and the internal grid representing the wind farm (33 kV) is given. Furthermore, 402002 bus is the infinite grid that can represent the remaining Ethiopian transmission network in this Master thesis work. Some of the buses are connection points to the remaining grid model.

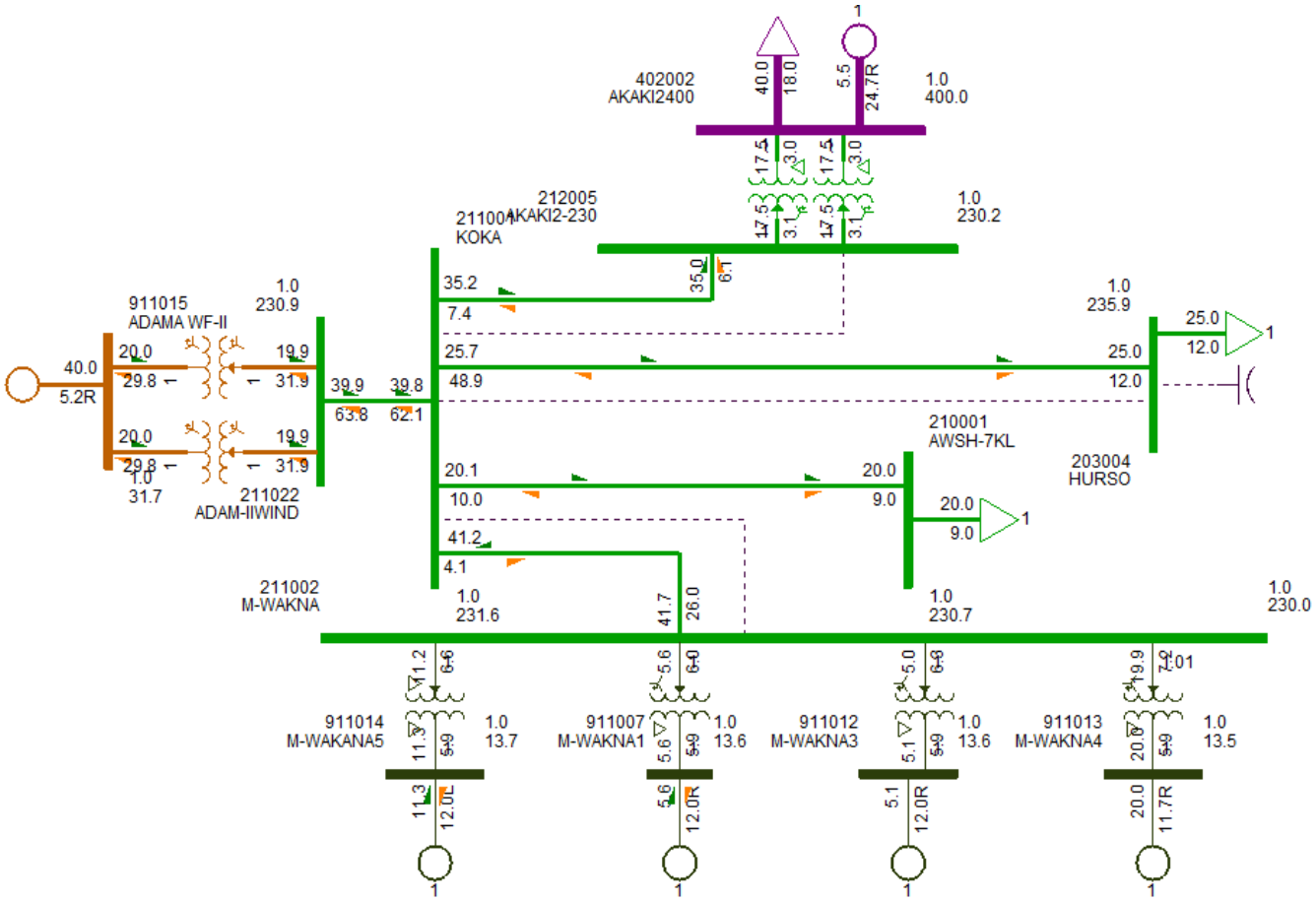

Figure 3. 10: A single line diagram of the grid model obtained using PSS/E.

The aggregated model of the wind farm obtained using in PSS/E is illustrated in Figure 3.11. The model consists of a wind turbine generator, transformers, and an overhead transmission line of 33 kV

(but the generator does not include an internal transformer). Thus, the transformer 33/230 kV is used to transform the wind farm voltage to desired level. The wind farm consists of a single DFIG aggregated source of active and reactive power. The wind generator is connected to the high voltage grid by a 230 kV overhead transmission line and a 33 kV cable.

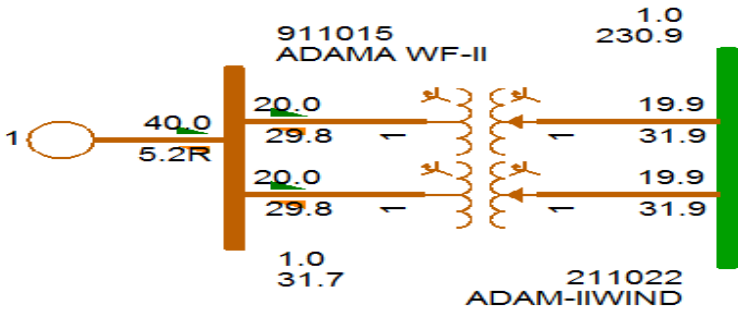

Figure 3. 11: The aggregated model of the wind farm obtained using PSS/E

CHAPTER 4

4 Simulation Studies and Results Analysis

4.1 Introduction

In this chapter, simulation studies have been carried out using PSS/E simulation software to study the capability of the wind farm to fulfill performance requirements connected to the grid and investigate compliance of the grid code by applying different scenarios into the grid. Consequently, simulation results are analyzed and discussed to investigate the impact of the wind farm integration on dynamic voltage performance and their influences on power system voltage stability. Finally, assessment of the wind farm performance in weak grid has been presented.

4.2 Performance of the Wind Farm in Steady State and Dynamic Operation

This section presents the steady-state simulations performed on the grid with the aggregated Adama II wind farm, to prove the regulation of voltage at the point of interconnection (POI). Results are analyzed and discussion of the result is also performed.

The power flow analysis carried out comprehends numerical calculations of active and reactive power flows and node voltages. PSS/E software is used, for the power flow analysis of the model, Ethiopian power grid with Adama II wind farm as described in Figure 3.10.

In this case special attention is given to the Point of Common Coupling (PCC) that is the point of connection of the wind farm with the remaining grid. The voltage at the PCC, the active power injected and the reactive power injected/absorbed in the PCC is analyzed as a part of the power flow study.

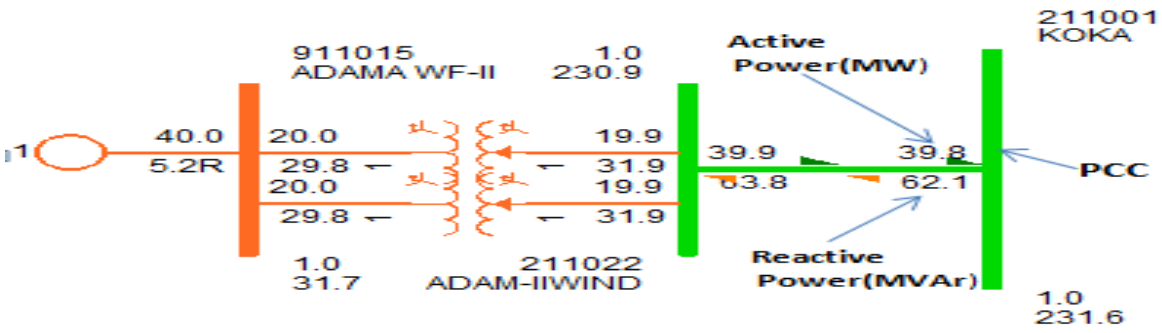

Figure 4. 1: The active, reactive power flow and the voltage magnitude presented in single line diagram

The active and reactive power flow of the branches and the voltage magnitude at each bus are depicted in Figure 4.1.

After developing the steady-state model of which the power system having the aggregated wind farm connected to the grid model as shown in Figure 3.10, the load flow analysis is performed in order to carry out the impact studies. Full Newton-Raphson method is used to perform the power flow studies in PSS/E. This is the power flow program which shows the convergence of the solution, as showing on the bottom of the window bar written as Met convergence tolerances.

```
SIEMENS POWER TECHNOLOGIES INTERNATIONAL
  50 BUS POWER SYSTEM SIMULATOR--PSS(R)E University-33.4.0
            INITIATED ON THU, JUL 13 2017  16:01

The Saved Case in file C:\Users\Anchinesh\Desktop\Adama II OK\Adama II.sav.sav was saved on TUE,
JUL 04 2017  12:54
Successfully cleaned Diagram

  ITER       DELTAP      BUS         DELTAQ      BUS        DELTA/V/      BUS       DELTAANG
BUS
   0         0.4000(   911015   )    0.6018(   211001   )
                                                            0.06514(   203004   )   0.14125(
911013   )
   1         0.0328(   911015   )    0.1224(   911015   )
                                     0.3921(   211002   )
                                                            0.02588(   911013   )   0.00603(
211002   )
   2         0.0006(   211002   )    0.0740(   911015   )
                                                            0.00506(   911015   )   0.00033(
911015   )
   3         0.0000(   211022   )    0.0011(   911015   )
                                                            0.00007(   911015   )   0.00000(
911015   )
   4         0.0000(   211022   )    0.0000(   911015   )

 Reached tolerance in 4 iterations

 Largest mismatch:      0.00 MW      0.00 Mvar      0.00 MVA at bus 211002 [M-WAKNA     230.00]
 System total absolute mismatch:                   0.01 MVA

 SWING BUS SUMMARY:
   BUS# X-- NAME --X BASKV      PGEN      PMAX     PMIN      QGEN      QMAX     QMIN
 402002 AKAKI2400   400.00       5.5    9999.0 -9999.0     -24.7    9999.0 -9999.0
```

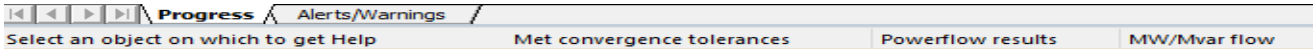

In Table 4.1, the voltages at different buses can be observed. It can be shown that almost all the buses except Hurso the voltages are normal as the desired value. Even if, the voltage at Hurso can be tolerable, the grid system might use the shunt reactor at Hurso busbar to bring the voltage into normal. The voltage at the PCC is 1.0395 p.u that is in the normal range whereas the normal maximum voltage limit is 1.05 p.u. The voltage is normal so no need to be compensated in order to bring the voltage under normal range. Therefore,the result indicates that the WTGs can regulate grid voltage at POI.

Table 4. 1: Voltages at different buses on the steady-state performance

Bus Number	Bus Name	Base kV	Code	Voltage (p.u)	Angle (deg)
203004	HURSO	230	1	1.0614	-1.92
210001	AWSH-7KL	230	1	1.0363	0.24
211001	KOKA	230	1	1.0395	1.32
211002	M-WAKNA	230	1	1.0000	4.9
211022	ADAM-IIWIND	230	1	1.0400	1.46
212005	AKAKI2-230	230	1	1.0059	0.26
402002	AKAKI2400	400	1	1.0000	0.0
911007	M-WAKNA1	13.8	3	0.9726	5.63
911012	M-WAKNA3	13.8	3	0.9703	5.7
911013	M-WAKNA4	13.8	-2	0.9605	7.92
911014	M-WAKANA5	13.8	3	0.9874	5.65
911015	ADAMA WF-II	33	2	1.0368	3.0

Table: 4.2 show the active and reactive power generated by different generating units (four units Melkawakena, aggregated wind generator of Adama II WF and the represented generation unit of the rest of the grid, AKAKI2400). It can be seen that WTGs are capable of adjusting power factor to a desired value, accordingly the reactive power needed to the grid.

Table 4. 2: Data of Active and Reactive power generated

Bus Number	Bus Name	Base kV	Code	Pgen (MW)	Qgen (MW)	Voltage (p.u)
402002	AKAKI2400	400	3	5.542	-24.7353	1.000
911007	M-WAKNA1	13.8	2	5.6258	-11.9542	0.9726
911012	M-WAKNA3	13.8	2	5.0543	-11.9542	0.9703
911013	M-WAKNA4	13.8	2	20	-11.9542	0.9605
911014	M-WAKANA5	13.8	-2	11.2643	-11.7	0.9874
911015	ADAMA WF-II	33	2	40	-5.2421	1.0368

After undergoing the steady-state simulation and observing the results of , the second case that is dynamic simulations are performed on the grid model under analysis. The response of the wind farm and that of the grid to the transmission line trip is analyzed and results are discussed.

Table 4. 3: Voltages at different buses after the transient performance

Bus Number	Bus Name	Base kV	Code	Voltage (p.u)	Angle (deg)
203004	HURSO	230	1	1.0618	11.4
210001	AWSH-7KL	230	1	1.0366	13.55
211001	KOKA	230	1	1.0399	14.63
211002	M-WAKNA	230	1	1.0074	18.2
211022	ADAM-IIWIND	230	1	1.0404	14.77
212005	AKAKI2-230	230	1	1.0022	13.59
402002	AKAKI2400	400	1	0.9956	13.33
911007	M-WAKNA1	13.8	2	0.9811	18.98
911012	M-WAKNA3	13.8	2	0.9783	19.05
911013	M-WAKNA4	13.8	2	0.9688	21.23
911014	M-WAKANA5	13.8	2	0.9993	18.94
911015	ADAMA WF-II	33	2	1.0371	16.29

Table 4. 4: Data of Active and Reactive power generated when the WF is out

Bus Number	Bus Name	Base kV	Code	Pgen (MW)	Qgen (MW)	Voltage (p.u)
402002	AKAKI2400	400	2	5.542	-24.7353	0.9956
911007	M-WAKNA1	13.8	2	5.6258	-11.9542	0.9811
911012	M-WAKNA3	13.8	2	5.0543	-11.9542	0.9783
911013	M-WAKNA4	13.8	2	20	-11.9542	0.9688
911014	M-WAKANA5	13.8	2	11.2643	-11.7	0.9993
911015	ADAMA WF-II	33	2	40	-5.2421	1.0371

The transient performance has been done ,when Adama II WF is out due to 230 kV transmission line trip from Adama II to Koka for 150 ms fault duration and then cleared. The voltages at different buses and active and reactive power generated after the transient performance are shown in Table 4.3 and 4.4 respectively. In this scenario, voltages are controlled mainly by conventional power plants since there is no WF. It can be observed that the voltage at each bus is more as compared to steady state but still normal to the desired value. Therefore,the results show the capability to control voltages within the transmission network is sufficient to compensate the impact of the wind farm .

4.2.1 Performance Analysis of Voltage at POI as Wind Speed Varies

Here is the power flow performance analysis for multiple scenarios with the model of Figure 3.10.

Table 4. 5: Power flow performance analysis for scenario - low wind speed of 3 m/s

Bus Number	203004	210001	211001	211002	211022	212005	402002	911007	911014	911015
Bus Name	HURSO	AWSH-7KL	KOKA (PCC)	M-WAKNA	ADAM-IIWIND	AKAKI2-230	AKAKI2 400	M-WAKNA 1	M-WAKANA 5	ADAMA WF-II
Base kV	230	230	230	230	230	230	400	13.8	13.8	33
Code	1	1	1	1	1	1	3	2	-2	2
Voltage (p.u)	1.0600	1.0349	1.0382	1.000	1.040	1.0019	1.000	0.9733	0.9875	1.0325

At low wind speed (3 m/s) the active power is almost zero. The stop will be rather soft and the impact on the voltage at the PCC will be small at such low wind speed.

Table 4. 6: Power flow performance for scenario - average wind speed of 14 m/s

Bus Number	203004	210001	211001	211002	211022	212005	402002	911007	911014	911015
Bus Name	HURSO	AWSH-7KL	KOKA (PCC)	M-WAKNA	ADAM-IIWIND	AKAKI2-230	AKAKI2 400	M-WAKNA 1	M-WAKANA 5	ADAMA WF-II
Base kV	230	230	230	230	230	230	400	13.8	13.8	33
Code	1	1	1	1	1	1	3	2	-2	2
Voltage (p.u)	1.0611	1.0360	1.0392	1.000	1.040	1.005	1.000	0.9728	0.9874	1.0342

Table 4. 7: Power flow performance for scenario - high wind speed of 25 m/s

Bus Number	203004	210001	211001	211002	211022	212005	402002	911007	911014	911015
Bus Name	HURSO	AWSH-7KL	KOKA (PCC)	M-WAKNA	ADAM-IIWIND	AKAKI2-230	AKAKI2 400	M-WAKNA 1	M-WAKANA5	ADAMA WF-II
Base kV	230	230	230	230	230	230	400	13.8	13.8	33
Code	1	1	1	1	1	1	3	2	-2	2
Voltage (p.u)	1.0617	1.0366	1.0398	1.000	1.040	1.007	1.000	0.9725	0.9874	1.0416

The impact may be larger at high wind speed (25 m/s) since the turbine produces at rated power on these occasions.

The result indicates that ,the voltage at the POI could be affected as wind speed varies.

4.3 Simulation Results Analysis of the Compliance of Grid Code on the Integration of Adama II Wind Farm

4.3.1 Regulation of Voltage at the Point of Interconnection

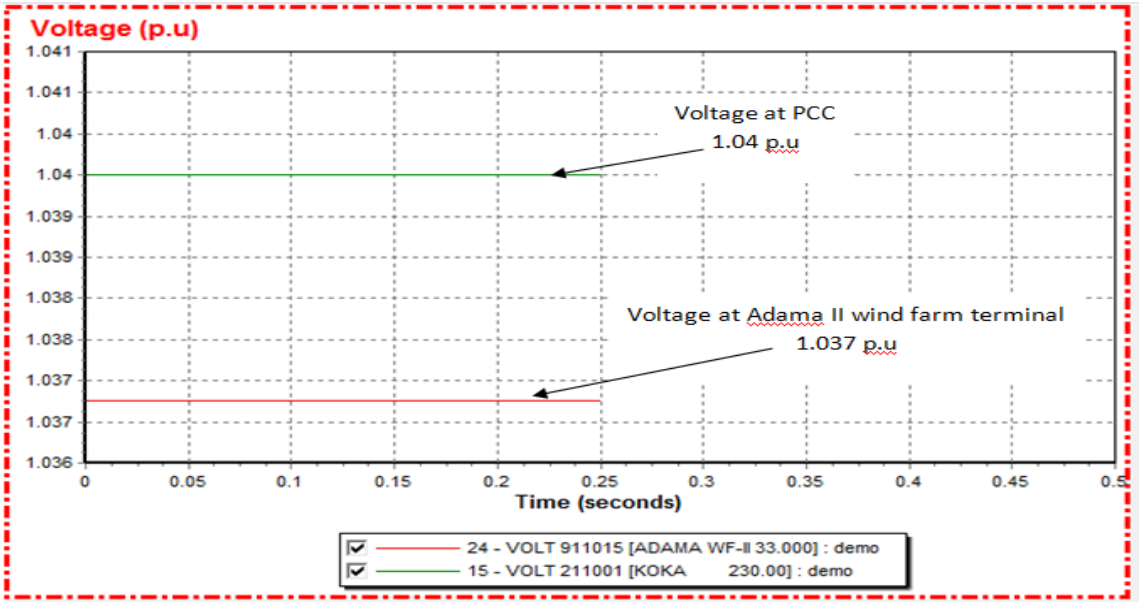

Figure 4. 2a: Voltage profile at the PCC and Adama II WFT

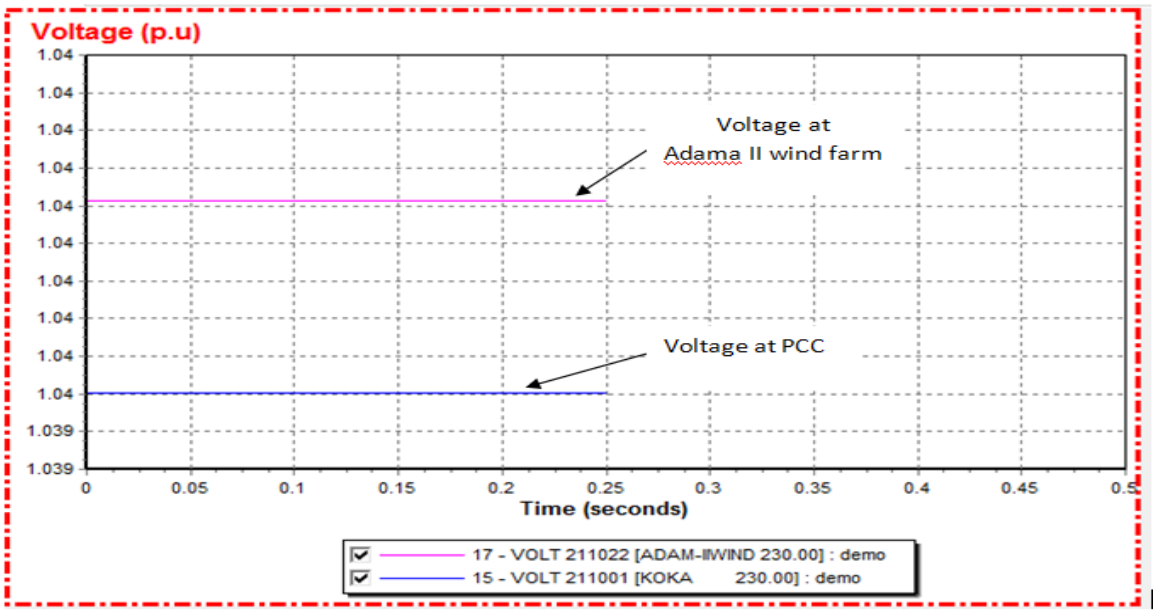

Figure 4. 2b: Voltage profile at the PCC and Adama II WF

Voltage at the PCC (POI) shall not exceed the apportioned levels (without exceeding voltage limit).This can be shown on Figure 4.2 b. As indicated in the Figure 4.2a the voltage at PCC is 1.04 p.u where as the voltage on the wind farm is 1.037 p.u this is due to different voltage level on the two

busbars. This means the terminal voltage of the Adama II wind farm (33 kV busbar) and the voltage at the PCC 230 kV. And also, it can be observed in Figure 4.2b that the voltage at PCC (Koka) is regulated by the wind farm.

4.3.2 Fault Ride Through Capability

The simulation test is carried out on the model illustrated in Figure 3.10 with the objective of assessing the fault ride through capability of the wind farm.

Dynamic simulation is carried out by creating a fault at a grid bus for 150 ms in order to determine the fault ride through capability of the wind farm. For all this steadystate and dynamic simulation Siemens PTI software Known as PSS®E is used.

For all simulations below, the following conditions have been applied:

- The fault applied is a bolted symmetrical three-phase.It is applied at Koka 230 kV busbar (PCC) which is the nearest high voltage grid one second after the start of the simulation.
- The simulation time is 3 seconds for voltage resposes of different buses and for observing power and reactive power response the simulation time is 7 seconds.

The result of this study was analyzed with respect to the grid connection requirements to investigate the fault ride-through capability of the wind farm.

Requirement compliance test is performed from an international grid code for this, the British grid code is used [4].The following grid code compliance requirement is considered.

i. The wind farm must remain transiently stable and connected for all HV voltages down to a minimum 0%.
ii. The maximum possible reactive current should be generated without exceeding the transient rating limit of the turbine
iii. Within 0.6 second following the fault clearance and restoration of the super grid voltage to at least 0.9 of the nominal, the active power output must be restored to at least 0.9 of the level available immediately before the fault .

Here are the responses of voltage at the PCC (Koka busbar) and the wind farm at the wind farm terminal (WFT) (33 kV bus voltage), active and reactive power of the wind farm.

The results of the simulation during and after the occurrence of the fault are shown in Figure 4.3 and Figure 4.4.

1 . Response of Voltage at the Faulty Bus(PCC), Bus 211001

Figure 4.3 shows that during the fault on bus 211001, the 230 kV bus voltage drops to 0 p.u. After fault clearance of 150 ms, the voltage gradually recovers to 1.032 p.u.

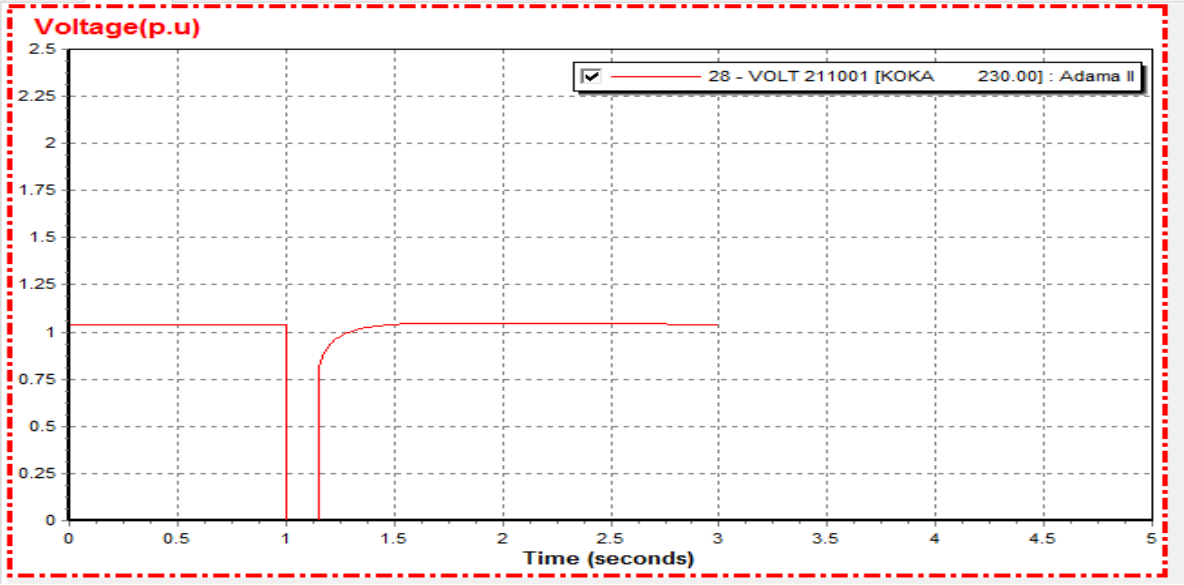

Figure 4.3: Response of voltage at the PCC, Bus 211001

2 . Response of Voltage at Terminals of WTG1 during the Fault:

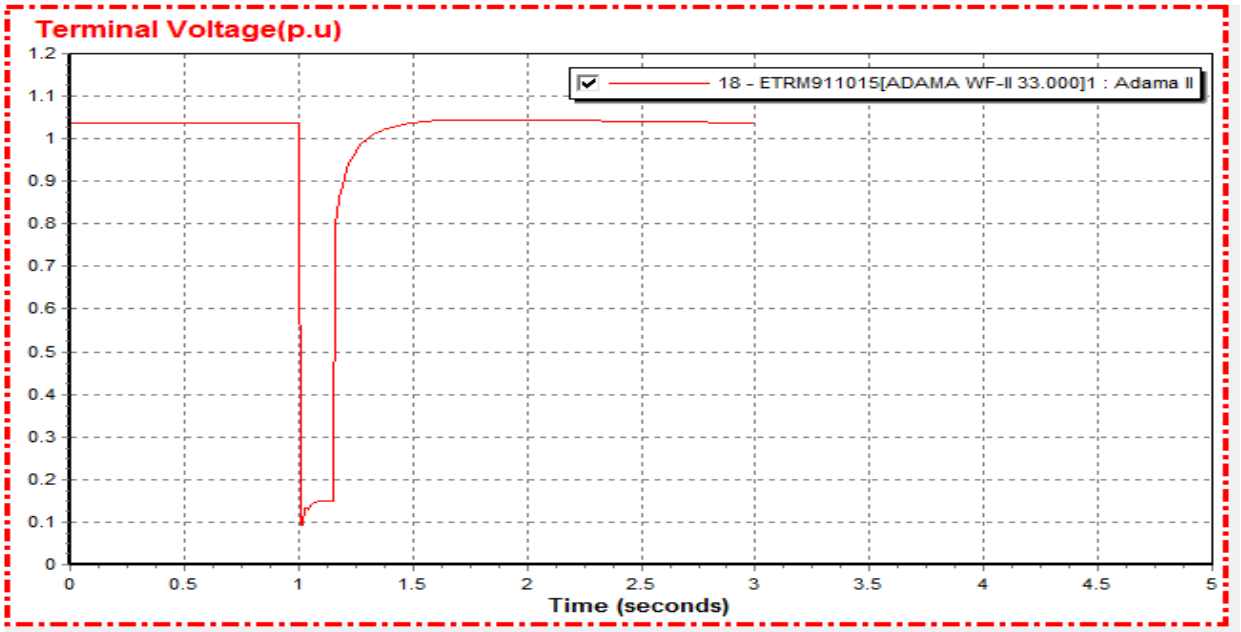

Figure 4.4: Response of voltage at terminals of WTG1 during the fault

Figure 4.4 shows WTG terminal voltage during the fault at Koka and Figure 4.3 clearly shows a similar pattern, except that during the fault the voltage at Koka is 0 p.u.

The range of terminal voltage drop to other WTGs is from 0.1 p.u to 0.15 p.u, depending on location of the installed units. The simulation results indicate that all DFIGs have the ability to ride through the fault, which is in compliance with wind grid code requirements.

3 . WTG1 Active Power Response during the Fault:

Figure 4.5 shows that during the fault the WT3G1electrical power output suddenly decreases to a very low value (0.0001 p.u). The difference between the mechanical input power and electrical output power causes an increase in the rotor speed and therefore the rotor starts to accelerate. The torsion oscillation in the drive-train model is reflected in the output power of the wind turbine. Oscillation of power output after the fault is cleared will cause mechanical stress in the drive train system. Approximately six seconds after the fault is cleared, the power output recovers to the pre-fault value of 40 MW.

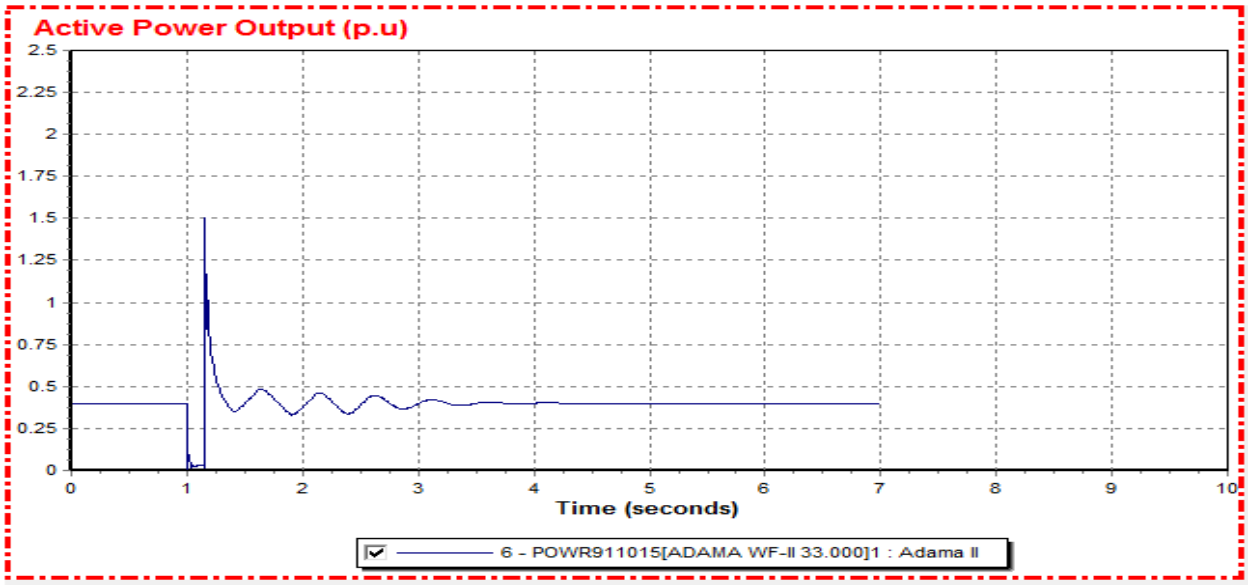

Figure 4.5: WT3G1 active power response during the fault

4 . WTG1 Reactive Power Response during the Fault:

During the fault, the rotor speed increases, giving a larger negative slip. This is because the electric power has decreased to almost zero whereas the mechanical power is assumed to be the same. As a result, WT3P1 part responds by altering the blade pitch to decrease mechanical power. The reactive

power output from selected wind turbine generator WTG1 is shown in Figure 4.6. Before the fault occurs, the generated reactive power is -0.05 p.u. It can be seen that each WTG units during the fault provide reactive power support to the grid, as is required by the wind grid code.

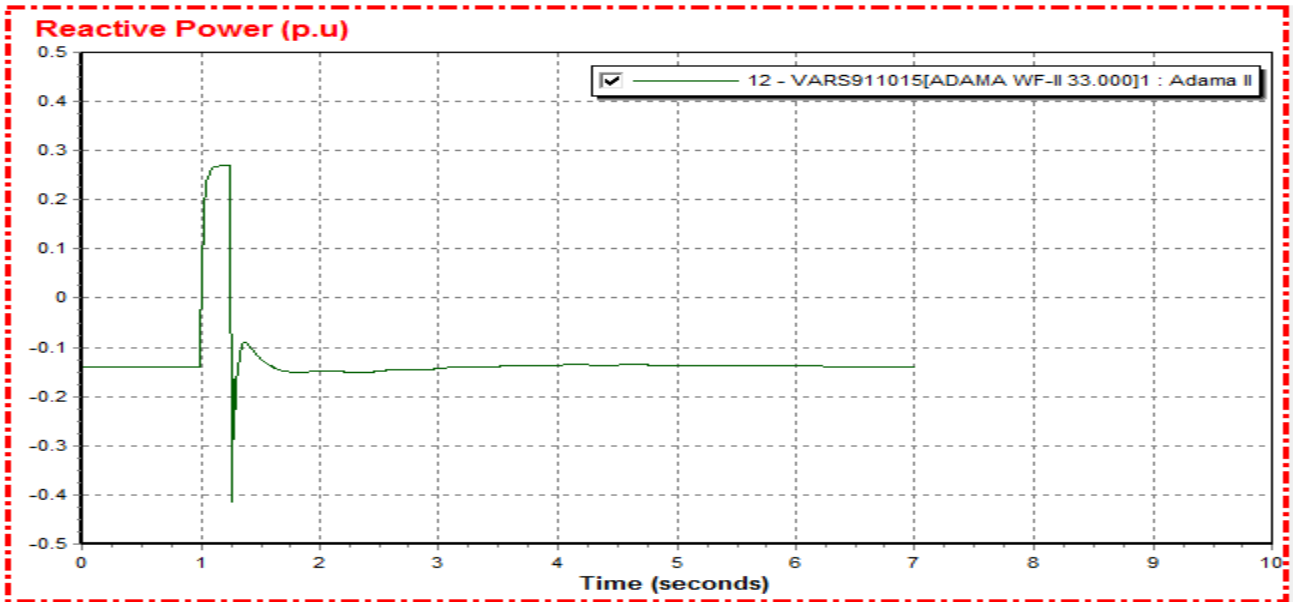

Figure 4. 6: WTG1 reactive power response during the fault

The results of the study shown in Figure 4.5 and 4.6 ,active and reactive power respectively for the wind farm for 3-phase fault of 150 ms depict that the wind farm has remained connected to the grid for the faults lasting for 150 ms . The study also demonstrated that the wind farm is capable of riding through the 230 kV system fault studied.

For all voltage dip durations greater than 150 ms the wind farm has remained connected to the grid . It is also investigated that, just after less than 1 s of restoration of the voltage to 90% of the nominal value, the wind farm has shown itself capable to supply about 90% of its pre-fault value. According to the studied cases the wind farm meets the fault ride-through capability requirement of the model in Figure 3.10. Fast recovery of voltage and power in this case mainly due to the ability of the DFIG model to control reactive power.

4.3.3 Reactive Power Capability without Active Power Generation

Figure 4.7 shows that during the fault the WTG electrical power output suddenly decreases to a very low value almost zero MW,and also, it can be seen that each WTG units provide reactive power support to the grid, as is required by the grid code even at zero active power generation.

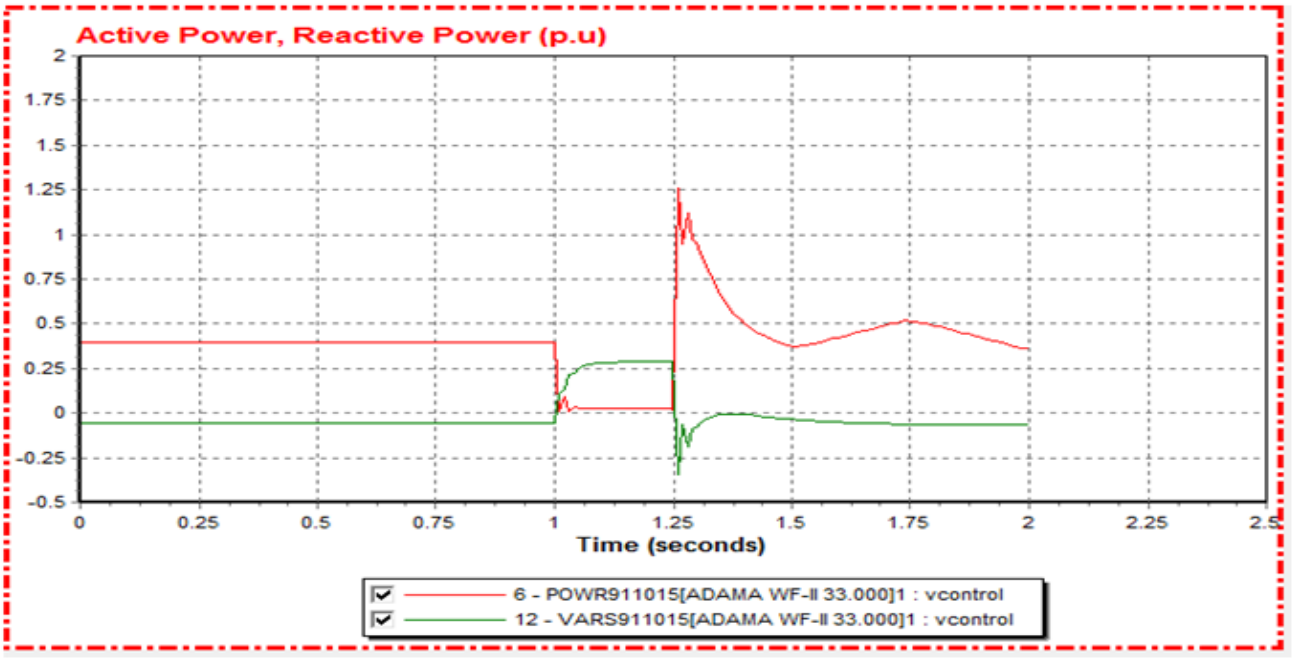

Figure 4. 7 : WTG1active and reactive power response

Therefore, voltage support continues without active power generation even following trips, this benefits weak grids and system with high wind penetration.

4.4 Results Analysis of Dynamic Behavior of the Grid model with Adama II Wind Farm

The dynamic simulations are performed to investigate the model response subjected to grid disturbance. A graphical analysis of the symmetrical short circuit fault on the grid, that is the fault location, is at Hurso where the far end of the WF for 150 ms duration of fault. These can be illustrated in Figures below. The fault lasts for 150 ms and is cleared.

Behavior of the following parameters of the grid and wind farm is analyzed here during and immediately following the disturbance:

- Voltage response at different buses.
- WTG active and reactive power response
- Current response
- Electrical and mechanical power
- WTG speed response
- Pitch angle response

This is the dynamic simulation program which shows the convergence of the solution.

```
SIEMENS POWER TECHNOLOGIES INTERNATIONAL

PTI INTERACTIVE POWER SYSTEM SIMULATOR--PSS(R)E UniversiTHU, JUL 13 2017  16:18

 INITIAL CONDITION LOAD FLOW USED 1 ITERATIONS

 ----------------------------- MACHINE INITIAL CONDITIONS -----------------------------
   BUS# X-- NAME --X BASKV ID  ETERM   EFD    POWER    VARS   P.F.  ANGLE   ID     IQ
 402002 AKAKI2400   400.00 1  1.0000 0.7776    5.54  -24.73 0.2185   2.69-0.2445 0.0669
 911007 M-WAKNA1    13.800 1  0.9726 0.8778    5.63  -11.95 0.4258   8.27-0.1201 0.0634
 911012 M-WAKNA3    13.800 1  0.9703 0.8731    5.05  -11.95 0.3894   8.08-0.1209 0.0572
 911013 M-WAKNA4    13.800 1  0.9605 0.8750   20.00  -11.95 0.8584  17.41-0.0884 0.2259
 911014 M-WAKANA5   13.800 1  0.9874 0.9151   11.26  -11.70 0.6936  10.71-0.1080 0.1241
 911015 ADAMA WF-II 33.000 1  1.0367 0.0000   40.00   -5.24 0.9915   3.00-0.0506 0.3858

 INITIAL CONDITIONS CHECK O.K.

 Channel output file is "C:\Users\Anchinesh\Desktop\Adama II OK\Adama II.out"
```

1 . Response of Voltage at the Faulty Bus (Bus 203004)

After the occurrence of the three-phase short circuit at the Bus 203004, the voltage drop occurs almost in the entire transmission system. More precisely, the closer the location of the fault, the greater will the voltage drop be (can be shown in Figure 4.9). This transient voltage drop lasts as long as the time of activity of protective relays in order to isolate the fault. In Figure 4.8, is shown the impact of short circuit fault at the faulted bus. Response of voltage could be see during and after the occurrence of the fault.After 1s of the short circuit fault occured, the voltage on bus 203004 drops down to 0 p.u and after the clearance of fault the voltage restores to its prefault value ,1.05 p.u.

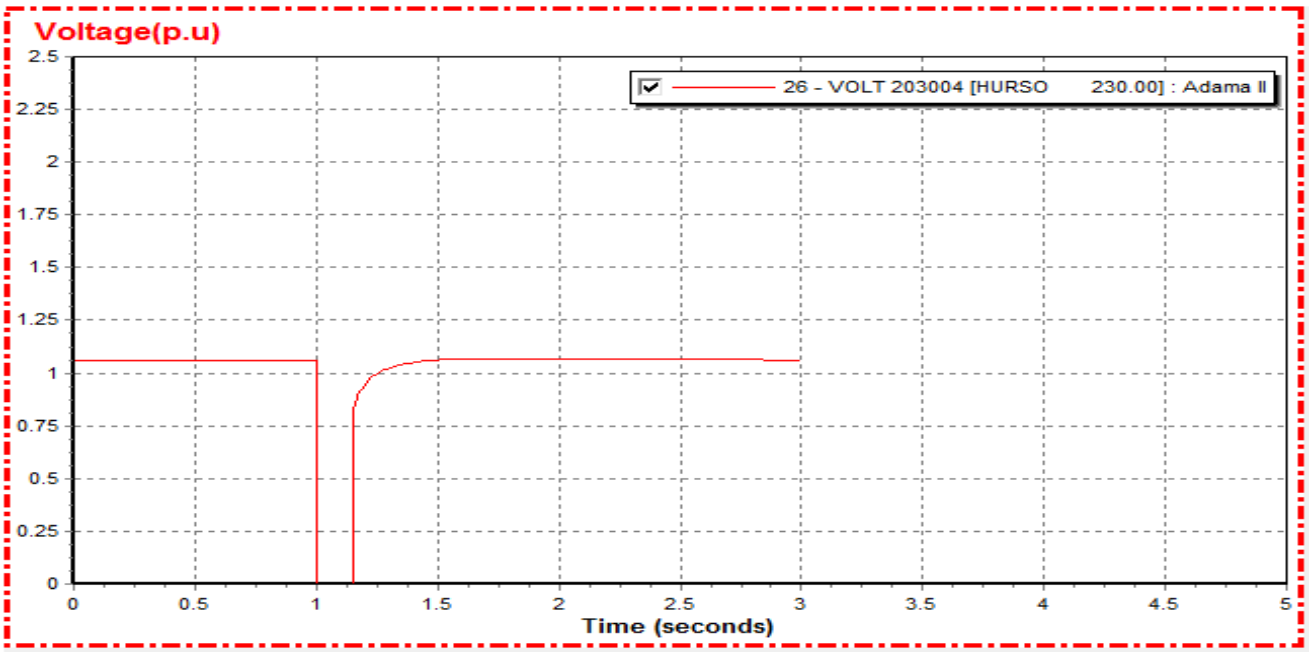

Figure 4. 8: Response of voltage at Hurso, Bus 203004

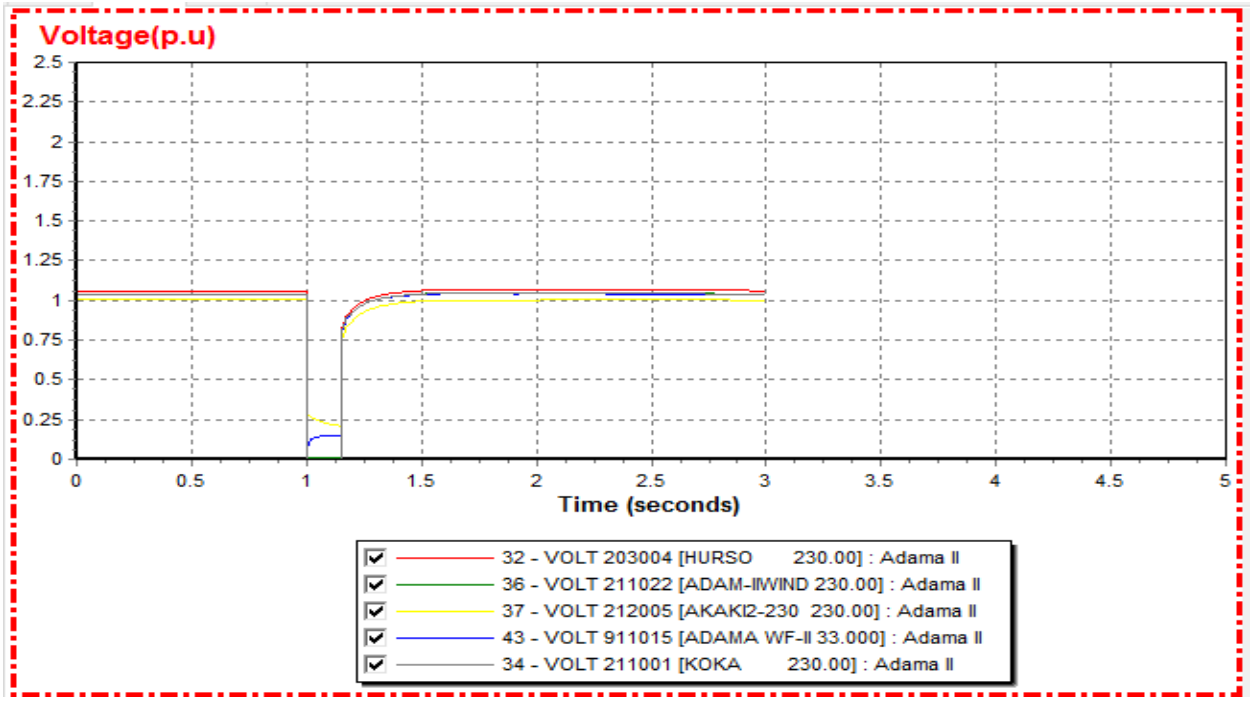

Figure 4. 9: Response of voltage at terminals of different buses during the fault

Therefore,the results indicate that the voltages are under the normal range(0.95-1.05).

2 . Active and Reactive Power Response

It can be seen in Figure 4.10 prior to the fault, the reactive power is almost zero and the wind farm operated at unity power factor. It can be seen that each WTG units during the fault provide reactive power support to the grid, as is required by the wind grid code.

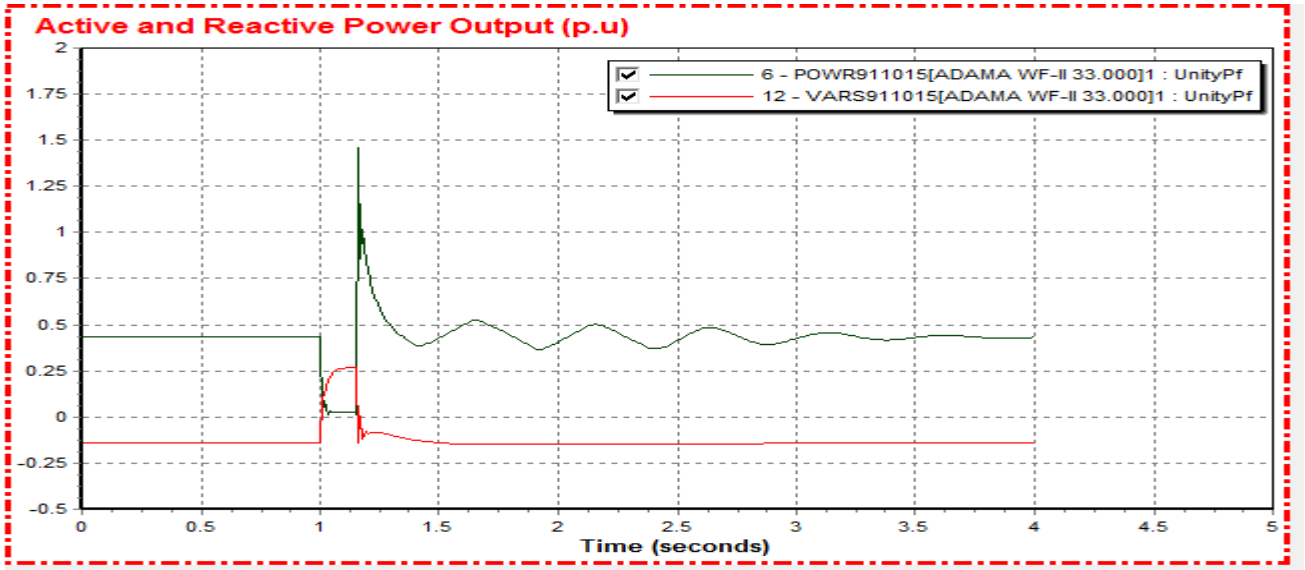

Figure 4. 10: Active and reactive power profile

3 . Current Response

The output current profile is shown in Figure 4.11. It can be seen the current level during fault is in between 0.391 p.u to 1.872 p.u and as the magnetizing impedance of generator is much bigger than its stator and rotor impedances it can be assumed whole current goes through the rotor-side converter and rotor winding. The converters are normally designed for a 10% overload and therefore flowing of the high current during fault will likely violate the rotor converter current limit and can damage the IGBTs inside converters.

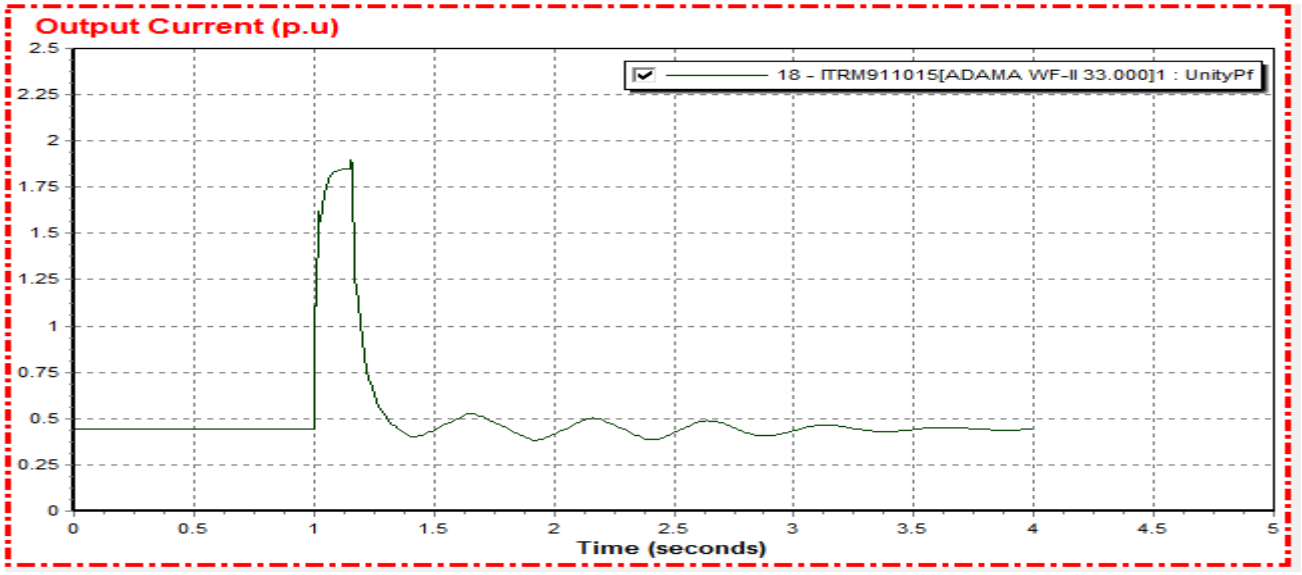

Figure 4. 11: Current profile

4 . Electrical and Mechanical Power

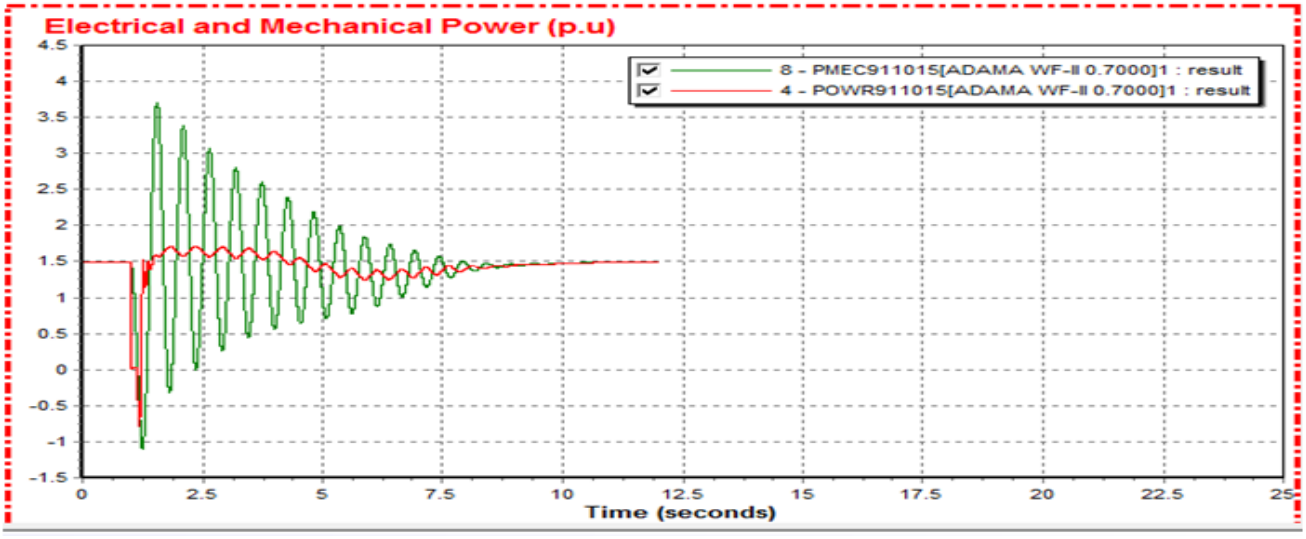

Figure 4.12: Electrical and mechanical power

As seen in Figure 4.12, as the fault occurred the electrical power suddenly decreases to a very low value and the difference between mechanical input power and electrical output power make an increasing in the rotor speed and therefore the rotor starts to accelerate. Both electrical and mechanical power oscillate around 12 seconds after fault is cleared, then it recovers to the pre-fault value after 12 seconds.

The peak of the mechanical power is considerably high, which is around 3.7 p.u during the first cycle of the oscillation. The scale of this magnitude indicates that the mechanical stress in the drive train is quite high.

During the fault, the mechanical input power is reduced by pitch control mechanism. The PMEC911015 plot shows the damped mechanical power output of the wind turbine due to the pitch controller action. It is assumed that the wind turbine works at its rated power at the fault instant. As the fault duration and the transient of voltage recovery is short, the wind speed can be assumed constant in the grid fault simulations.

5. WTG1 Speed Response during the Fault

Figure 4.13 shows the generator rotor speed response after the occurrence of the fault at Koka busbar for 150 ms. The generator speed is oscillating for about 8 seconds after the fault. After the fault is cleared, the rotor speed recovers to the pre-fault value at some 16 seconds later.

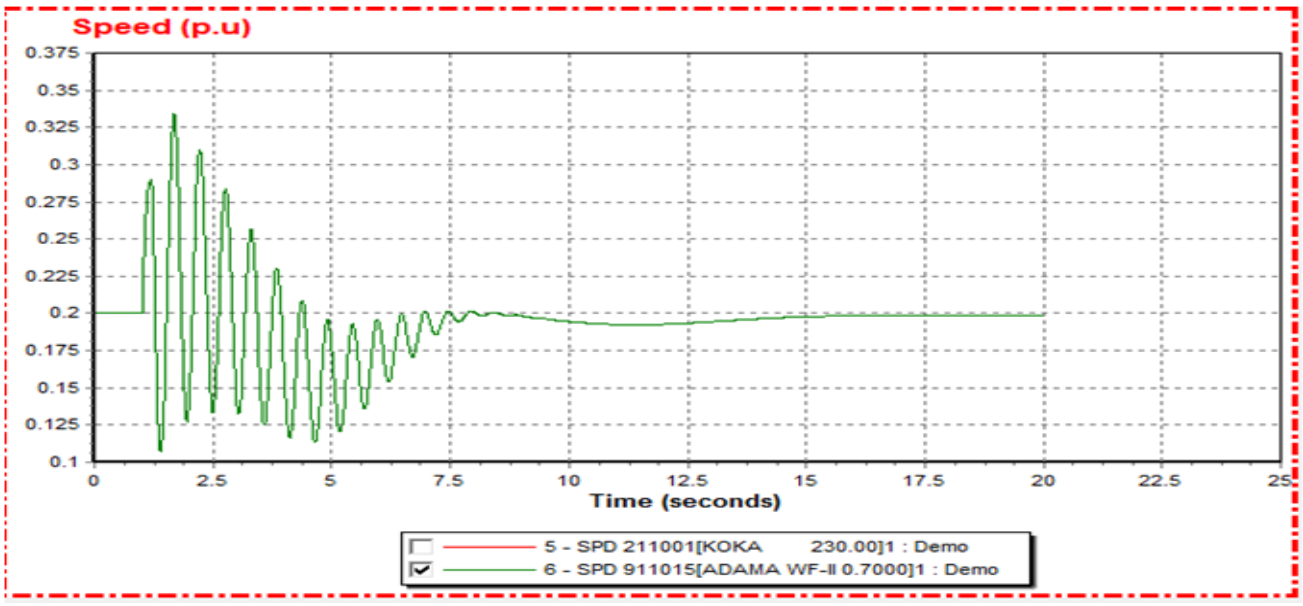

Figure 4. 13: WTG1 speed response during the fault

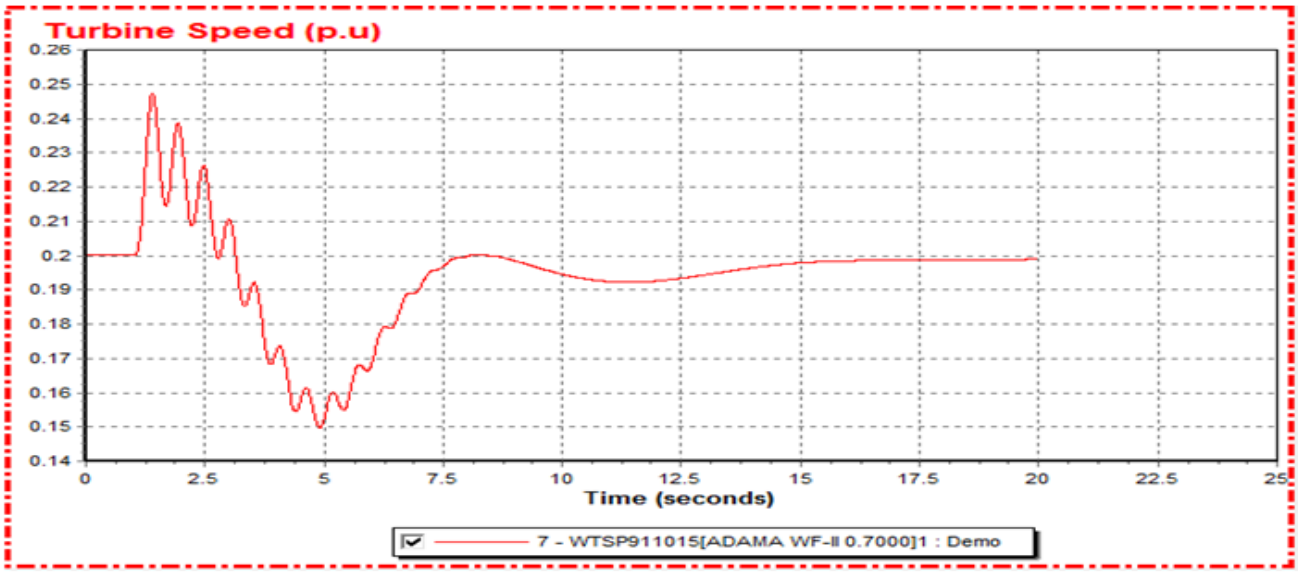

Figure 4. 14: Turbine speed response during the fault

6. Pitch Angle Response

As shown in Figure 4.15, the pitch angle is increased during the fault in order to reduce the power input from wind turbine. The pitch angle is oscillating; this is because the pitch angle is controlled by the speed of the turbine. After fault clearance, the turbine shaft speed decreases (can be seen in Figure 4.14), while the pitch angle increases due to the effect of pitch compensation controller trying to reduce the input power to the turbine by increasing the pitch angle.

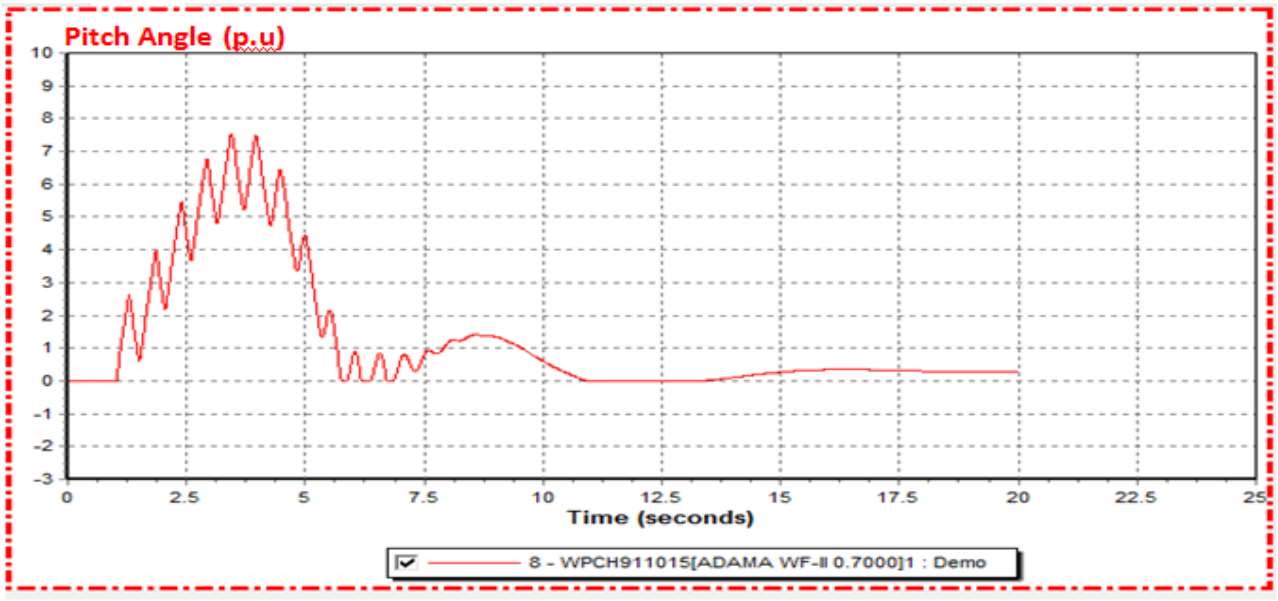

Figure 4. 15: Pitch angle response during the fault

4.5 Results Analysis of DFIG Voltage Control Strategy

The interaction between the power system and the generic wind turbines model during a grid fault is assessed through simulations in PSS/E. The analyses focus on DFIG voltage control effect.

The following simulations illustrate the effect of the DFIG voltage control on both the power system (at the PCC) and the wind generator terminal voltage stability during the grid fault . Case 1: The DFIG is not equipped with voltage control capability,and Case 2: The DFIG is equipped with voltage control capability.

The disturbance in the simulation study is a three-phase symmetrical short-circuit fault at the PCC (Koka bus). The fault duration is 150 milliseconds.During the fault the voltage at PCC is dropped to zero and thus no electrical power transfer from wind turbine to the grid.

The DFIG Equipped with/without Voltage Controller

The simulation study in PSS/E, when the reactive control mode of the model is set to a constant reactive power (varflg=0 **)** the current in q-direction is also constant during the fault .when Qmax and Qmin =0,i.e the turbine maintains a power factor of unity(it can be observed in Appendix D) in this case the DFIG is not equipped with voltage controller. It was found that the voltage at Adama II WF is 1.056 p.u which exceeds the normal limit of 1.05 p.u . It has been shown in Figure 4.16 that the DFIG equiped without voltage controller cannot recover to normal acceptable grid voltage .

In the second case ,simulation study in PSS/E, the vltflg is set to 1 **.** This means that the terminal voltage control is enabled. The reactive power command is equal to the reference value and the internal voltage magnitude is limited in the closed loop controller. The upper and lower limits of the internal voltage magnitude are Vterm+XIQmax and Vterm+XIQmin, respectively. In the simulation, the voltage drop limits XIQmax and XIQmin must be set by user (it can be observed in Appendix D.2). It was found that using the typical voltage drop limit values given in PSS/E, i.e. XIQmax=0.6, the voltage at Adama II WF is 1.035 p.u .So that the DFIG equiped with voltage controller is able to recover following a grid fault after 1.625 sec.This can be illustrated in Figure 4.16. If the upper and lower limits of the voltage controller are fixed; rather it is dependent on the terminal voltage level in second case.

Figure 4.18 shows effects of DFIG voltage control at the terminal of the wind farm and as a result the voltage is successfully recovered with 1.625 sec. with maximum voltage drop limit set at 0.6.

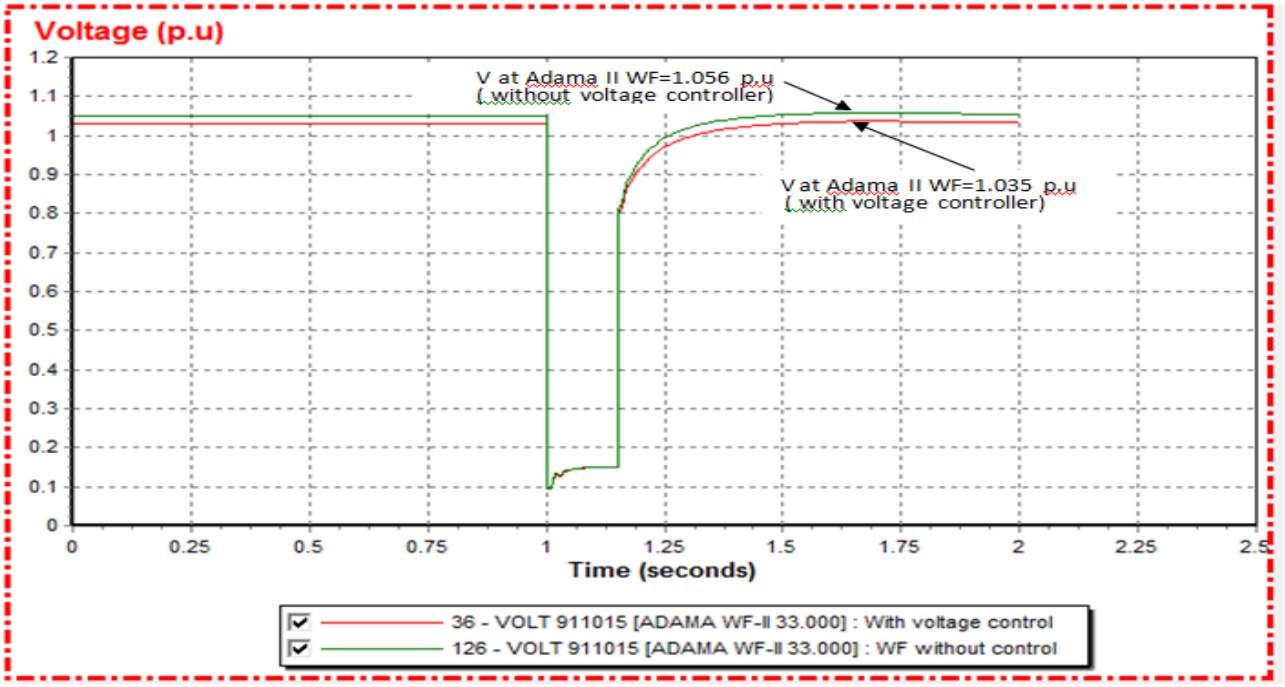

Figure 4. 16:Effects of DFIG voltage control capability at the wind farm bus

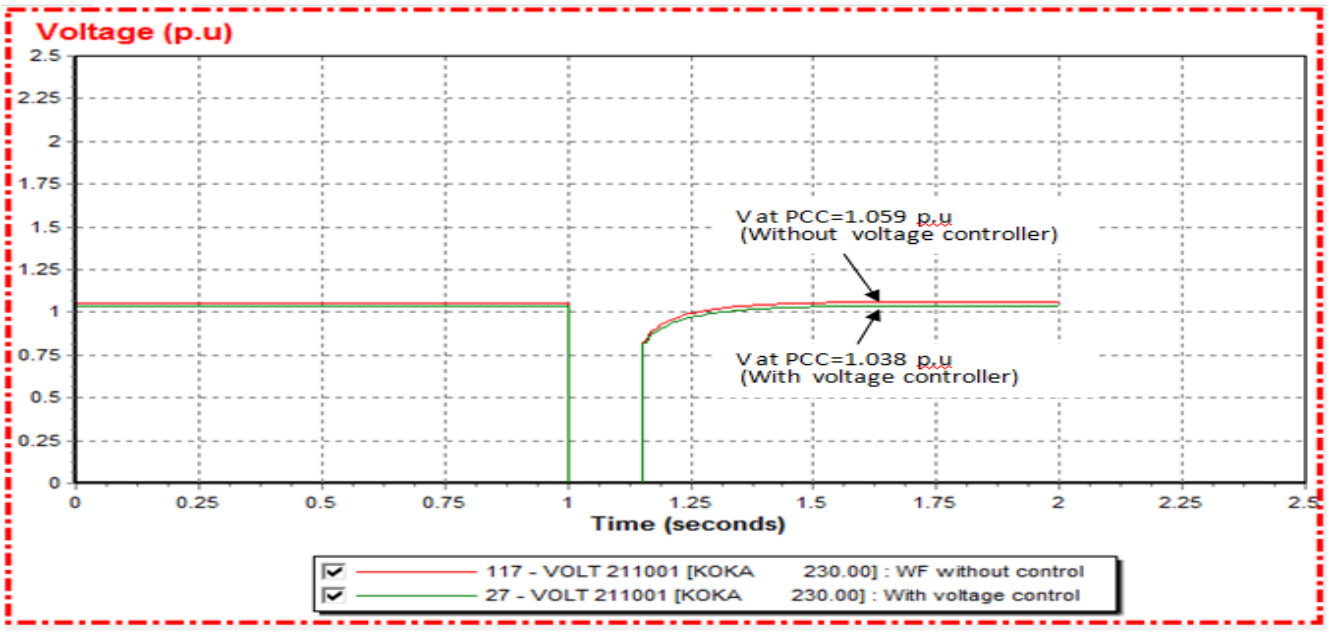

Figure 4. 17 :Effects of DFIG voltage control at PCC

The wind turbine terminal voltage has a similar pattern, except that during the fault the retaining terminal voltage is 0.15 p.u, which is considerably higher than the PCC voltage.

Figure 4.17 shows that during the fault voltage on the PCC drops to zero. After fault clearing, the voltage gradually recovers 1.038 p.u with voltage control strategy but the DFIG equiped without

voltage controller cannot recover to normal acceptable grid voltage, since the voltage at PCC is 1.059 p.u which exceeds the normal limit of 1.05 p.u.

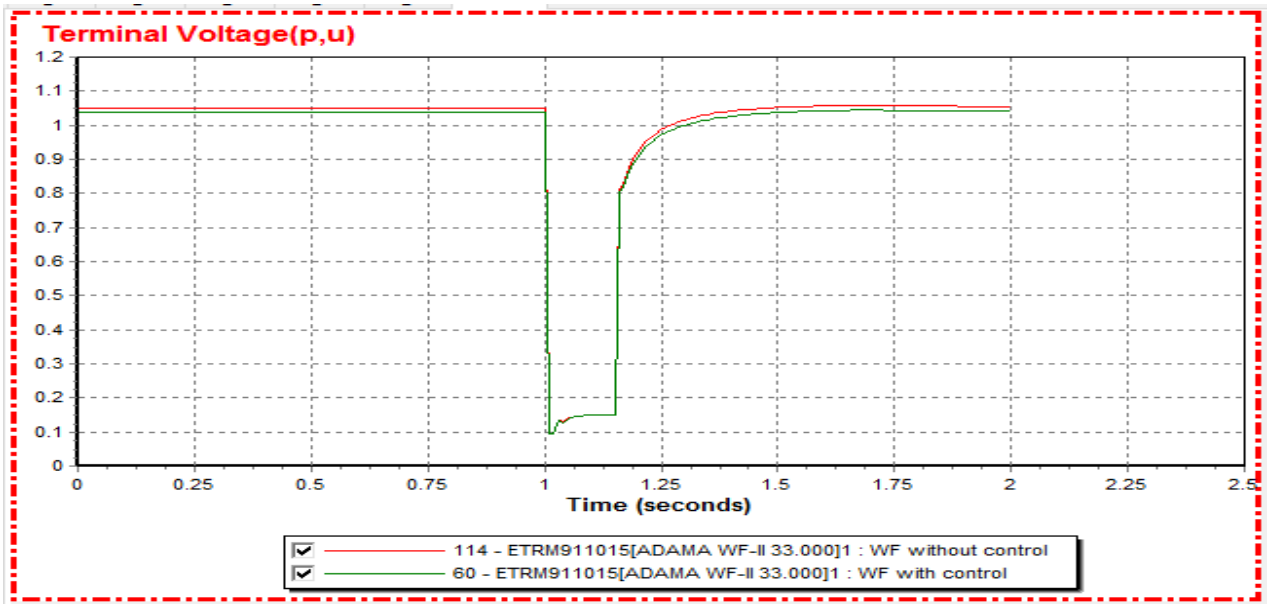

Figure 4. 18 Effects of DFIG voltage control at the terminal of the wind farm

Dynamic simulations were carried out ,and these simulation results indicated in Figures 4.16 - 4.18 that, terminal voltage variation is smoothest in the case of DFIG variable-speed wind turbines with enabled voltage control capability since it enhances the DFIG wind turbine capability during grid faults as compared to DFIG WT not equipped with voltage control capability. Therefore as observed in Figures 4.17, wind turbines possess enough capability to inject reactive power into the PCC to support the voltage during short-circuit when equipped with voltage controller. And also the wind farm is able to fulfill the slow and fast control characteristics as spelt out in international grid codes.

4.6 Results of the Wind Turbine / Wind Power Plant Voltage Control

According to section 2.4.1 wind power plant voltage control characteristic will be applied for analyzing its influence on the power system voltage stability.

In order to evaluate the effects of the wind power plant voltage control on the power system voltage stability, two simulations are carried out. Two cases are employed to verify the contribution of wind power plant voltage control: Case 1: With both the wind turbine/wind power plant and synchronous generator voltage controller and Case 2: Only with the wind turbine/wind power plant voltage controller.

Case 1: Regulation of Voltage on the Power System with both Controller

A three phase short circuit of 150 ms (on t=1.0 s) at the PCC (Koka) is simulated. Voltage at the Koka and Adama II wind farm are employed to demonstrate the system voltage behavior.

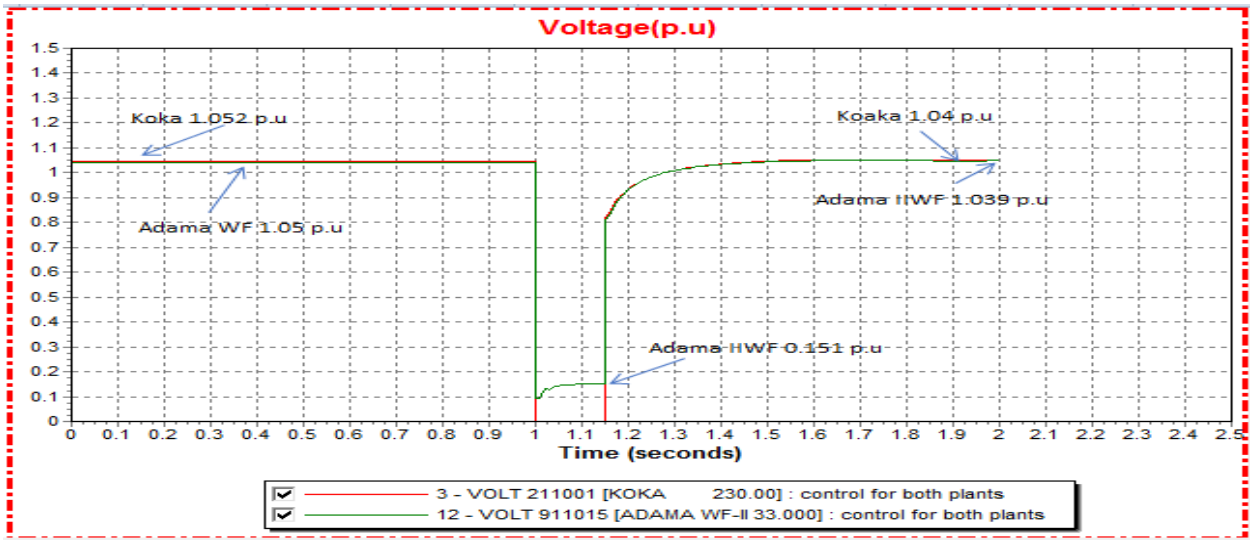

Figure 4. 19:Case 1. Voltage at the PCC and Adama II Wind Farm

Case 2: Regulation of Voltage on the Power System with only WT/WP Controller

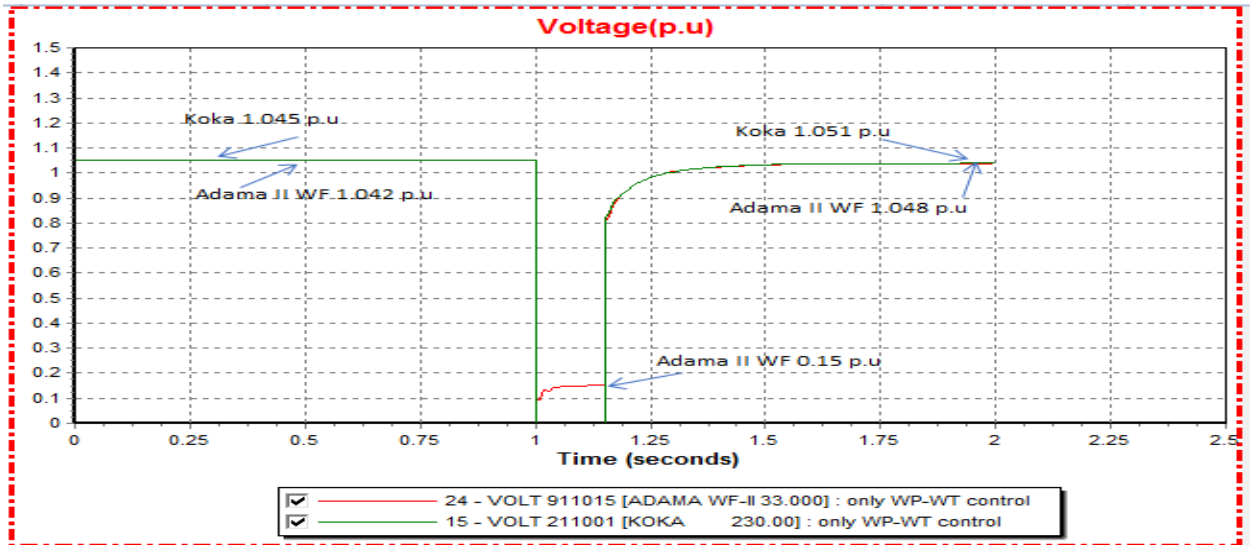

Figure 4.20:Case 2. Voltage at the PCC and Adama II Wind Farm

In Figure 4.19 and Figure 4.20, the voltages at the PCC and WG are illustrated. The effect of the wind turbine voltage controller can be visible and it improves the system voltage stability. As a result, the control of individual wind turbine regulates total wind plant reactive power.

4.7 Performance Analysis of the Wind Farm in Weak Grid

Since there is a high probability of the standard voltage values being violated, it is necessary to consider possible voltage fluctuations and limit violations in weak grids. In general, with and without wind power the issue of interest is the amount of voltage limit that can be observed at remote bus bar of which the far end of the wind farm with which the maximum (peak) load and light load is connected. The influence of the point of electrical interconnection between a wind farm and the rest of the power system on the bus voltage performance has been analyzed in Table 4.8.

Table 4. 8: Voltages of system light and peak load with wind farm and with no wind farm connection

Bus Name	Bus Number	Voltage of Light load With WF (p.u)	Voltage of Light load Without WF (p.u)	Voltage of Peak load With WF (p.u)	Voltage of Peak load Without WF (p.u)	Transmission line distance from Adama II WF(km)
ADAM-IIWIND	211022	1.0158	1.0296	1.0000	1.0000	0
KOKA	211001	1.0197	1.0328	0.9987	0.9984	10
AKAKI2-230	212005	1.0172	1.0305	0.9811	0.9808	97
AWSH-7KL	210001	1.0220	1.0353	0.9822	0.9820	129
M-WAKNA	211002	1.0000	1.0000	1.0000	1.0000	163
HURSO	203004	1.0495	1.0639	0.9342	0.9339	315

So studying the effects of such an electrical connection on voltage performance is also important for this work. In the present study, several interconnection scenarios have been analyzed by using the system light load with WF, system light load without WF, system peak load with WF and system peak load Without WF.

Figure 4.21 reveals this fact by connecting wind turbines at one of the remote end substations of the Ethiopian power system or the feeder substation, Hurso in this case at far end of the wind farm.

The voltage profile of six buses 211022, 211001, 212005,210001,211002 and 203004 are considered with the two cases only, the first case is system light load With WF and secondly system peak load Without WF to illustrate voltage profile of a weak grid. The voltage level is shown for no wind farm connection and with wind farm connection both for maximum and minimum loading conditions.

When no wind turbines are connected to the grid the main concern for utilities is that minimum voltage level which will be experienced at the far end of the feeder (in this case at Hurso) when consumer load is at its maximum. So the voltage profile for a feeder is that the highest voltage at the substation bus bar and it drops to reach the minimum at the far 0.934 p.u below the acceptable range.

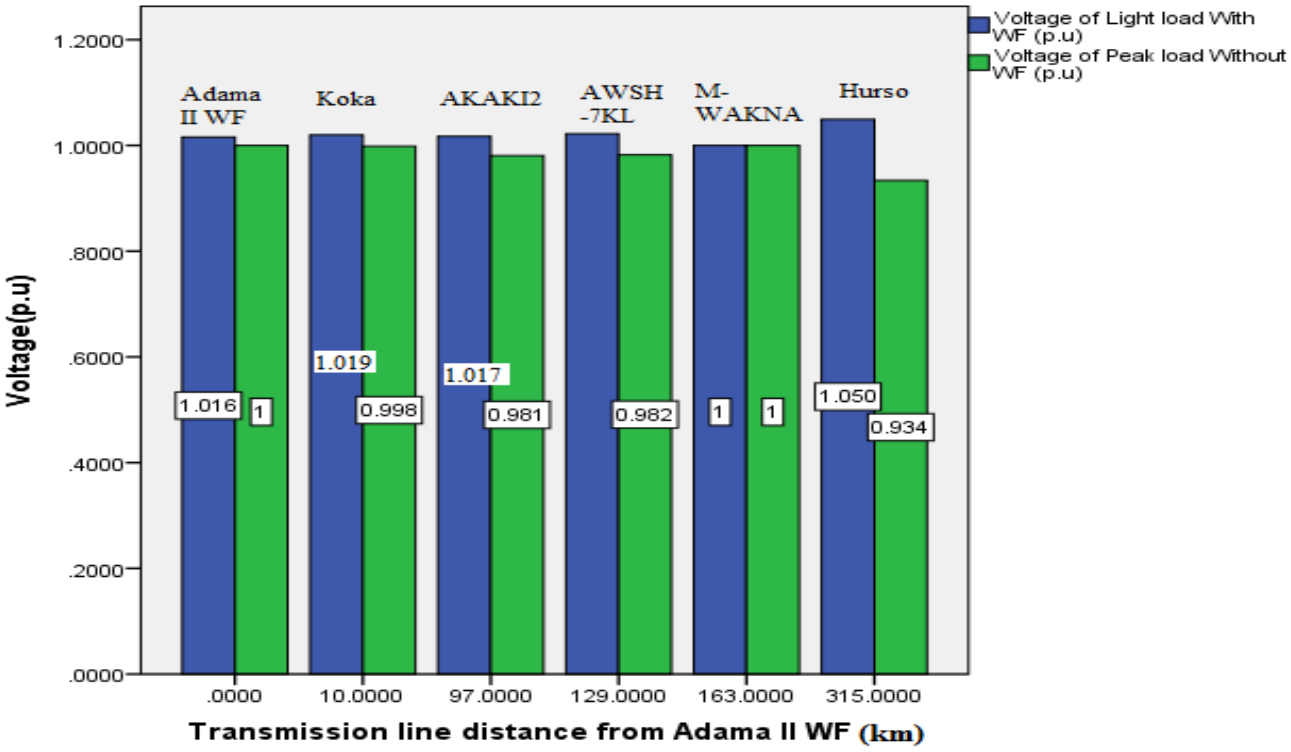

Figure 4. 21. Voltage profile for buses at different location of system light and peak load with wind farm and with no wind farm connection

Therefore the settings of the transformers by the utility during low load is such, that the voltage at the consumer closest to the substation will experience a voltage close to the maximum value (blue bar) and that the voltage is close to the minimum value at the far end when the load is high (green bar). This operation ensures that the capacity of the feeder is utilized to its maximum.

The situation is completely different when wind turbines are connected to the feeder. Due to the power production at the wind turbine the voltage level will be higher than in the no wind case (green bar). The voltage level can even exceed the maximum allowed when the consumer load is low and the power output from the wind turbines is high. This is what limits the capacity of the feeder. The voltage profile of the feeder depends on the line impedance, the point of connection of the wind turbines and on the wind power production and the consumer load.

CHAPTER 5

5 Conclusions, Recommendation and Future Work

5.1 Introduction

In this study, analysis of dynamic voltage stability and also assessment of technical requirements of the integrated Adama II wind farm on Ethiopian grid has been performed. For this purpose, a simplified model of Ethiopian power system was set up that has been used for static and dynamic studies of the impact of wind power on this system. Before integrating the wind farm an aggregation technique was developed to reduce the wind farm from multi number of turbine representation in to single turbine representation for stability analysis.

5.2 Conclusions

The thesis analyzes the voltage control capability of the farm that has been implemented on Adama II wind farm during a short circuit fault at PCC to study its influence on the power system dynamic voltage stability. In order to evaluate the effects, two cases are employed. These simulations are carried out on the wind generator terminal voltage equipped with and without voltage controller.

Adama II wind farm with FTR is aggregated to STR and the developed model has been verified for its accuracy. The result of the simulation has given 0.1 MW (0.065% of total active power transferred) and 0.008 MVAR reactive power flow (0.57% of the total reactive power transferred) difference between full turbine representation and single turbine representation of Adama II WF.

After carried out detailed analysis of the contingency scenario of that a bolted symmetrical three-phase fault applied at the PCC for 150 ms then is cleared, based on this analysis the compliance of the grid code: Fault Ride-Through capability, voltage regulation at PCC; active and reactive power behavior of the wind farm could be investigated. After fault clearance, the voltage recovers to 1.032 p.u at the PCC and within 0.6 second following the fault clearance other buses restored to the super grid voltage, and also the active and the reactive power restored to 0.9 of the pre fault value. The results show the wind farm integrated to the power grid fulfill the wind grid code requirements.

The voltage at the PCC gradually recovers to 1.038 p.u with voltage control strategy and 1.059 p.u without voltage controller that exceeds the normal limit of 1.05 p.u, after the clearance of short circuit fault.

It is concluded that the capability of DFIG wind farm controller can improve power system dynamic behavior. Finally, the wind farm performance in weak grid application has been discussed. This can be observed when no wind farm is connected to the remote end substations of the grid, Hurso in this case at far end of the wind farm at its maximum load .The voltage profile of the substation bus bar drops to the minimum, 0.934 p.u below the acceptable range. On the other hand, the voltage level can exceed the maximum allowed when the power output from the wind farm is high are connected with the low load at Hurso, the voltage reach the maximum 1.0639 p.u above the acceptable range.

In conclusion, the thesis study has revealed analysis of the dynamic voltage stability on Adama II wind farm penetration into the existing Ethiopian grid using PSS/E 33 simulation software.

5.3 Recommendation

The investigations carried out in this thesis reveal that DFIG wind farm controllers can improve power system dynamic voltage stability. Therefore, it is recommended that EEP may equip all wind farms with voltage controllers so that the voltages at selected nodes in the high voltage grid can be controlled.

5.4 Suggestions for Future Work

- Further work as extention of this Master thesis may be to consider the grid including all the wind farms and carryout detailed investigations concerning the production and absorption of reactive power at the wind farms.
- The model considered in this study does not include the rotor voltage and current limiters. Thus, a model including the influence of rotor current and voltage limits on the wind turbine may be developed to investigate the voltage stability of the integrated system.
- The dynamic voltage stability of the wind farm on the power system has been investigated in the present work. As the wind farm is going to be a major source of power in future, it may originate new challenges such as system security, power quality and system stability problems. Research work may be carried out to investigate the effects of wind farm integration on system security, power quality and power system stability.

References

[1] L. Munteanu, A. L. Bratcu, N.-A. Cutulilis, and E. Ceanga. " Optimal Control of Wind Energy Systems, Springer."

[2] F. Shewarega, I. Erlich and José L. Rueda. "Impact of Large Offshore Wind Farms on Power System Transient Stability ." Seattle, 2009.

[3] Getachew Bekele, Abdulfetah Abdela. "Investigation of Wind Farm Interaction with Ethiopian Electric Power Corporation's Grid." Energy Procedia_, Addis Ababa,Ethiopia: ELSEVIER Ltd., 2012.

[4] Belachew Bantyirga Gessesse . "Integration of Large Wind Farms into Weak Power Grids – Emphasis on the Ethiopian Interconnected System (ICS) ." 2013

[5] MOHAMMAD SEYEDI . "Evaluation of the DFIG Wind Turbine Built-in Model in PSS/E ." Sweden, 2009.

[6] Gabriele Michalke. "Variable Speed Wind Turbines - Modelling, Control, and Impact on Power Systems." 2008.

[7] Thomas Ackermann. *Wind Power in Power Systems.* Stockholm, Sweden, 2005 .

[8] Mohamed Amer Hassn Abomahdi , Manish Kumar Srivastava . "Control of Grid Voltage and Power of Doubly Fed Induction Generator wind turbines during grid faults ." *IOSR Journal of Electrical and Electronics Engineering (IOSR-JEEE)*, Jul – Aug. 2014: PP 12-21 .

[9] Anca D. Hansen,Gabriele Michalke,Poul Sørensen and Torsten LunCo-ordinated Voltage Control of DFIG Wind Turbines in Uninterrupted Operation during Grid FaultsWIND ENERGY Denmark 2006

[10] Teshale Taddese. "Study of Doubly Fed Induction Generator Control under Grid Fault Conditions." Addis Ababa,Ethiopia, May,2016.

[11] Chen, Z. "Issues of Connecting Wind Farms into Power Systems ." IEEE/PES Transmission and Distribution Conference & Exhibition. Asia and Pacific Dalian, China, 2005.

[12] J. Hossain and H. R. Pota,2014.

[13] P.Kundur. *Power System Stability and Control.* 1994.

[14] Ö.S. Mutlu, E. Akpınar, and A. Balikci. "Power Quality Analysis of Wind Farm Connected to Alacati Substation in Turkey." *Renewable Energy Journal*, 2009: pp. 1312–1318.

[15] I. de Alegria, J. Andreu, J. Martin, P. Ibanez, J. Villate, and H. Camblong. "Connection requirements for wind farms:A survey on technical requierements and regulation." Renewable and Sustainable Energy Reviews (2007): pp. 1858–1872.

[16] J. Hethey and M. S. Leweson. "Probabilistic Analysis of Reactive Power Control Strategies for Wind Farms." M.Sc. thesis, 2008.

[17] Li-Jun Cai, István Erlich and Jens FortmanDynamic Voltage Stability Analysis for Power Systems with Wind Power Plants using Relative Gain Array (RGA)

[18] Akhmatov V. "Electrical Power and Energy Systems." System Stability Of Large Wind Power Networks A Danish Study Case, 2006.

[19] E. Muljadi, C. Butterfield, a. Ellis, J. Mechenbier, J. Hochheimer, R. Young, N. Miller, R. Delmerico, R. Zavadil, and J. Smith. "Equivalencing the collector system of a." 2006: p. 9 .

[20] Ethiopian Energy Authority(EEA). "Ethiopia National Electricity Transmission Grid Code – Draft Version 02." February,2016.

[21] J.H KEHLER. "Wind Power Facility Technical Requirements." November 15, 2004.

[22] I. Erlich, M. Wilch and C. Feltes. "Reactive Power Generation by DFIG Based Wind Farms with AC Grid Connection ."

[23] Eduard Muljadi Abraham Ellis . *Western*

[24] *Ordinance on System Services by Wind Energy Plants (System Service Ordinance – SDLWindV)[Online]. Available: http://www.erneuerbare-energien.de.* [Online]. Available: http://www.erneuerbare-energien.de.

[25] Lars Lindgren, Jörgen Svensson and Lars Gertmar . "Generic models for Wind Power Plants Needs and previous work ." Elforsk rapport , July, 2012.

[26] Nicholas W. Miller . "Voltage And Reactive Power Control." *BPA Voltage Control Technical Conference.* August 23, 2011 .

[27] Patterson, J. "Final project report western electric coordinating council wind." 2014.

[28] M. P. Panumpabi. "Large wind farm aggregation and model validation." 2011.

[29] H. Eshetu . "Investigation and analysis of ashegoda wind farm integration impact onEthiopia power grid ." 2010.

[30] Mesfin Megra . "Impact of Large Scale Wind Power Integration on Ethiopian Power System Transient Stability ." March, 2017:p30,33

Appendices

Appendix A

A. Micrositting of Adama II wind farm

ADAMA Ⅱ WIND POWER PROJECT
GENERAL LAYOUT
(Adama二期风电场工程总平面布置图)

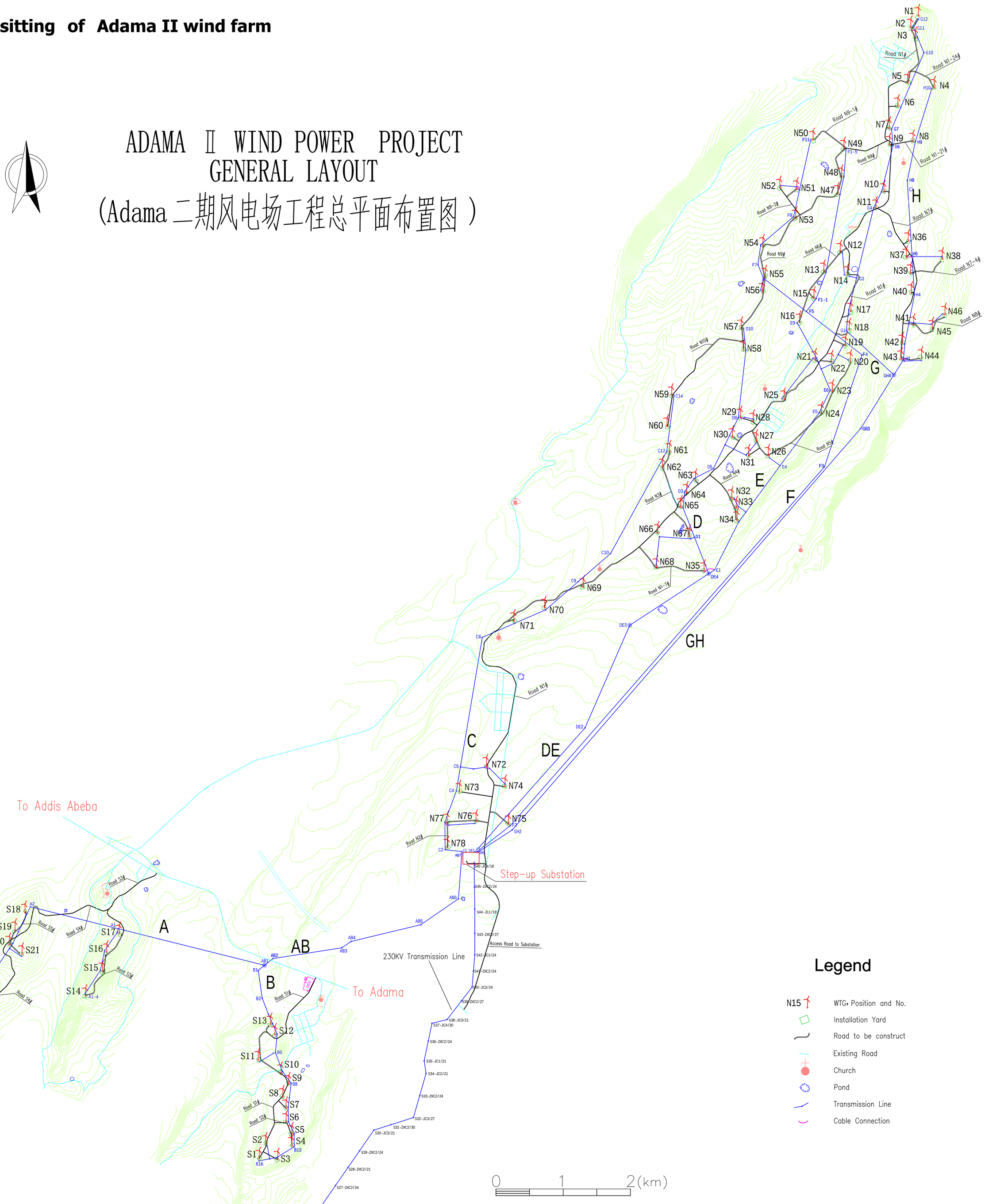

PROJECT	ADAMA Ⅱ WIND POWER PROJECT						
EMPLOYER	ETHIOPIAN ELECTRIC POWER CORPORATION (EEPCo)						
CONTRACTOR	HYDROCHINA-CGCOC JV						
DESIGNER	中国水电顾问集团北京勘测设计研究院 HYDROCHINA BEIJING ENGINEERING CORPORATION					PAGE	
						SHEET	
			DESIGENED			SCALE	
			CHECKED		LAYOUT OF ADAMA Ⅱ WIND POWER PROJECT		
			AUDITED			VER.	
REV.	DATE	DESCRIPTION	APPROVED		DWG. NO.	00	

Appendix B: Technical Data for the Cable and Overhead Line

TableB.1: Technical Data for the Cable and Overhead Line

	Type	R (ohm/km)	X (ohm/km)	C (µF/km)
Under Ground cable	ZRC-YJV22-3*50	0.494	0.143	0.155
	ZRC-YJV22-3*95	0.246	0.116	0.233
	ZRC-YJV22-3*95	0.246	0.128	0.188
	ZRC-YJV22-3*185	0.128	0.105	0.275
Over Head TL	LGJ-95	0.015	0.01	0.27

Appendix C: Parameters of all the Clusters of Adama II Wind Farm

Table C.1: GPS data, distance between each tower and branch impedance of all clusters

Cluster A									
Tower ID No.	Y(m)	X(m)	Branch		Distance (Km)	R(pu / kM)	X(pu/ kM)	C(µF/ km)	Z (pu/ kM)
			From	To					
S 14	944583.1	517705.6	S 14	S 15	0.45	0.011	0.005	0.270	0.012
S 15	944955.2	517959.1	S 15	S 16	0.29	0.007	0.003	0.270	0.008
S 16	945238.8	518020.9	S 16	S 17	0.33	0.008	0.003	0.270	0.009
S 17	945516.4	518207.1	S 17	CCG1	0.10	0.003	0.001	0.270	0.003
S 18	945829.5	516805.6	S 18	CCG1	1.40	0.035	0.014	0.270	0.038
S 19	945564.4	516657.8	S 19	S 18	0.30	0.008	0.003	0.270	0.008
S 20	945353.4	516572.1	S 19	S 20	0.23	0.006	0.002	0.440	0.006
S 21	945211.1	516761.8	S 20	S 21	0.24	0.006	0.002	0.270	0.006
S 22	944405.9	516021.5	S 21	S 22	1.09	0.027	0.011	0.270	0.029
S 23	944187.0	515947.1	S 22	S 23	0.23	0.006	0.002	0.270	0.006
S 24	944001.8	516018.5	S 23	S 24	0.20	0.005	0.002	0.440	0.005
Cluster B									
S1	942168.1	520288.1	S1	S2	0.24	0.006	0.002	0.270	0.006
S2	942385.6	520384.9	S2	S3	0.29	0.007	0.003	0.270	0.008
S3	942152.1	520563.6	S3	S4	0.30	0.007	0.003	0.270	0.008
S4	942358.7	520774.3	S4	S5	0.18	0.004	0.002	0.270	0.005
S5	942536.0	520774.0	S5	S6	0.20	0.005	0.002	0.270	0.005
S6	942713.6	520687.9	S6	S7	0.20	0.005	0.002	0.270	0.005
S7	942917.4	520687.9	S7	S8	0.18	0.004	0.002	0.270	0.005
S8	943086.2	520639.4	S8	S9	0.21	0.005	0.002	0.270	0.006

Tower ID No.	Y(m)	X(m)	Branch		Distance (Km)	R(pu / kM)	X(pu/ kM)	C(μF/ km)	Z (pu/ kM)
			From	To					
S9	943279.6	520727.9	S9	S10	0.20	0.005	0.002	0.270	0.005
S10	943441.0	520614.8	S10	S11	0.39	0.010	0.004	0.270	0.011
S11	943638.4	520273.9	S11	S12	0.45	0.011	0.004	0.270	0.012
S12	944008.3	520522.9	S12	S13	0.17	0.004	0.002	0.270	0.005
S13	944164.8	520458.7	S13	CC	3.57	0.053	0.038	0.440	0.065
Cluster C									
N59	953525.3	526422.1	N59	N60	0.47	0.012	0.005	0.270	0.013
N60	953063.8	526352.7	N60	N61	0.38	0.010	0.004	0.270	0.010
N61	952684.0	526390.6	N61	N62	0.25	0.006	0.003	0.270	0.007
N62	952452.6	526283.9	N62	N69	2.14	0.053	0.021	0.270	0.057
N69	950671.6	525106.4	N69	N70	0.65	0.016	0.006	0.270	0.017
N70	950364.8	524534.2	N70	N71	0.50	0.013	0.005	0.270	0.013
N71	950165.1	524074.3	N71	N72	2.46	0.062	0.025	0.440	0.066
N74	947705.8	523943.9	N74	N72	0.41	0.010	0.004	0.270	0.011
N72	948012.1	523667.6	N72	N73	0.56	0.014	0.006	0.440	0.015
N73	947627.2	523267.0	N73	N77	0.50	0.013	0.005	0.270	0.014
N76	947185.9	523511.1	N76	N77	0.43	0.011	0.004	0.270	0.012
N77	947169.4	523083.2	N77	N78	0.37	0.009	0.004	0.440	0.010
N78	946794.7	523087.2	N78	CC	0.15	0.002	0.002	0.440	0.003
Cluster D									
N57	954520.9	527455.0	N57	N58	0.33	0.008	0.003	0.270	0.009
N58	954196.9	527490.3	N58	N29	1.00	0.025	0.010	0.270	0.027
N28	953134.7	527633.2	N28	N29	0.20	0.005	0.002	0.270	0.005
N29	953195.3	527445.9	N29	N30	0.31	0.008	0.003	0.270	0.008
N30	952904.5	527326.0	N30	CCG2	0.85	0.013	0.009	0.270	0.015
N27	952843.8	527678.3	N27	N31	0.25	0.006	0.003	0.270	0.007
N31	952620.8	527564.5	N31	N30	0.37	0.009	0.004	0.440	0.010
N63	952258.8	526775.1	N63	N64	0.23	0.006	0.002	0.270	0.006
N64	952073.0	526645.5	N64	N65	0.23	0.006	0.002	0.270	0.006
N65	951862.4	526556.8	N65	CCG3	0.46	0.007	0.005	0.270	0.008
N68	950968.2	526196.4	N68	N66	0.51	0.013	0.005	0.270	0.014
N66	951475.5	526213.4	N66	N67	0.47	0.012	0.005	0.270	0.013
N67	951424.2	526684.7	N67	CCG4	5.00	0.074	0.053	0.440	0.091

Cluster E									
Tower ID No.	Y(m)	X(m)	Branch		Distance (Km)	R(pu / kM)	X(pu/ kM)	C(µF/ km)	Z (pu/ kM)
			From	To					
N16	954609.9	528324.1	N16	N21	0.61	0.015	0.006	0.270	0.016
N25	953467.7	528093.3	N25	N21	0.74	0.019	0.007	0.270	0.020
N21	954050.2	528555.0	N21	CCG1	0.25	0.004	0.003	0.270	0.004
N22	954023.4	528800.7	N22	N21	0.25	0.006	0.002	0.440	0.007
N19	954265.0	529004.5	N19	N20	0.25	0.006	0.002	0.270	0.007
N20	954030.9	529079.0	N20	CCG2	0.28	0.004	0.003	0.270	0.005
N23	953586.0	528809.9	N23	N24	0.37	0.009	0.004	0.270	0.010
N24	953257.0	528647.6	N24	N26	1.01	0.025	0.010	0.270	0.027
N26	952623.9	527858.4	N26	CCG3	1.06	0.027	0.011	0.270	0.029
N32	951994.7	527314.2	N32	N33	0.16	0.004	0.002	0.270	0.004
N33	951851.8	527381.4	N33	CCG4	0.18	0.003	0.002	0.270	0.003
N34	951667.6	527394.3	N34	N35	0.90	0.023	0.009	0.270	0.024
N35	950908.8	526903.7	N35	CCG5	5.61	0.083	0.059	0.440	0.102
Cluster F									
N52	956614.1	528029.8	N52	N51	0.25	0.006	0.003	0.270	0.007
N51	956591.6	528281.3	N51	N53	0.44	0.011	0.004	0.270	0.012
N50	957327.4	528524.1	N50	N51	0.77	0.019	0.008	0.270	0.021
N53	956156.5	528265.3	N53	N54	0.64	0.016	0.006	0.270	0.017
N54	955745.8	527779.4	N54	N55	0.46	0.011	0.005	0.270	0.012
N56	955066.4	527772.9	N56	N55	0.23	0.006	0.002	0.270	0.006
N55	955289.3	527813.8	N55	CCG1	0.79	0.012	0.008	0.440	0.014
N49	957195.6	528984.1	N49	N48	0.42	0.010	0.004	0.270	0.011
N48	956782.0	528948.1	N48	N47	0.27	0.007	0.003	0.270	0.007
N47	956520.6	528890.9	N47	N13	1.17	0.029	0.012	0.270	0.032
N13	955368.5	528684.4	N13	N15	0.42	0.011	0.004	0.270	0.011
N15	954972.7	528536.9	N15	CCG2	5.00	0.074	0.053	0.440	0.091
N78	947143.9	523995.6	N78	CCG3	0.09	0.001	0.001	0.440	0.002
Cluster G									
N1	959170.0	530089.7	N1	N2	0.21	0.005	0.002	0.270	0.006
N2	958996.4	529977.2	N2	N3	0.18	0.004	0.002	0.270	0.005
N3	958835.3	530046.6	N3	N5	0.67	0.017	0.007	0.270	0.018
N5	958172.4	529930.3	N5	N6	0.38	0.009	0.004	0.270	0.010
N6	957824.7	529785.3	N6	N7	0.35	0.009	0.004	0.270	0.009
N7	957496.3	529658.7	N7	N9	0.24	0.006	0.002	0.270	0.007

Tower ID No.	Y(m)	X(m)	Branch		Distance (Km)	R(pu / kM)	X(pu/ kM)	C(µF/ km)	Z (pu/ kM)
			From	To					
N9	957253.7	529659.7	N9	N10	0.71	0.018	0.007	0.270	0.019
N10	956550.4	529577.4	N10	N11	0.27	0.007	0.003	0.270	0.007
N11	956307.8	529458.6	N11	CCG1	1.08	0.027	0.011	0.440	0.029
N14	955314.1	529034.9	N14	N12	0.36	0.009	0.004	0.270	0.010
N12	955660.7	528927.7	N14	CCG2	0.55	0.014	0.006	0.440	0.015
N17	954770.4	529087.1	N17	N18	0.27	0.007	0.003	0.270	0.007
N18	954498.1	529062.6	N18	CCG3	5.45	0.136	0.058	0.440	0.148
Cluster H									
N4	958099.1	530324.5	N4	N8	0.86	0.021	0.009	0.270	0.023
N8	957300.6	530010.1	N8	N36	1.48	0.037	0.015	0.270	0.040
N36	955818.3	529938.3	N36	N37	0.24	0.006	0.002	0.270	0.007
N37	955575.6	529910.8	N37	N39	0.24	0.006	0.002	0.270	0.007
N38	955551.4	530443.4	N38	N37	0.53	0.013	0.005	0.270	0.014
N39	955342.2	529975.3	N39	N40	0.30	0.007	0.003	0.270	0.008
N40	955044.3	529984.8	N40	CCG1	0.48	0.007	0.005	0.270	0.009
N46	954723.3	530485.3	N46	N45	0.28	0.007	0.003	0.270	0.008
N45	954514.9	530299.2	N45	N41	0.29	0.007	0.003	0.270	0.008
N41	954565.6	530018.5	N41	CCG2	0.32	0.005	0.003	0.440	0.006
N42	954296.8	529853.2	N42	N43	0.24	0.006	0.002	0.270	0.006
N44	954077.8	530136.1	N44	N43	0.30	0.008	0.003	0.270	0.008
N43	954061.7	529834.1	N43	CCG3	5.00	0.074	0.053	0.440	0.091

Appendix D: Wind Turbine and Network Parameters

Table D.1:WT3G1 Generator model data

Symbol	Description	Value
Xeq	Equivalent reactance for current injection(pu) 0.8	0.8
Kpll	PLL first integrator gain	30
Kipll	PLL second integrator gain	1
PLLMX	PLL maximum limit	0.1
Prated	Turbine MW rating	1.5
Number of lumped wind turbines		102

Table D.2:WT3E1 Wind turbine electrical model data

Symbol	Description	Value
Tfv	Filter time constant in voltage regulator(sec)	0.15
Kpv	Proportional gain in voltage regulator(pu)	18
Kiv	Integrator gain in voltage regulator(pu)	5
Xc	Line drop compensation reactance(pu)	0.05
Tfp	Filter time constant in torque regulator(sec)	0.05
Kpp	Proportional gain in torque regulator(pu)	3
Kip	Integrator gain in torque regulator(pu)	0.6
PMX	Max limit in torque regulator(pu)	1.12
PMN	Min limit in torque regulator(pu)	0.1
QMX	Max limit in voltage regulator (pu)	0.296
QMN	Min limit in voltage regulator(pu)	-0.6
IPmax	Max reactive current limit(pu)	1.1
Trv	Voltage sensor time constant(sec)	0.05
RPMX	Max power order derivative(pu)	0.45
RPMN	Min power order derivative(pu)	-0.45
T_Power	Power filter time constant(sec)	5
Kqi	MVAR/Voltage gain	0
VMINCL	Min voltage limit	0.9
VMAXCL	Max voltage limit	1.2
Kqv	Volt/ MVAR gain	40
XIQmin	XIQmin-min limit	-0.5
XIQmax	XIQmax-max limit	0.4
Tv	Lag time constant in wind Var controller	0.05
Tp	Pelec. Filter in fast PF controller	0.05
Fn	A portion of on –line wind turbine	1.0
Wpmin	Shaft speed at Pmin,pu	0.69
Wp20	Shaft speed at 20% rated power,pu	0.78
Wp40	Shaft speed at 40% rated power,pu	0.98
Wp60	Shaft speed at 60% rated power,pu	1.12
Pwp	Minimum power at wp100 speed,pu	0.74
Wp100	Shaft speed at 100% rated power,pu	1.2

Table D.3:WT3T1 Wind turbine model data

Symbol	Description	Value
VW	Initial wind, pu of rated windspeed	1.25
H	Total inertia constant,MW*sec/MVA	4.95
DAMP	Machine damping factor , pu P/puspeed	0.00
Kaero	Aerodynamic gain factor	0.007
Theta2	Blade pitch at twice rated wind speed (deg)	21.98
Htfrac	Turbine inertia fraction (Hturb/H)	0.875
Frec1	First shaft torsional resonant frequency(Hz)	1.8
DSHAFT	Shaft damping factor (pu)	1.5

Table D.4:WT3T1 Pitch model data

Symbol	Description	Value
Tp	Blade response time constant(sec)	0.3
Kpp	Proportional gain of PI regulator(pu)	150
Kip	Integrator gain of PI regulator(pu)	25
Kpc	Proportional gain of the compensator(pu)	3
Kic	Integrator gain of the compensator(pu)	30
TetaMin	Lower pitch angle limit(deg)	0
TetaMax	Upper pitch angle limit(deg)	27
RTeta	Upper pitch angle rate limit(deg/sec)	10
PMX	Power reference(pu on MBASE)	1

Appendix E: The Plants Turbine and Generator Specification [Feasibility study]

Table E.1: Adama II wind power plant turbine generator specifications

Generator type	DFIG, Doubly fed Induction Generator
Drive	Direct drive
Rated Output Voltage	0.69kV
Rated Power	1500kW
Frequency	50HZ
Power factor	$\geq$0.98
Start up wind speed	3.5m/s
Cut in wind speed	3.5m/s
Rated wind speed	14.5m/s
Cutout wind speed	25m/s
Blade length	37m
Converter	Full power IGBT converter

Table E.2: Adama II wind power plant unit transformer specifications

Unit transformer capacity	1.6MVA
Voltage level	33±2 x 2.5%/0.69kV(33/0.69/0.4kV)
Connection Group	D,yn11
Short circuit impedance	6.5%
Number of Winding	Three winding

TableE.3: Adama II wind power plant main transformer specifications

main transformer capacity	90MVA
Voltage level	230±8 x 1.25%/33kV(230/33kV)
Connection Group	Yn,d11
Short circuit impedance	14%
Number of Winding	Two winding